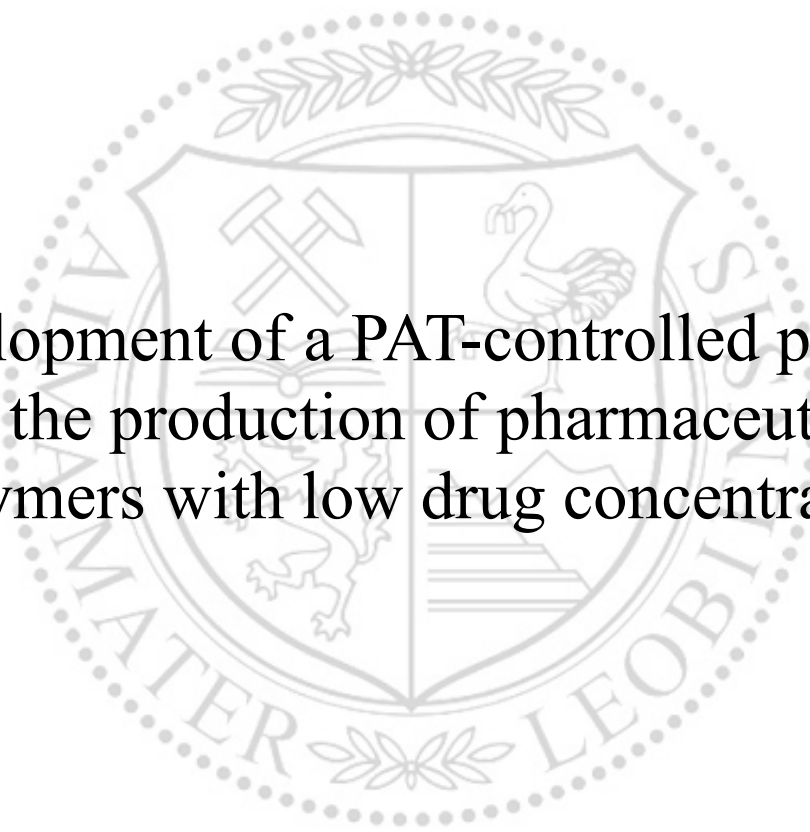




Chair of Polymer Processing

Master's Thesis



Development of a PAT-controlled process
for the production of pharmaceutical
polymers with low drug concentration

Nikolaus Heindl, BSc

May 2020

EIDESSTATTLICHE ERKLÄRUNG

Ich erkläre an Eides statt, dass ich diese Arbeit selbständig verfasst, andere als die angegebenen Quellen und Hilfsmittel nicht benutzt, und mich auch sonst keiner unerlaubten Hilfsmittel bedient habe.

Ich erkläre, dass ich die Richtlinien des Senats der Montanuniversität Leoben zu "Gute wissenschaftliche Praxis" gelesen, verstanden und befolgt habe.

Weiters erkläre ich, dass die elektronische und gedruckte Version der eingereichten wissenschaftlichen Abschlussarbeit formal und inhaltlich identisch sind.

Datum 25.05.2020



Unterschrift Verfasser/in
Nikolaus, Heindl

Abstract

Aim and motivation for this master thesis was the development of a novel continuous hot-melt extrusion-based compounding process, where a micro-feeder is added to a standard twin-screw extruder.

Target of this innovative production method is to produce extrudates with an active pharmaceutical ingredient (API) loading, which reaches a concentration as little as 0,1 $\omega/\omega\%$. By reaching such low concentration-levels, this method could be applied for the production of drug eluting polymers, in a continuous process. The low API concentrations were enabled by the implementation of a novel microfeeder into the compounding process.

The main objective was to assess the underlying process characteristics and parameters for the production of extrudates with an API concentration of 0,1 to 0,5 $\omega/\omega\%$. Furthermore, the implementation of an in-line process analytical tool (PAT) was assessed and investigated. Additionally, a capability analysis of the applied key technologies, with special emphasis on the microfeeder was performed. Ultimately, a comparison between a pre-blend production method and the newly developed compounding process was performed.

The tested formulation was comprised of Fenofibrate as API and polyvinylpyrrolidone-vinyl acetate (Kollidon[®] VA64) as polymer matrix. For the compounding process, a pharma-grade twin-screw extruder was used with an optimized screw geometry to suit the processes requirements. Additionally, a new powder guiding system was developed, to facilitate the integration of the microfeeder into the process. A UV/Vis spectrometer as PAT was integrated, to analyze, inline, the extrudates API concentration. The extrudates were furthermore analyzed by high pressure liquid chromatography (HPLC).

A capability analysis of the microfeeder showed reproduceable feed rates with sufficient accuracy between 85 % (for 1 g/h) and 97 % (for 5 g/h) for various rates over a timespan of two hours. The implementation of the UV/Vis based PAT showed the feasibility of the concept, in principle, did however encounter certain obstacles in the execution due to problems with weak signal-intensity. Off-line API content analysis of the extrudates via HPLC successfully verified the capability of the compounding processes. In several different compounding processes, the feasibility and reproducibility of the process was assessed and proven. In a complimentary compounding experiment, the variability of the API concentration during ongoing processing was successfully shown. The intended concentration of API in the extrudates was met with an average of more than 90 % accuracy. A comparison between this experiment and an extrusion experiment based on the pre-blend production method showed superiority of the new microfeeder based compounding method in terms of accuracy for higher API concentration.

In conclusion it can be said, that this thesis' main objective, the development of a continuous compounding process for extrudates with API concentrations down to 0,1 $\omega/\omega\%$, was successfully accomplished within the realms of possibility.

Kurzfassung

Motivation dieser Masterarbeit war die Entwicklung eines kontinuierlichen compoundier-Prozesses, bestehend aus einem Microfeeder und einem Doppelschneckenextruder.

Ziel dieses innovativen Prozesses war die Herstellung von Extrudaten mit einem Wirkstoffgehalt (API) von bis zu 0,1 $\omega/\omega\%$. Eine Anwendungsmöglichkeit für diesen Prozess wäre die kontinuierliche Herstellung von „drug eluting polymers“ mit hoch wirksamen APIs. Die geringen Wirkstoffkonzentrationen in den Extrudaten wurden durch die Einbindung des neuen Microfeeders in den Prozess ermöglicht.

Primäres Ziel war die Überprüfung des Prozesses, um dessen Charakteristiken, Grenze und Möglichkeiten zur Herstellung von Extrudaten mit Wirkstoffkonzentrationen zwischen 0,1 und 0,5 $\omega/\omega\%$ zu ermitteln. Zusätzlich wurde die Implementierung einer in-line Prozessüberwachung zur Kontrolle der API-Konzentration im Extrudat (PAT) geprüft. Weiteres wurde eine Prozessfähigkeitsanalyse von allen Technologien mit zentraler Bedeutung, mit besonderem Augenmerk auf den Microfeeder, für den Prozess durchgeführt. Schlussendlich wurde der neu entwickelte Compoundier-Prozess mit dem derzeit üblichen „pre-blend“ Herstellungsverfahren verglichen.

Die getestete Formulierung besteht aus dem Wirkstoff Fenofibrat und Polyvinylpyrrolidon-Vinylacetat (Kollidon® VA64) als Matrixpolymer. Für den Extrusionsprozess wurde ein Pharma-Doppelschneckenextruder mit einer für die Prozessanforderungen optimierten Schneckenengeometrie eingesetzt. Des Weiteren wurde ein neues „powder guiding system“ entwickelt, um die Integration des Microfeeders in den Prozess zu ermöglichen. Zur in-line Überwachung des Wirkstoffgehalts im Extrudat wurde ein UV/Vis Spektrometer als „process analytical tool“ (PAT) integriert. Zusätzlich wurden die Extrudate mittels Hochleistungsflüssigkeitschromatographie (HPLC) analysiert.

Eine Prozessfähigkeitsanalyse des Microfeeders zeigte reproduzierbare Förderraten mit einer Genauigkeit zwischen 85 % (für 1 g/h) und 97 % (für 5 g/h) für unterschiedliche Förderraten in einem Zeitraum von zwei Stunden. Das Konzept der Implementierung des auf UV/Vis basierenden PAT erwies sich als machbar, unterlag jedoch Problemen bei der Umsetzung aufgrund von nicht ausreichender Intensität der gemessenen Signale. Eine off-line Analyse des API-Gehalts der Extrudate mittels HPLC verifizierte erfolgreich die Fähigkeit des compounding-Prozesses. In mehreren Versuchen wurden die Machbarkeit sowie die Reproduzierbarkeit des Prozesses bewiesen. Zusätzlich wurde die Möglichkeit zu Änderung der API-Konzentration im Extrudat während des laufenden Prozesses gezeigt. Die geplante API-Konzentration in den Extrudaten wurde mit einer durchschnittlichen Genauigkeit von über 90 % erreicht. Ein Vergleich zwischen diesem Experiment und einem Extrusionsversuch basierend auf der „pre-blend“-Herstellungsmethode zeigte die überlegene Genauigkeit des neuen Microfeeder basierenden Compoundier-Prozesses für höhere Wirkstoffkonzentrationen.

Zusammenfassend kann gesagt werden, dass das zentrale Ziel dieser Masterarbeit, die Entwicklung eines kontinuierlichen Compoundier-Prozesses für die Herstellung von Extrudaten mit einem API-Gehalt von bis zu 0,1 $\omega/\omega\%$ im Rahmen der gegebenen Möglichkeiten erfolgreich erreicht wurde.

Acknowledgement

Thanks go firstly to the "Research Center Pharmaceutical Engineering" in Graz under the scientific leadership of Univ.-Prof. Dr. Johannes Khinast for giving me the opportunity to conduct and author this master thesis.

Many thanks also go to my advisor Stephan Sacher from the RCPE for all his guidance, input and continuous support during my work. Additionally, I want to thank Johannes Poms and Julia Kruisz for their help with specific topics. I would also like to acknowledge the input from my colleagues Carolina Alva and Sara Fathollahi as well as to the entire team of the RCPE's pilot plant under Daniel Kaiser for their active support during all challenges. Lastly, I want to thank Jesús Alberto Afonso Urich and the "HPLC-team" for their essential help.

Special thanks go to the Institute of Polymer Processing at the Montanuniversitaet Leoben, headed by Univ.-Prof. Dipl.-Ing. Dr. mont. Clemens Holzer.

I wish to express my sincere thankfulness to Stephan Schuschnigg for advising my work at the institute as well as for all of his vital inputs and suggestions during the formation of this thesis. Additionally, I want to thank all my fellow students, with special regards to Lukas Hentschel and Martin Hubmann for their encouragement. At last I want to thank all my fellow students for their support and the shared time in Leoben.

Finally, I take this opportunity to express my sincere gratitude to my entire family and especially my parents Katrin and Matthias. They supported and encouraged me during my time at University with an enduring endorsement, facilitating my achievements during the years of studies.

Table of contents

1	<i>Introduction</i>	1
2	<i>Objectives</i>	2
3	<i>State of the art</i>	3
3.1	Definitions	3
3.2	Drug eluting polymers	3
3.2.1	Polymer matrixes	6
3.2.2	Active pharmaceutical ingredients (API)	9
3.2.3	Formulation.....	10
3.3	Processes	12
3.3.1	Twin-screw extrusion	13
3.3.2	Feeder	19
3.3.3	Process analytical technology	23
3.3.4	UV/Vis spectroscopy	25
3.3.5	HPLC	27
3.4	Research topic	28
3.4.1	Current production technique and its limitations	28
3.4.2	New micro-feeding solution and its challenges	29
4	<i>Materials and methods</i>	30
4.1	Materials	30
4.1.1	API	30
4.1.2	Matrix.....	31
4.2	Equipment and methods	32
4.2.1	UV/Vis spectroscopy for API feasibility test	32
4.2.2	Microfeeder.....	32
4.2.3	Pre-blend preparation	34
4.2.4	Twin-screw extruder	34
4.2.5	UV/Vis spectroscopy as PAT.....	38
4.2.6	Residence time distribution	39
4.2.7	HPLC analysis	39
5	<i>Experiments</i>	40
5.1	Feasibility test of API	40
5.2	Capability analysis of equipment	40
5.2.1	Microfeeder.....	40
5.2.2	HPLC analysis	41
5.3	Compounding experiments	41
5.3.1	Preceding extrusion trials	41
5.3.2	Pre-blend experiment with PAT	43
5.3.3	Compounding experiments with microfeeder	44

6	<i>Results and discussion</i>	49
6.1	Feasibility test of API	49
6.2	Capability analysis of equipment	49
6.2.1	Microfeeder	49
6.2.2	HPLC analysis	55
6.2.3	Residence time distribution	55
6.3	Compounding experiments	57
6.3.1	Pre-blend experiment with PAT	57
6.3.2	Compounding experiments with microfeeder	59
6.4	Comparison between pre-blend feeding and microfeeding	68
7	<i>Conclusion and perspective</i>	70
8	<i>Literature</i>	72
9	<i>Appendix</i>	78
9.1	Abbreviations and symbols	78
9.2	List of figures	81
9.3	List of tables	82

1 Introduction

Currently, pharmaceutical science faces the problem that many newly developed drugs are highly active, but lack in bioavailability [55]. One approach that has high potential in solving this problem for many applications are drug eluting systems. This form of drug administration causes a predefined release of the active pharmaceutical ingredients (API) over a certain period of time. Additionally, it can increase the bioavailability of many drugs [33]. Such systems can be built of a polymer matrix containing the API. The properties of such drug eluting polymers strongly depend on the used materials and the architecture, leading to different variations in release type [17]. One important aspect for the bioavailability is the degree of crystallinity of the API in the formulation [30, 34]. Crystallinity strongly decreases the bioavailability, often leading to the necessity of single-phase amorphous systems [42, 51]. One proven method for the creation of such systems is hot melt extrusion (HME) [14].

Lately, hot melt extrusion has gained much attention in the pharmaceutical industry, due to its many possibilities and its suitability for continuous processing opposed to the current batch-wise production methods [36, 66]. Especially twin-screw extruders are a convincing technology, due to their accuracy and versatility [35]. A bottleneck in the production of low drug-dose extrudates are the capabilities of feeders. Here, mostly loss in weight feeders are applied. Due to their construction, the feed rates cannot be sufficiently low for HME-produced low dose formulations [25]. However, due to the high potency of many APIs, doses in the milli- or even microgram range are necessitated. The therefore small quantities that have to be introduced into a production process can lead to problems with guaranteeing blend homogeneity and content uniformity [48]. A novel microfeeder used in this thesis can solve this problem by providing constant feed rates in the range down to one gram per hour.

Continuous processes also arise the question of continuous product quality control. Since the publishing of the FDA in 2004, the field of process analytical technology (PAT) is gaining even more momentum in the pharmaceutical technology as an answer [66]. Applied or investigated technologies for the application as PAT are monitoring of process variables and in-line observation with tools such as spectrometers [34]. With the via PAT gained information, the stability and quality of a controlled continuous process can be determined. For this, the data has to be analyzed. Chemometric methods to do so are, among others, statistical mathematics and multivariate data analysis [24].

In this thesis, a continuous hot melt extrusion process was established that produces extrudates with an API-concentration between 0,1 and 0,5 $\omega/\omega\%$, resembling the smallest concentrations possible with this setup. This was realized by integrating the above mentioned microfeeder, providing feed rates between 1 to 5 g/h, directly into the extrusion process. After a capability analysis of the employed techniques, several approaches of the process setup were tested. The process feasibility, stability and repeatability were investigated via analysis of the extrudates by means of HPLC. Additionally, in-line monitoring of the API-concentration in the extrudate was attempted.

2 Objectives

The objectives of this thesis are:

- 1) Determining whether it is possible to achieve reproduceable, stable feed rates between one and five gram per hour with the microfeeder for the applied material.
- 2) To implement a process analytical tool on the basis of UV/Vis spectroscopy to measure the concentrations in the extrudate in-line and verify the in-line monitoring, as well as the entire process with means of high-pressure liquid chromatography.
- 3) To prove that it is possible to implement the microfeeder in a hot melt extrusion process and produce extrudates with concentrations of the material fed by the microfeeder between 0,1 and 0,5 $\omega/\omega\%$ in a stable manner for repeatable intervals of one hour.

3 State of the art

3.1 Definitions

Active pharmaceutical ingredient (API): "An active ingredient is any component that provides pharmacological activity or other direct effect in the diagnosis, cure, mitigation, treatment, or prevention of disease, or to affect the structure or any function of the body of man or animals." [67]

Matrix system: An active pharmaceutical ingredient is dissolved or dispersed in a non-active polymer, which forms the matrix carrying the API [75].

Release rate: A release rate defines the amount of active pharmaceutical ingredient that is released from the drug delivery system over a specified period of time into the surrounding system [55].

Dissolution: "Dissolution can be defined as a process, by which molecules of a solute (such as an active agent) are dissolved in a solvent vehicle." [11]

Controlled therapeutic systems: Drug delivery systems with temporal control which deliver the drug(s) over an extended period of time, at a definite location via controlled release dosage forms with predefined release rates [17, 75].

Sustained release: In a sustained release form, the drug eluting system maintains a certain rate of drug release over a prolonged period of time [55].

Immediate release: In an immediate release form, the drug is dissolved into the surrounding system without any means of delaying the dissolution or absorption of the drug [55].

Biocompatibility: Biocompatibility describes the compatibility between a technical and a biological system [75].

Biodegradability: Biodegradability describes the prospect of an enzymatic or hydrolytic degradation of the molecules by the body, leading to a practically complete removal of the material from the system [75].

Bioavailability: Bioavailability describes the proportion of a substance, which is unaltered available to the body's circulation (therefor reaching the systemic circulation) in respect to the amount of administered API [27].

3.2 Drug eluting polymers

A drug eluting system is a form of drug-administration for one or more active pharmaceutical ingredients, which releases the substances at a predefined release rate continuously into the entire system or at a specific location. This rate can be constant (zero-order release), gradually decreasing (first order release), or any other type of predefined release pattern [33].

There are several factors which are to be considered when designing the delivery form of APIs. One is the therapeutic index (TI). It is the ratio between an APIs mean lethal dose (the dose where 50 % of laboratory test-animals die) and the mean effective dose (the dose where the expected effect occurs in 50 % of all cases). Therefor the TI is a restraining factor, when

designing the administration form and dose of APIs. With a low TI, a constant but accurate drug release is desired over a discontinuous form with high peaks, as it is e.g. caused by orally administered tablets.

Drug eluting polymers are a system, which make it possible to achieve constant API concentration in the tissue / body over a certain period of time by releasing the API with a constant rate into the surrounding tissue [47, 75]. Figure 1 shows the difference of drug concentration in plasma over time for the two mentioned delivery methods.

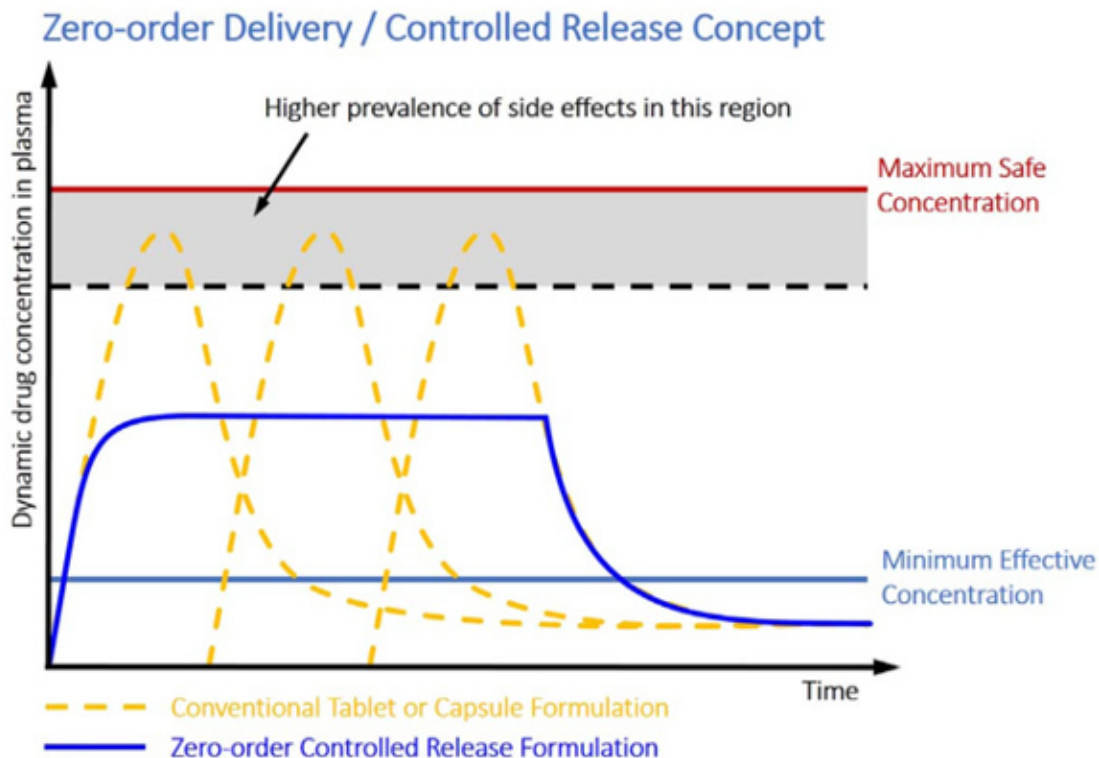


Figure 1: Concentration of API in plasma for different delivery forms [59]

Discontinuous administration forms have the disadvantage of the first kinetic order, meaning that the API gets quickly dispensed into the body at the starting phase, leading to a peak in API concentration, followed by an exponential decline. This effect could be minimized by a more frequent administration, which however, carries the disadvantage of more effort [75].

Due to this constant oscillation between the maximal and minimal dose, more API than necessary is administered. This problem can be solved by a system with a constant release (zero order) over a certain period of time, leading – besides other things – to a reduction of possible side effects and an increase in the therapy's safety [75].

In summary, the advantages of drug eluting systems (especially if) made of polymers are [47]:

- The level of API(s) in the plasma or entire system are kept at a desired therapeutic level.
- API(s) with short in vivo half-lives are available in the system for a predefined time at predefined levels.
- Side effects of the API(s) can be reduced due to the overall lower administration of the drug(s).
- By local drug administration via drug eluting implants the APIs side effect can be constrained to a specific area.
- The administration of drugs via drug eluting systems can lead to a more efficient use of resources by reducing the amount of wasted API.

Apart from that, polymer-based drug-eluting-systems have the big advantage that the release rate is primarily predefined by the polymers properties and only weakly depends on the surrounding environmental conditions, allowing to design systems with high reproducibility [47]. One further advantage of using polymers as matrix for APIs is the possibility to create a delivery system for poorly bioavailable substances [17].

However, the above-mentioned advantages are accompanied by several disadvantages [47]:

- The (polymer) material as well as all byproducts have to be sufficiently biocompatible to avoid any undesired side effects.
- In the case of drug eluting implants, the surgical implantation as well as the possible discomfort caused by the implant's presence, have to be considered.
- Malfunctioning of the system can never be entirely ruled out.

There are several schemes how controlled therapeutic systems can be designed. The most important ones are matrix-systems (biodegradable and non-biodegradable) and membrane-systems [75]. Current methods of drug administration via drug eluting polymers are: oral drug delivery (immediate or sustained/targeted), parenteral drug delivery (subcutaneous, intramuscular, intraocular, or intraosseous), and others (transmucosal, transdermal, or intravaginal) [62].

In the case of drug eluting systems consisting of a polymer matrix, hot melt extrusion is one possible technique for the fabricating of those drug eluting polymers. One major reason for using HME is, that all melt-able materials can be considered as matrix or binding agent. Furthermore, they can be applied as modifying agents. Finally, hydrophilic materials can be mixed with hydrophobic ones, as long as at least sufficiently available component in the mixture is in a molten state at processing temperature. Ingredients that are not molten or dissolved in the matrix at processing temperature are incorporated in the matrix and therefore still present in the final product [25].

3.2.1 Polymer matrixes

3.2.1.1 Polymers in „drug eluting polymers “

The selection of the matrix-polymer for drug eluting polymers is primarily depending on the intended purpose of the final product. In perspective to drug eluting polymers, one important aspect is the release type: There is the “immediate release”-type, used for enhancing the bioavailability of APIs as well as the location of their release in the system, and there is the “sustained release”-type, which provides a constant supply of a predefined API amount over time [17].

Examples for possible polymers used as “immediate release” are polyethylene oxide (PEO), polyethylene glycol (PEG), polyvinylpyrrolidone (PVP) as well as copolymers such as vinylpyrrolidone/vinyl acetate (PVP-VA).

Polymers suitable for a “sustained release” rate are for example ethylene vinyl acetate (EVA), polyvinyl acetate (PVA) and poly(L-lactic acid) (PLA) [17].

Other used or tested polymers for drug eluting systems include: synthetic biodegradable polymers (aliphatic polyesters, poly(ortho esters), polyurethanes, and polyanhydrides) synthetic non-biodegradable polymers (polyvinyl lactam polymers, ethylene-co-vinyl-acetate, acrylic polyesters, polyethylene glycol, and polyethylene oxide) and natural polymers (cellulose derivatives, starch, and chitosan) [62].

In many cases the difference between polymers in sustained release and immediate release is the biodegradability of the polymers. Four different degradation mechanisms are prevalent: polymer dissolution, non-specific hydrolysis, enzymatic degradation, and dissociation of polymer-polymer complexes [75].

The requirements for polymers in HME-manufactured drug eluting systems are primarily: thermoplasticity / processability, a glass transition temperature (T_g) in processable range, especially in consideration of the other components, a thermal stability that is sufficiently higher than the T_g to enable a degradation-free process, bio-compatibility, and a thermodynamically desired character to obtain solubility or insolubility [17, 75]. Of course, similar to equal requirements are valid for additives like plasticizers and drug-release modifiers [75].

There are various ways, in which the properties of the polymer influence the diffusion rate of the API and therefore the drug release. Factors which decrease the diffusion rate are for example a higher molecular weight, stiffness of the polymers main chain, the degree of cross-linking, interactions between the molecules and a higher degree of crystallinity. An increase can be caused by a higher filler and plasticizer content [75].

Additionally, issues such as sterilization, e.g. of the implants, is an important and complex matter. Especially due to the sensitivity of many polymers and APIs to heat and / or humidity, moist-heat-sterilization cannot be applied, and alternatives have to be utilized [62].

3.2.1.2 Polyvinylpyrrolidone

Polyvinylpyrrolidone was developed in the 1930s by Prof. Reppe at I.G. Farben. It is the product of radically polymerized N-vinyl-2-pyrrolidone (synthesis shown in Figure 2). At start it has been primarily used as blood-plasma-substitute in WWII. Nowadays its main application lies in the fields of pharmaceuticals, cosmetics and the food industry. This fact is due to its good biological compatibility (and low toxicity), its resistance to thermal degradation, its extrudability and binder-quality, as well as its film forming and adhesive characteristics. Furthermore, it provides reliable API-dissolution rates for sustained release formulations and enhances the bioavailability for various APIs [57]. It is water soluble and has recrystallization inhibiting characteristics, which makes it a suitable candidate for immediate release formulations [1, 42].

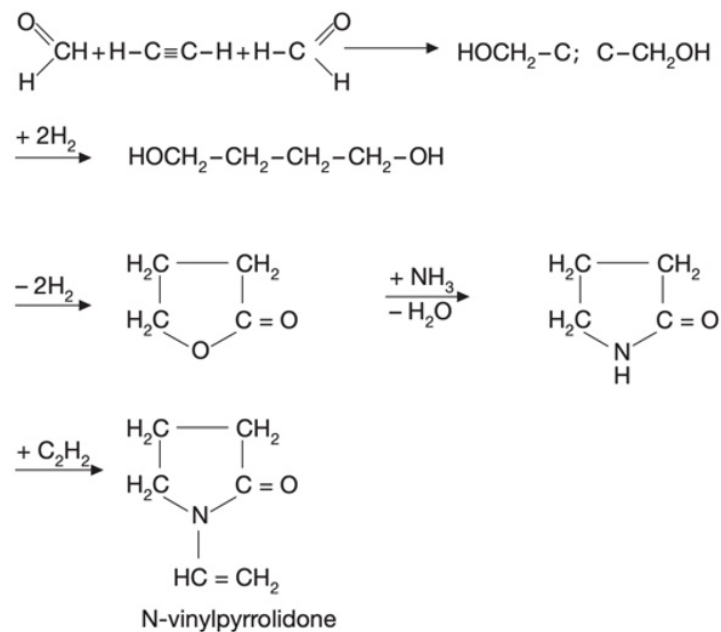


Figure 2: Synthesis of N-Vinyl-2-pyrrolidone [13]

There are 4 different grades of PVP for the use in pharmaceuticals supplied by BASF, DE. They primarily differ in their molecular weight and glass transition temperature [1].

3.2.1.2.1 Soluble polyvinylpyrrolidone (Povidone)

Soluble polyvinylpyrrolidone is produced through free radical polymerization of N-vinyl-2-pyrrolidone in water using hydrogen peroxides as initiator (see Figure 3). Thanks to the polymerization mechanism, the reaction can be stopped at any point, allowing to fabricate PVP in any desired range of molecular weight. For low molecular weight versions of PVP which are used, among others, for injectables, the polymerization is often carried out in an organic solvent like 2-propanol [12].

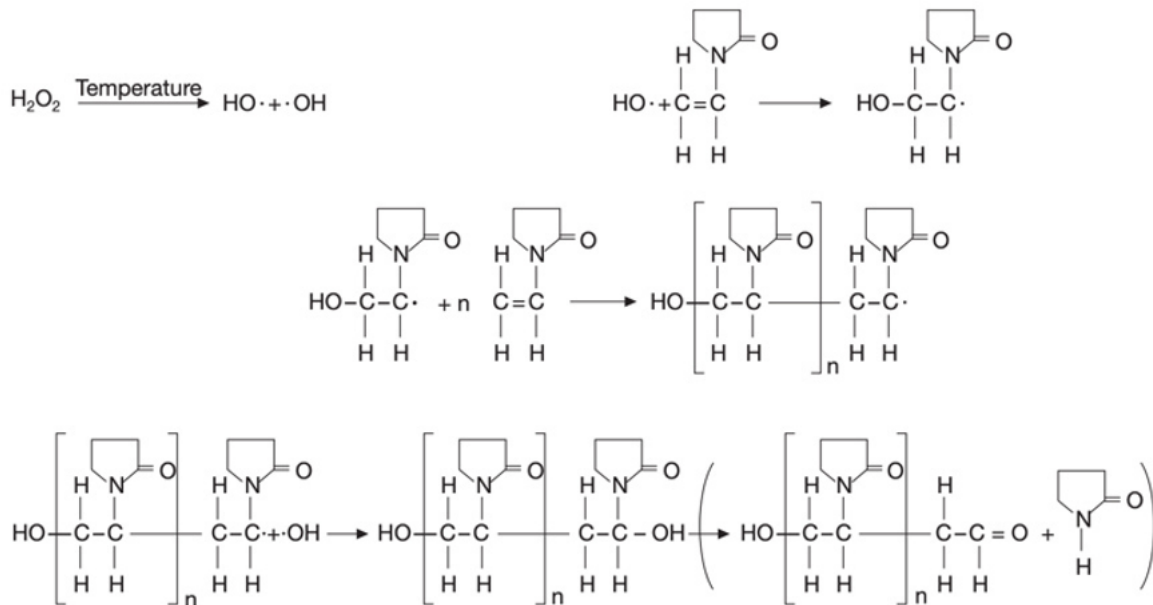


Figure 3: Polymerization of soluble PVP in water [13]

3.2.1.2.2 Insoluble polyvinylpyrrolidone (Crospovidone)

The insoluble version of polyvinylpyrrolidone is fabricated by popcorn-polymerization of N-vinylpyrrolidone [2]. The strong crosslinking created during the popcorn-polymerization is responsible for the polymer's properties. Among them is the swelling of the polymer without gelling in liquids such as water, making it a suitable disintegration agent in tablets [12].

3.2.1.2.3 Spray dried polyvinyl acetate containing Povidone

19 % of Povidone are added to an in aqueous dispersion radically polymerized vinyl acetate with a molecular weight average of around $50.000 \text{ g}\cdot\text{mol}^{-1}$. After further addition of auxiliaries for stabilization and the improvement of the flowing behavior, the polymer is spray dried. It is not water soluble due to its high molecular weight polyvinyl acetate content. Therefore, it is used as powder in solid dosage forms [13].

3.2.1.2.4 Vinylpyrrolidone-vinyl acetate copolymer (Copovidone)

In the presence of initiators, N-vinyl-2-pyrrolidone can also be copolymerized with vinyl acetate via free radical polymerization in isopropanol solution (see Figure 4). The solvent is necessary due to the insolubility of vinyl acetate in water. For "Kollidon[®] VA64" (a type of Copovidone) supplied by BASF, the resulting vinylpyrrolidone-vinyl acetate copolymer (PVP-VA) contains the two components in a ratio of 6 : 4. Due to the vinyl acetates properties, the resulting polymer has a slightly higher hydrophilic character and is water soluble. This gives the products made from Kollidon VA64 their favorable properties, as soluble or dry binders and film-forming agents, particularly for solid dosage forms [12].

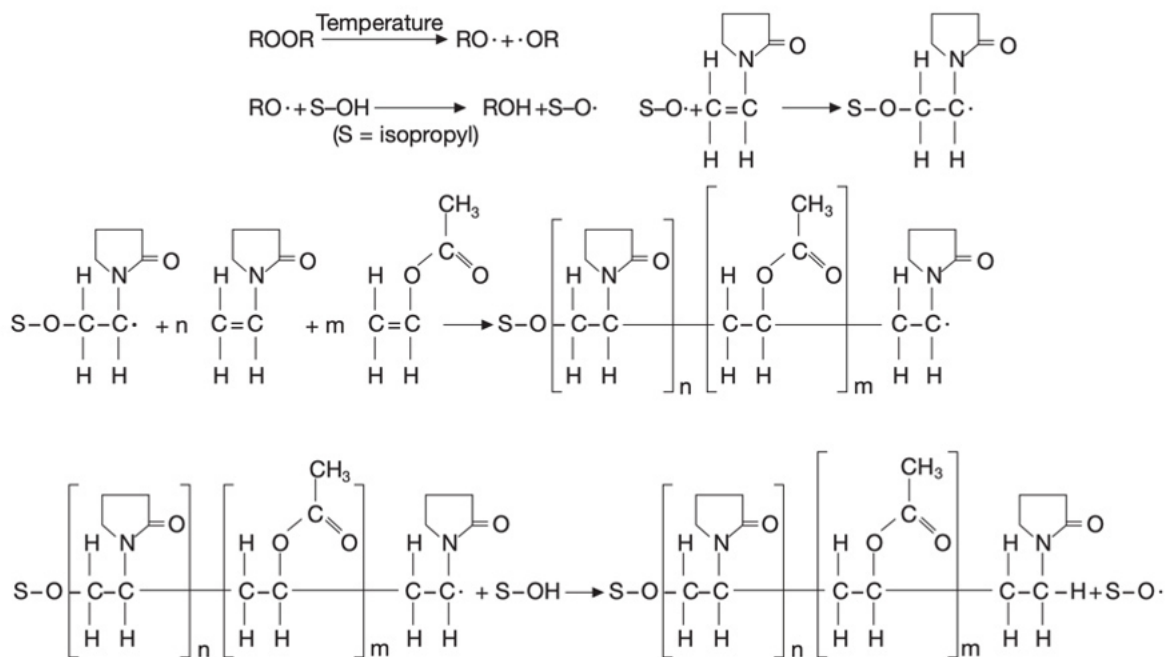


Figure 4: Synthesis of PVP-VA via free radical polymerization [13]

Kollidon VA64 is a spray dried polymer resulting in a typical hollow spherical structure for this process. The hollow spherical particles of normal Kollidon VA64 are mostly broken compared to the mainly intact particles of Kollidon VA64 Fine. The resulting irregularity of the particles is an important factor for the powders flowing properties [13]. Spray drying is the procedure to turn a liquid emulsion or suspension into a powder by spraying the liquid into a gaseous drying medium resulting in a removal of the liquid by evaporation. Some of the major advantages of spray drying are the rapid liquid evaporation, the variability of the process, the high throughput rate, and that it is a continuous process [8].

The effects of PVP-VA on the human body, when administered orally via food supplements or in tablet form, were investigated by the "European Food Safety Authority". They concluded, that due to its high molecular weight average PVP-VA barely gets absorbed and leaves the body essentially intact. Furthermore, several feeding-studies of PVP-VA on laboratory rats and dogs ended without any observed adverse effects [23].

3.2.2 Active pharmaceutical ingredients (API)

3.2.2.1 APIs in „drug eluting polymers“

Bioavailability describes the proportion of a substance that is unaltered available to the body's circulation (therefor reaching the systemic circulation) in respect to the amount of administered API [27]. Approximately half of all newly developed molecular drugs, particularly the new synthetic drugs, are poorly water soluble [16, 53]. In the biopharmaceutical classification system (BCS), they are therefore falling under category II for "poorly water-soluble compounds with low bioavailability". Because of the APIs poor water solubility and

bioavailability, administration to the body can be a big challenge, as absorption by the human body is low [27]. In order to avoid the need of high dosage by oral administration and its potential side effects triggered by the poor bioavailability, new drug formulations and administration forms are necessary, which enhance the solubility and therefore bioavailability of those APIs [53].

Solubility and bioavailability of poorly water-soluble APIs can be strongly influenced by the thermodynamic state of the API in a matrix. Hence, one very important aspect that has to be considered is the degree of crystallinity of the API [30, 34]. From the standpoint of bioavailability and drug release an amorphous state is preferred due to the better solubility of the drug. However, in many cases the crystalline form of APIs is the physically and chemically more stable one. A polymer based matrix system is one possibility to achieve a stable amorphous state of an API [17, 34].

3.2.2.2 Fenofibrate

One of those poorly water-soluble, and therefore badly bioavailable BCS class II drugs, is Fenofibrate (FFB) (see Figure 5) [53]. Belonging to the group of fibrates (a class of amphiphilic carboxylic acids), Fenofibrate acquires its bioactivity through esterase in form of its metabolite (an intermediate product of metabolism) „fenofibric acid“ [28, 29]. One positive aspect of this is, that Fenofibrate develops a good permeability leading to a high bioavailability once it is dissolved [40].

The effects it has on the human body are a cholesterol and triglyceride reduction in plasma as well as a rise in high density lipoprotein cholesterol. Because of this, Fenofibrate is regularly used to treat hypertriglyceridemia, combined hyperlipidemia and further metabolic disorders. By doing so it reduces the possibility of cardiovascular events, helping their prevention [29].

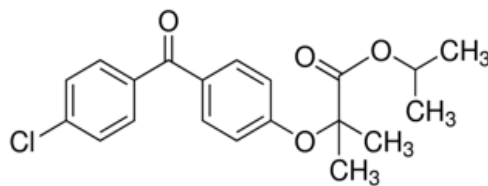


Figure 5: Chemical structure of Fenofibrate [60]

3.2.3 Formulation

In the case considered here, miscibility results in the formation of a single-phase amorphous system after two liquids (molten components), one being an amorphous polymer and the other an amorphous API, are mixed together [42, 51]. Since many APIs are only available in the thermodynamically more stable crystalline state, energy is required to transform them to the higher-energy amorphous state [42]. On a molecular level, this mixing can be achieved in two ways: 1) via a solvent, where both components are dissolved together and the solvent is then removed, or 2) by direct mixing of the two components in e.g. their molten state [14].

In both ways the components have to be thermodynamically miscible during the process to form a single-phase system. However, thermodynamic miscibility during the process often results in disturbance of the thermodynamic equilibrium of the components, which further results in their tendency to re-equilibrate after the process. One effect that worsens this is that low particle sizes reduce the thermodynamic stability. This triggers possible phase-separation. Therefore, it's the thermodynamics which are determining whether such an agitated system remains a single phase or becomes unstable, resulting in phase separation. In latter case, one amorphous phase would tend to go back into the energy-favored state of crystallinity [42]. For many cases it is only the slow speed of the thermodynamic processes which leads to a quasi-kinetically stable state that is sufficient for the intended use [51]. This stabilization technique of an amorphous solid dispersions can be achieved via the "freezing effect". Here, the rapid cooling of the mixture obstructs the recrystallisation of one phase through the solidification or sufficient rise in viscosity of the other [1, 65]. For a polymer based formulation, that effect relies upon a high glass transition temperature and interactions between the two components such as hydrogen bonding, leading to a more rigid structure [37, 42]. Other factors influencing the kinetic stability of amorphous solid dispersions are storage temperature and humidity, humidity being the bigger determinant due to the plasticizing effect of the moisture in the polymeric matrix, which in turn leads to local dissolution and recrystallisation of the API [16]. Additionally, the remaining crystallinity plays an important role in recrystallization due the effects of nucleation [1].

Polymer properties that influence the stability of an APIs amorphous state in a polymer matrix are the glass transition and melting temperature, the viscosity, and consequently the molecular weight. They have to be kept in mind in the design of the formulation [17, 34, 42]. One suitable and widely proven technique for mixing an API into a polymer matrix is via HME [42]. During that process, both components are exposed to high temperatures, pressure and mechanical forces. This leads to either melting or dissolving of a crystalline API [15]. Therein lies a major advantage of HME in creating amorphous solid dispersions [27].

To theoretically predict the solubility of two substances in each other, the three-dimensional Hansen's solubility parameters [31] can be applied. They are based on the Hildebrand theoretical solubility parameters, which in turn are based on the principle that "equal dissolves equal". According to Hansen, the solubility can be embodied by three single parameters which each represent a different intermolecular force. Those parameters are: δ_d for the dispersion component (or Van der Waals' forces), δ_p for the polar component, and δ_h for hydrogen bonding components. A total solubility parameter δ_{tot} then can be calculated according to equation (1).

$$\delta_{tot} = \sqrt{\delta_d^2 + \delta_p^2 + \delta_h^2} \quad (1)$$

Ultimately, those parameters can be used to give a first estimate about the miscibility of two components by directly comparing them to each other. The smaller the differences between δ_d , δ_p , δ_h , and especially δ_{tot} , the more likely is their miscibility [10, 31]. It is to be noted that slightly different values for the solubility parameters can be the caused by different calculation

methods. As a guideline, it can be said, that substances with $\Delta\delta < 7 \text{ MPa}^{1/2}$ are most likely to be miscible, whereas substances with $\Delta\delta > 10 \text{ MPa}^{1/2}$ are most likely not to be miscible [32]. For the substances used in this thesis, the following values can be found in the literature [42]:

Table 1: Hansen solubility parameters for used substances

	$\delta_d \text{ (MPa}^{1/2}\text{)}$	$\delta_p \text{ (MPa}^{1/2}\text{)}$	$\delta_h \text{ (MPa}^{1/2}\text{)}$	$\delta_{tot} \text{ (MPa}^{1/2}\text{)}$
Fenofibrate	19,8	4,2	6,7	21,4
Kollidon VA64	17,4	0,5	9,2	19,7

Considering this, it can be expected that, the polymer Kollidon VA64 has good miscibility with the API Fenofibrate.

In a pharmaceutical context the components of these processes should inherit certain characteristics, which are also relevant [53]:

- A sufficient level of purity must be met by both components.
- They have to be thermally stable during the entire manufacturing (extrusion) process as well as during the later storage time.
- The anticipated in vivo behavior (and for drug eluting formulations their release pattern and bioavailability) has to be taken into account.

In terms of a formulation, which consists of Fenofibrate and polyvinylpyrrolidone – vinyl acetate, it is reported that hot melt extrusion is a suitable technique to create amorphous solid dispersions. With help of the wide variety of existing types of PVP-VA, proper extrudability, dissolution rates and stability of Fenofibrate in PVP-VA can be achieved [1, 32]. Furthermore, the amount of drug loading (weight percentage of Fenofibrate in the PVP-VA matrix) has a significant effect on the mentioned properties [1]. That said, in formulations with low Fenofibrate drug loading the release is strongly influenced by the polymer's viscosity. In formulations with high Fenofibrate loading on the other side, the molecular weight of PVP is less of an impact factor. For a PVP matrix consisting of Kollidon 12PF a drug loading of 25 % is achievable via HME with the API still remaining in amorphous state. [1].

3.3 Processes

In the field of drug-development continuous processing techniques are intensively investigated due to their advantages over current methods. Several obstacles have to be overcome until continuous processes, including hot melt extrusion (HME), can be commonly applied. Among them are the alignment of the throughput from individual processing units, the ability of adequate surveillance of all relevant processing parameters responsible for a conforming product and the means to control those parameters allowing a stable and overseen production process [36].

3.3.1 Twin-screw extrusion

3.3.1.1 General overview

Two types of cylindrical twin-screw extruders (TSE) are distinguished: co-rotating- and counter-rotating-ones. Further, one differentiates between intermeshing and non-intermeshing. At intermeshing screws, the flights only have a small clearance between them, leading to a self-cleaning effect of the screws [41].

The extruder can be separated into several zones according to the dominant process happening there (see Figure 6). The main zones are the intake-, melting-, mixing-, conveying-, and the pressure build-up zone. Furthermore, zones for side-feeding and degassing can be implemented [41]. The screw can be adapted to the needs of the different zones by individual screw elements, which are described in detail in chapter 3.3.1.3.

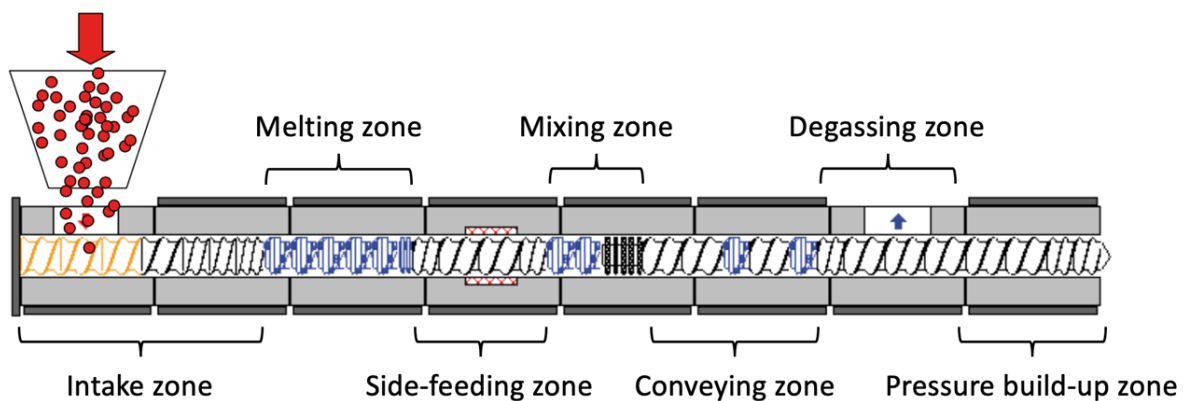


Figure 6: Processing zones of a twin-screw extruder (Figure adapted from [41])

3.3.1.1.1 Intake zone

The main task of the intake zone is to convey the polymer from the inlet into the barrel and to compress the polymer. Additionally, air is removed, which has been drawn in during the intake. The most relevant parameters for this zone are the screw speed, the mass throughput, the processed material and its properties, the free volume, and the friction at the barrel wall. When feeding materials with low bulk density, special attention has to be given to the removal of gas from the intake zone [41].

3.3.1.1.2 Melting zone

In this zone, the polymer is molten to a certain degree and the dispersion of the components is carried out. This process is, again, strongly influenced by the screw speed and the mass throughput, but also by other factors such as the heat flux, heat conduction, and by the material properties such as the melting enthalpy or the particle size. The necessary length of this zone strongly depends on those factors and, ultimately, on the time needed until the

material is molten. This time can be influenced by the degree of filling as well as the polymer melting temperature, particle size, and melt viscosity.

The required energy to melt the polymer is primarily generated by the shear forces created from the screw. Therefore, most (e.g. ~80 %) of the provided mechanical energy is applied in this zone. The goal of controlling the barrel-temperatures lies primarily in the energetic isolation of the inner barrel walls and can also be responsible for the formation of a melt film on the inner walls. This film plays an important role in the upkeeping of the shear forces between barrel and the screw.

For the processing of low-density polymers, the melting zone should not be operated fully filled. Otherwise fluidization in the intake zone could be the result. This is easily achieved by avoiding any pressure build up in the melting zone. This, however, results in the necessity for considerably longer melting zones [41].

3.3.1.1.3 Mixing zone

In the mixing zone, the homogenization of the melt, including the temperature, and the distribution of additives and fillers takes place. This is strongly influenced by the screw speed, the mass throughput, and most of all the screw geometry. In general, mixing-results are best at lower throughput and higher screw-speeds. In these zones mixing can further be improved by a high melt filling degree [41].

3.3.1.1.4 Conveying zone

This zone is responsible for conveying the melt. Once again, the main influential material properties are the screw speed, the material throughput, the screws pitch (here often bigger than 1D), and the polymer properties. These zones are usually only partially filled since the sole purpose is that of a "spacer" between different zones. Nevertheless, due to the nature of the conveying technique via screws, a certain amount of mixing and material stress is applied in the leakage flow between barrel and screw [41].

3.3.1.1.5 Pressure build-up zone

In this zone (also called discharging zone), the pressure necessary to overcome the resistance from the die and any following units such as a filter is built up. Besides the usual influential factors such as the zones length, especially the pitch, but also the clearance between screw and barrel, play an important role. Another aspect relevant in this zone are the number of screw flights. They create individual product flows (three product flows for double flighted screws in TSE) leading to metering fluctuations. Consequently, the energy intake in this zone is relatively high. To avoid too high energy input to the material and throughput fluctuations, alternatives such as a melt pump can be used [41].

3.3.1.2 Compounding process

In a compounding process two or more materials are mixed in an extrusion process. The differences can lie in properties such as chemical composition, moisture content, color, density, temperature, viscosity, particle size etc. [41]. These materials can be introduced into the extruder from individual feeders to be mixed inside the compounder. Alternatively, they can be fed as mixed pre-blend [17]. Either way, it is the prime objective to modify the polymer or compound towards the desired properties [75].

In hot melt extrusion, two of the most common mixing processes are the incorporation of fillers and additives and the blending of polymers. Twin-screw extruders are a well proven tool for such processes. They manage to combine the melting of polymers, the incorporation and distribution of fillers, and the actual extrusion in one process. Additionally, a variety of supporting technologies, such as special screw configurations or peripheral apparatuses, have been developed, to further enhance the twin-screw extruders mixing performance [41].

One important aspect of compounding is that local concentration-variations are undeniably undesired. One reason for variations in local concentration can be caused by pre-mixing materials with different particle sizes (e.g. pellets with powder) creating the risk of the component's segregation during or before the process. Therefore, when working with a pre-blend, it is of advantage to have the components in similar dimensions [17].

The amount of energy input into the compounding process should be as much as necessary, while at the same time being as little as possible. Especially due to the risk of possible degradation of the matrix or the API. The energy-input can be controlled by the process parameters (as mentioned above, e.g. screw speed and material-throughput) as well as by the screw geometry itself [17].

To melt a crystalline API, it is necessary to overcome its lattice energy. This is done by the shear-stress created from the extruder on the API-filled polymer melt [42]. In co-rotation twin-screw extruders, this process starts before a compression zone is reached. The advantage being, that the particles start to get molten before any agglomeration happens. Breaking up those agglomerates to melt the components would increase the necessary overall energy input. Due to the existing elongational deformation in twin-screw extruders, this process is further dampened [17].

3.3.1.3 Screw geometry

Usually, the screws of TSEs are composed of many individual screw elements (some examples shown in Figure 7) arranged on shafts, allowing to adapt and optimize an extruder for the intended process. Those elements can vary in function, shape, pitch, length, pitch direction, and the number of flights. Conveying elements are labeled by the ratio of "pitch / length". In the case of intermeshing-self-wiping elements, neighboring elements are symmetrical and have the same geometry [1]. Besides from the geometry, the self-wiping characteristic comes from small clearances between the screws themselves and the barrel [41]. For mixing purposes, the screw design can be considered one of the main influential factors when targeting high content uniformity [70].

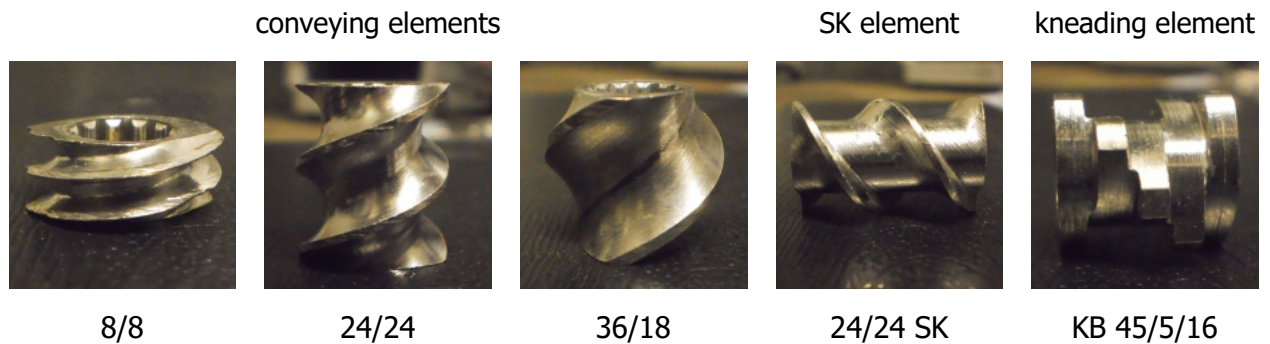


Figure 7: Different screw elements

3.3.1.3.1 Conveying elements

The prime task of conveying elements is the transportation of the polymer. This can be at the material-intake, or between different processing steps. Therefore, the polymer does not necessarily have to be molten. Mostly double-flighted screw elements are used in this section. Due to the geometry of the screw elements, the polymer is moving in the form of an "8" from one screw to the other. By changing the pitch, different conveying-speeds of the material can be achieved. The efficiency of the transport always depends on friction between product, screw and barrel [41].

3.3.1.3.2 SK elements

SK-elements (from "Schub-Kante") increase the free cross section in the barrel (Figure 7: 24/24 SK). This can improve the product transport especially in the intake zone. In combination with a higher pitch, it can also increase the open surface of the melt at degassing zones. The disadvantage of those elements with an undercut flight is, that the self-wiping character is lost [41].

3.3.1.3.3 Kneading elements

Kneading elements (Figure 7: KB 45/5/16) are usually built of several kneading discs, which have the same cross section as conveying elements. Therefore, they are also self-wiping. Differences between elements are the number of discs, their width, and the angle of the discs being stacked (in the case of KB 45/5/16 there are 5 discs with a 45° angle and a total length of 16 mm). The main purpose of kneading elements is the melting of the polymer and the dispersion of fillers. Depending on the stacking angle, the kneading discs can form a spiral-like element. This results in a certain conveying capacity. Elements with large stacking angles, however, increase the amount of axial mixing due to the gaps between the disc-tips. The disc width is responsible for the dispersive effect of the element due to the bigger amount of material that is sheared by it. The buildup of shear forces takes place primarily between the two screws, but also between the screws and the barrel [41]. Kneading elements can be categorized according to their forward-, backward-, or neutral-conveying characteristics.

3.3.1.3.4 Backward-pumping elements

Since a co-rotating TSE is an axially open system, pressure buildup can only happen at sections where the polymer flow is disturbed. This can be, for example, kneading blocks, the die, or backward pumping elements. One type of backward pumping element is an element with a negative pitch, intending to transport the polymer backwards. This system is fundamentally open but creates a strong enough obstacle for the polymer passing through, that pressure is built up. The melt-plug, resulting from that, can have a supporting effect on the mixing processes. It is also needed as a flow-restrictor at the beginning of a vacuum degassing [41].

3.3.1.3.5 Mixing elements

Mixing of polymers and fillers can be supported by special mixing elements. Contrary to kneading elements, they do not intend to apply too much mechanical stress on the melt, but rather support the incorporation by distributive mixing. This at times leads to a reduction of the self-wiping property. Among this last group are elements such as segment mixing elements. They are built similarly to normal conveying elements but have small gaps in the screw flanks that allow a certain backflow of the melt. Therefore, an operation in a filled zone, applying a certain backpressure, improves the mixing efficiency of the elements [41].

3.3.1.4 Residence time distribution

The residence time (RT) is the time a material (or particle) resides in the operation unit [45]. As in all continuous processes, the mean residence time for particles in the process does not show a precise peak, but is rather distributed over a period of time [41]. The mean residence time (τ) can be calculated as the fraction of the hold-up-Volume (V) and the volumetric flow rate (\dot{V}), or, constant densities given, mass (m) divided by mass-flow rate (\dot{m}) as shown in equation (2) [44].

$$\tau = \frac{V}{\dot{V}} = \frac{m}{\dot{m}} \quad (2)$$

The residence time distribution (RTD) of a process can be measured by a tracer response experiment, where a tracer is being introduced into the process. This introduction has to be done impulsively, to avoid compromising the measurement. Two parameters, time and the concentration of tracer leaving the process, are continuously measured from this moment on. This data can be graphed to show the resulting concentration profile $c(t)$ (see Figure 8). When normalized to the curves integral, this profile equals the residence time distribution $E(t)$ [22]. The residence time distribution therefor is a probability density function.

From this function, distinctive parameters can be obtained. Those are the mean residence time (τ), indicating the center of the distribution (average time an element spends in the process), and the times (t_x) until 5, 50, or 95 % of the tracer have left the process [45]. Together with the standard deviation, indicating the width of the distribution, the shape of the curve can be characterized. It is important to consider, that each deviation between the actual process and

the monitored process results in a falsification of the result. This includes a possible effect from the application of a tracer [22].

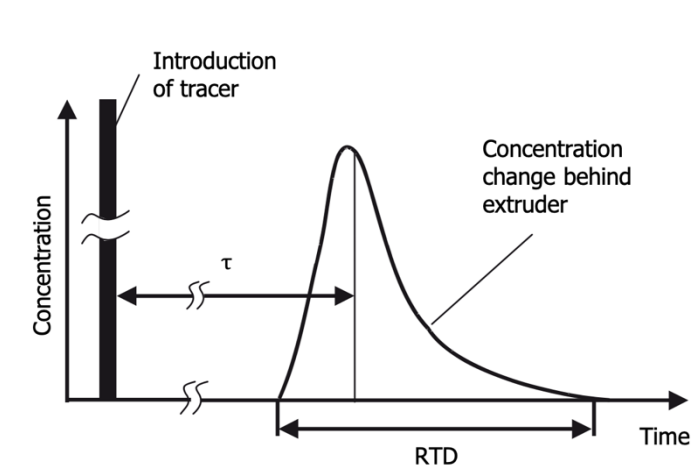


Figure 8: Residence time distribution (Figure adapted from [41])

Effects of the residence time distribution in an extrusion process are multifarious. The minimum RT is especially relevant for dispersive mixing characteristics of the process, whereas the maximum RT is important for the processing of heat sensitive material [41]. A short RTD can allow sharp batch transitions during a process, whereas long mean residence times and broad RTDs dampen disturbances in the process by their longitudinal distributive mixing [20, 44]. This helps to compensate fluctuations in e.g. the feed rate. For a homogeneous product, mixing in a cross section of the barrel, as well as axial mixing (correlated to the RTD) is necessary to compensate feeder fluctuations. Furthermore, also the self-cleaning ability can be resembled by the RTD. The shape of the RTD has a huge impact on the final product quality and the process itself. Thus, a significant amount of information about the process can be obtained from it [41].

The RTD in an HME-process can be influenced by several factors. The width of the RTD is strongly depending on the flow profile of the melt in the screw channel. Relevant factors are, besides from the processed material, the throughput (in fully filled screw sections), the screws pitch (if the screw is partially filled), the reverse flow, screw speed, and the screw configuration. Whereas simple conveying screws have a very narrow RTD, kneading, mixing, and especially backward conveying elements strongly widen the RTD. In general, the minimum residence time drastically depends on the investigated process, but usually lies somewhere between 5 to 15 s [41].

3.3.1.5 Hot melt extrusion in pharmaceutical technology

The reason hot melt extrusion is increasingly applied in the production of pharmaceuticals is based on several benefits [15, 25, 50, 73]:

- It is a continuous process with good reproducibility.
- It combines several processes such as melting, mixing and forming of extrudates.
- It permits the simple combination of several processing units into one continuous line.
- Due to the adaptability of the screw as well as the entire process, multiple materials can be processed, yet securing optimal mixing of the components, which leads to a uniform dispersion and distribution.
- The combination of several processing steps into one continuous process leads to economic advantages.

Additionally, some possibilities arise especially for the development and production of many pharmaceutical formulations:

- The solubility and therefore bioavailability of poorly water-soluble drugs can be enhanced.
- It is a solvent free process preventing the need of solvent extraction.
- Content uniformity can be greatly improved and guaranteed.
- Fine particles can be dispersed uniformly in the process.
- No direct influence on chemical processes such as pH-instability or hydrolysis from solvents is given.

The most relevant shortfalls of the HME process are [17, 25, 50, 75]:

- It is a thermal process, making polymer and drug stability a crucial aspect.
- Mechanical stress is applied onto the components.
- Not all polymers are extrudable without problems.
- Radical and oxidative degradation of components are possible.

3.3.2 Feeder

The importance of a constant and accurate feed rate becomes evident, if one is aiming for a continuous manufacturing process. In the case of inaccurate feeding, the fluctuating material-stream is passed on from one unit to the other, resulting in instabilities in the entire process. For that reason, the feeding equipment is of considerable importance, especially when working in the pharmaceutical industry, where API-doses have to be met precisely [20, 70].

There are two main methods of feeding: gravimetric / loss-in-weight (LIW) and volumetric feeders. The disadvantage of volumetric feeding lies in the actual mass flow, which can vary strongly due to variation in bulk density and / or fluctuations in screw loading [25]. In order

to guarantee a constant and accurate feed rate (as is required in pharmaceutical technology) loss-in-weight feeders are commonly used. One advantage being, that the mass-throughput of the extruder can be precisely controlled via starve-feeding. This leads to an independency of a twin-screw extruders mass throughput from process parameters like screw speed [17, 25]. When multiple materials are processed simultaneously, there is the possibility to either pre-mix them and feed them into the extruder via a single feeder, or there is the possibility of using several feeders that simultaneously feed the separate materials into the extruder [25].

In the feeder, the material is usually stored in a hopper. Their design must be aligned with the requirements of the material used. Considerations must be given to the size of the hopper, the surface-properties, the geometry and finally the cleanability. The hopper size is especially important in case of continuous extrusions. In order to avoid unnecessary process-interruptions from refilling and recalibrating the feeders, many feeders can switch to volumetric feeding during the refill process. To avoid bridging and to assure a constant supply of material to the feeder-screw (therefor guaranteeing a uniform filling of it), agitators like stirrers are frequently used [25].

From the hopper, the material has to be transferred into the process unit (e.g. the extruder). One method is by utilizing twin- or single screws. Twin-screw feeders are applied when free flowing materials are transferred that still need an additional regulation of the flow-behavior, or if additional forces have to be applied on a cohesive material. Due to the possible self-cleaning abilities, also adhesive materials can be conveyed [9]. Depending on the material and feeder used, different screw geometries can be applied, to adapt the feeder to the materials properties and optimize the feeder output. Established screw geometries are concave (coarse or fine) and auger (coarse or fine). The different screw geometries lead to different feeding-capacities. Mainly depending on the free volume between the barrel and the screw(s), as well as the size of the void created by the screws. One big advantage of the twin-screw construction is the screws self-cleaning-effect. This is especially helpful, when agglomerating and "surface-adhering" materials have to be fed, which would otherwise reduce the throughput, the consistency, and thereby the overall performance of the process [20].

Consequently, the optimal feeder configuration is primarily influenced by the desired feed rate and the material properties [9]. So far, the selection of the proper setup is mainly based on "trial and error", demanding for experience or the will to invest effort until a suitable arrangement is found [21]. Reasons for this are, that, despite their relatively simple appearing principle, their performance is strongly depending on the characteristics of the fed materials. Influential factors can be the variability of material characteristics, flow properties, particle size, and bulk density [9]. When working with several feeders in one process, their alignment and coordination is another significant impact factor on the content uniformity [70].

3.3.2.1 Loss-in-weight feeder

In the pharmaceutical industry, twin-screw loss-in-weight feeders are commonly used, due to their accurate, versatile, and closed system [35]. Loss-in-weight feeders are composed of a scale, a feeding element in combination with a motor, a controller, and a hopper where the material is stored (see Figure 9) [25].

The scale allows the controller to constantly meter the current mass of material in the hopper. Therefore, a rate of material loss can be calculated in relation to a specific motor speed. This allows to calculate a correlation between different motor-speeds and material-loss rates during the calibration of the feeder. With these values, a feed rate can be calculated and the rotational speed of the motor driving the feeding element can be adjusted to the desired value depending on the current mass-loss rate [17, 25]. After calibration, gravimetric feeders can also feed in volumetric mode. This feature is usually used during the refilling phases of the feeder. In that phase, the current mass loss-and-gain rate are strongly biased by the effects of the material refill, which handicaps any meaningful measurements. Such effects can range from a change in bulk density to the need of removing lids etc. from the feeder. As a consequence, small fluctuations and instabilities in the feed rate cannot be ruled out during this interval [9].

Typical feeding elements for powders are single or twin-screws with case-specific screw designs, but also vibrational feeders or belt-feeders are used [25]. As already mentioned, the screw geometry plays an especially important role.

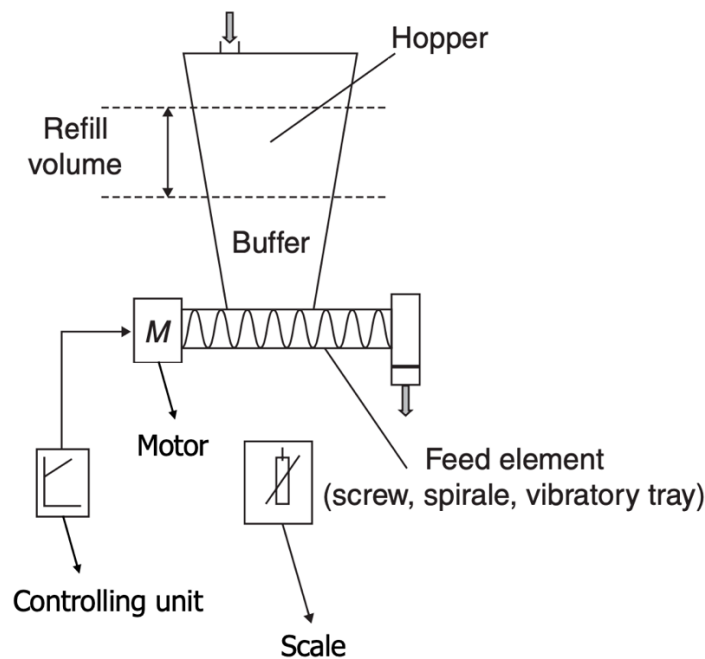


Figure 9: Operating principle of LIW-feeder (Figure adapted from [17])

3.3.2.2 Microfeeder

Due to the high potency of many APIs, doses in the range of milli- or even micrograms are necessary in certain formulations. Resulting therefrom, it is often required to introduce just small quantities of these substances into a manufacturing process. This triggers several problems in the process design and realization if one aims to secure blend-homogeneity and content-uniformity during the process without affecting the pharmaceutical activity and

chemical stability of the components [48]. Measures to overcome that shortfall often turn out to be complicated or ineffective. Common methods for the production of low and ultra-low dose mixtures are dry blending, granulation techniques, compression techniques, and spray drying techniques. Also, HME can be considered a suitable technique, usually utilizing dry pre-blends of matrix and API in the desired low dose concentration [52].

Due to these additional techniques required to establish a blend with the desired concentrations, the implementation of a truly streamlined continuous process is often not feasible. To avoid extra production-steps to overcome the above-mentioned challenges small scale (powder) feeding is very much desirable. Unfortunately, the smaller the feed rate of powders, the more hindrances must be overcome. To be mentioned are for example poor powder-flowability or the buildup of agglomerates and chunks. Even with the gravimetric control of loss in weight feeders a sufficiently stable mass flow may turn out impossible, when effects like this kick in. The result then is a flow rate that conforms to the desired rate according to a time-integrated rate but contains oscillations in the feed rate that can be between medium to high frequencies. Often this is enough to ultimately result in a non-constant concentration of different ingredients leading to a process with an irregular output [48].

Different methods of microfeeding have been tested or utilized so far: Powder microfeeding via a capillary that is excited by an ultrasonic source. With this setup feed rates down to 0,036 g/h of ultrafine dry copper powder could be reached [77]. Another approach tested was to utilize a gravimetric powder micro dosing system consisting of a vibratory sieve that is mounted on a chute. With this construction continuous feed rates of 3 g/h of pharmaceutical powders with specific properties (e.g. diameter) have been achieved [7].

The microfeeder used for this thesis is a slightly adapted version of the feeder described by Besenhard et al. [5]. Its specific aspects will be further explained in chapter "4.2.2 Microfeeder". It is a volumetric feeding system based on volumetric displacement. The feedstock is stored in a vertical cylinder from where it is pushed out by a piston and is transported into the process via a scraper (see Figure 10). The piston-speed is the main influential factor of the feed rate. Utilizing a leadscrew in combination with a transmission, very constant and slow piston-speeds can be achieved. In combination with the cylinder diameter as another factor to influence the feed rate constant feed rates of fine powders down to 1 g/h can be achieved. It has to be noted, that this result is only valid for a feedstock without a density gradient. Apart from the filling-process, also the movement of the piston, which pushes the powder, has a significant impact on the density-gradient. To achieve a powder stock without a change in density during the feeding process, pre-conditioning via tapping, vibrations and compression is of importance. The specific measurements necessary depend on the powder properties. Another way to solve this problem is via an adaptable piston-speed controlled via real-time, loss-in-weight control or by means of pre-recorded process data. Once a proper pre-conditioning routine is established, recurring calibrations of the process will not be necessary any longer. In order to adapt this system in a continuous-process suitable fashion, several exchangeable pistons can be used during the running process to avoid process interruption by the filling process. Ultimately, it can be concluded, that solutions for most of the microfeeder problems are present, even though most of the time it is possible to use the process in its basic form due to the accurate feed rates that can be achieved with proper pre-conditioning of suitable powders [5].

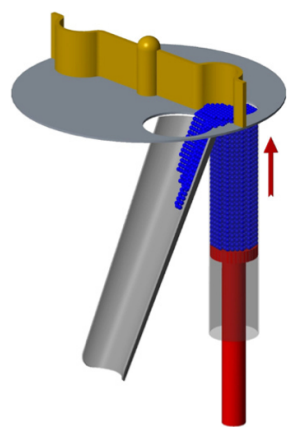


Figure 10: Operating principle of the microfeeders volumetric feeding system [5]

3.3.3 Process analytical technology

3.3.3.1 Data acquisition

Until lately pharmaceuticals have mostly been produced batchwise with quality control for each individual batch. This allows for a good assessment of the product quality. Yet, discontinuous production-processes are slowly becoming outdated, as process analysis and process control are being introduced in pharmaceutical production techniques.

In 2004, a "Guidance for Industry" was published by the "U.S. Department of Health and Human Services'" "Food and Drug Administration" (FDA), who established an official risk assessment for process analytical technology in pharmaceutical technology [66]. According to this "guidance" the FDA defines PAT as a system for "designing, analyzing, and controlling manufacturing through timely measurements (i.e. during processing) of critical quality and performance attributes of raw and in-process materials and processes, with the goal of ensuring final product quality" [66]. Hereby, the term "analytical" is primarily referring to the analytical methods which can be integrated into a process for the above-mentioned reasons [66]. Nevertheless, PAT can be used to help understand a process with its various components and influential parameters. This is especially important to consider, as the proper understanding of a process is imperative to ensure its correct design [58]. The main goal of PAT is to ensure the quality of the product by monitoring the process and guaranteeing the process robustness (which in turn leads to the desired product attributes), instead of testing samples of the final drug product [66]. Continuous manufacturing techniques consequently demand continuous in- / or online control [58]. In the pharmaceutical production technique this leads to a change in production-processes, i.e. to a "Quality by Design" (QbD) approach [58]. The most important advantages of PAT for the production of pharmaceuticals are a reduction of process cycle time, a reduction of rejected waste, an increased automation, and thereby, fewer human errors [66].

Three types of process-analyzation can be distinguished: off-line tools (a sample is removed from the process stream; often also described as "at-line" tools), on-line tools (a sample is

taken from the process and returned after analyzation), and invasive-, respectively non-invasive in-line tools (samples are not removed from stream) [66].

With a properly installed PAT, several aspects of a process can be monitored. Among them are the control of the raw material purity, as well as the detection of other contaminations and the possibility to monitor the process setting including the impact of process instabilities [66]. Examples of process parameters from the extruder that can be monitored are the screw speed, the torque, and the temperature profile. Complimentary methods such as rheological in- or on-line techniques (e.g. in-line viscosimeter) can be applied. For these values to be useful in PAT it is important to know and understand the correlation of the individual parameters [58].

Further in- and on-line methods, which can be implemented in an extrusion process, are optical systems such as: near-infrared (NIR), mid-infrared (MIR), Raman and ultraviolet/visible light (UV/Vis) spectroscopy. But also, non-optical methods such as terahertz and ultrasonic techniques can be applied [34]. With such techniques many aspects of the process such as the crystallinity in solid amorphous dispersions can be measured via a PAT system. However, the feasibility of such tools strongly depends on the applied API and matrix [34].

These tools generate a large amount of data that needs analysis for a useful interpretation and usage. Analysis can be accomplished with multivariate data analysis as well as "artificial intelligence" and mathematical statistics. For the UV-Vis analysis we are using the multivariate data analysis and for the other experiments statistics is applied.

3.3.3.2 Multivariate data analysis

The output of PATs are often huge amounts of data. They can contain a lot of important or helpful information, yet, pure data is not necessarily useful. First, relevant information has to be extracted from recorded data.

One discipline which addresses this issue is chemometrics. Chemometrics focuses on extracting relevant information from recorded process data with statistical and mathematical methods. The objective is to extract the relevant information and find correlations in the data. One method is principal component analysis (PCA). Hereby the goal is to describe the variation in the data with as few variables as possible. Correlations of the underlying data structure are analyzed and shown, leading to the use of principal properties (dimensionless) instead of normal variables [24].

"Soft independent modelling of class analogy" (SIMCA) is one method that can be used to classify data. A restriction which has to be met for this classification is, that all variables have to express similarity and are therefore approximatable into a PC model with only a few components. From this model, the classification of the individual objects is carried out with specific tolerance intervals as criteria [63]. Through this method one can drastically reduce the design, while still showing the relevant information. Multivariate data analysis is a useful tool to simplify complex data sets and make them easier to understand by visualizing correlations and dependencies in the process. It can be implemented as a comprehending tool for process monitoring, control, fault detection, and diagnosis. This is done by creating high dimensional data from samples, which are described by many variables. This data can include information about the raw materials, process conditions and steps, and the state of the final product [56].

3.3.4 UV/Vis spectroscopy

This method of analyzing substances works with the wavelength of ultraviolet light and visible light (200 - 400 nm and 400 - 800 nm). It is based on interactions between the sample and the light. Molecules can absorb photons and thereby acquire their energy, leading to the alteration of the energetic state of an electron. Therefore, the absorbed energy of the light corresponds to a specific electron transition. What wavelengths are absorbed and how the energy gained affects the state of electrons in the molecule, strongly depends on its structure and composition. This correlation gives indications of a molecule's structure from the wavelength it absorbs and from the intensity of absorption [76].

In the case of organic molecules, four electron transitions with different energies based on the atomic bonds are possible: $\sigma \rightarrow \sigma^* > n \rightarrow \sigma^* > \pi \rightarrow \pi^*$ (conjugated) $> n \rightarrow \pi^*$. The $\pi \rightarrow \pi^*$ and $n \rightarrow \pi^*$ transitions (also called chromophores) lead to clear peaks that are caused among others by double bonds such as C=C, C=O, N=N but also aromatic rings. When attached to such chromophores, unshared electron-pairs of functional groups such as -OR, -SH, -OH can affect these chromophores by increasing their absorptivity and shifting their wavelength. They are called auxochromes. Therefore, it is also possible to assign certain functional groups to one or more typical electron-transition. In inorganic materials, two more transitions can occur: the d-d transition and the charge-transfer transition [76].

The UV/Vis-spectrometer consists of five significant components [76]:

- Light source: Consisting of a tungsten-halogen lamp (for the visible light) combined with a deuterium lamp (for the UV light), giving the spectrometer the entire range from ultraviolet to visible light (200 - 800 nm).
- Monochromator: The monochromator (often gratings) is necessary to reduce the broad spectrum of the lamps to a narrow monochromatic band of wavelengths.
- Sample compartment: Usually the sample for UV-analysis is prepared in solution. Hereby great care has to be taken to avoid any influences of the solvent, such as reaction with the sample or an influencing of the absorption spectra, on the result. The dissolved sample is usually put in a quartz-cell due to the materials transparency at the desired wavelengths. But also solid samples such as films can be analyzed as long as they are sufficient transparent. Often the sample as well as the reference sample can be measured simultaneously via a double-beam setup.
- Detector: It typically consists of a photomultiplier or a photodiode which converts light into electrical signals, the detector measures how much light of a specific wavelength passes from the source through the sample.
- Data collection and processing system: Finally, a processing system is needed to transform the acquired results in an evaluable spectrum.

It has to be pointed out, that only the main components and their most basic principle are described here. Many different versions of spectrometers exist on the market, which employ several distinctive alterations and methods.

UV/Vis spectroscopy is most commonly applied to determine the concentration of a substance in a solution (quantitative analysis). It is important to know, that a molecule can absorb, transmit, scatter or reflect an energetic wave, when being hit by it. Of those effects only the first two are of relevance for absorption-spectroscopy. The basis for this is the Beer-Lambert's law (equation (3)), which sets a relation between the absorption of a substance (A), its molar attenuation coefficient (k), the length of the optical path (l), and the substances concentration (c).

$$A = klc \quad (3)$$

To acquire the absorbance of a substance, the measured transmittance has to be converted. The transmission (T) is the ratio between the initial radiation (I_0) and the transmitted amount of radiation (I) through the sample (see equation (4)).

$$T = \frac{I}{I_0} \quad (4)$$

The correlation between the absorbance (A) and the transmittance (T) is then given in equation (5).

$$A = \log_{10} \left(\frac{I_0}{I} \right) = \log_{10} \left(\frac{1}{T} \right) = klc \quad (5)$$

This relation reveals why an absorption spectrum is preferred for the purpose of a quantitative analysis. Due to the linear correlation between absorbance and concentration, calculation is considerably simplified. For a qualitative analysis however, the transmission spectrum is usually preferred due to the more distinct display of weak peaks in the spectrum based on the correlation between absorbance and transmittance [54, 64].

In a hot melt extrusion process UV/Vis-Spectroscopy can be applied to monitor color change during the process e.g. for indication of changes in the molecular mass [72]. It can also be used for "live" in-line monitoring of color changes triggered by pigments. This offers the possibility of measuring the residence time distribution [26]. Yet, so far, UV/Vis-in-line-spectroscopy devices for HME processes are not standard in manufacturing of pharmaceuticals and are therefore rarely used for quantification of APIs in amorphous solutions [73].

3.3.5 HPLC

Nowadays, high pressure liquid chromatography (HPLC) is one of the most important tools for the drug discovery, development, and production. It is based on chromatographic separation. A characteristic of this method is the presence of a mobile phase. It contains the dispersed analyte and transports it in a stationary phase with a high surface area. The interactions between the stationary phase and the analyte are the relevant mechanism for operation. Those interactions are responsible for a separation of the individual molecule sizes by creating a retention time gradient. Due to the consequences of those surface interactions, molecules with a low interaction energy need a great surface area for a sufficient molecule separation.

A variety of different chromatographic systems exists. They can be differentiated by the mobile phase which is being used, dividing the systems in liquid- and gas chromatography. These systems can further be divided depending on the stationary phase. For liquid chromatography, the systems may be liquid-liquid or liquid-solid chromatography.

In liquid-solid systems, the stationary phase was initially the polar phase whereas the liquid phase was the non-polar one. Nowadays the polarity of the phases is mostly reversed leading to a non-polar stationary phase, often composed of hydrophobic surface-modified silica, and a polar mobile phase. Therefore, this more modern technology is termed reverse phase (RP-HPLC), whereas the older system with a non-polar mobile phase is called normal phase (NP-HPLC). Rather than polar forces, dispersive forces (hydrophobic or van der Waals interactions) are employed in RP-HPLC. This gives the newer system the advantage, that liquids such as water can be used for sample preparation. Furthermore, due to the weakness of the employed forces, small alterations (in an absolute perspective) in the interactions have a big overall impact (in a relative perspective) on the separation of the components. Hence, also closely related components with only little variances in surface interaction can be reliably distinguished [39].

A typical HPLC is built of five components [39]:

- Solvent reservoirs: here the necessary amount of mobile phase (solvent) for the analysis is stored. Especial attention has to be appointed to the purity of the substances.
- Pump: the mobile phase and the sample solution (consisting of a solvent and the analyt) are forced through the system with a specific pressure.
- Injector: the injector inserts the sample solution into the mobile phase's stream for analysis in the column. Modern systems are equipped with autosamplers, which allow the automated analysis of an entire sequence without the need of constant human interference or supervision.
- Column: here the actual analytical process takes place. In the column the sample solution's components are separated by the differences in the surface interactions of the molecules. A variety of columns exists, which allows to select from the setup that suits best for a different analysts and separation procedures. The columns themselves are mostly made out of stainless steel and are filled with the stationary phase that consists of one to five micrometers small particles of a rigid porous material. Generally, a bigger

surface area leads to a longer retention time, which in turn leads to a better separation, producing a better result.

- Detector: the registration of all components, which pass through the column, is done by the detector. Different detectors can be applied, which register specific material properties. The most usual type is a UV-detector. With it a continuous measurement of the absorbance at a specific wavelength from the sample is possible. If more wavelengths have to be registered simultaneously, a diode array may be applied. During measurement the presence and composition of the analyte leaving the column changes with time, leading to a change in spectrum depending on the process-time scale.
- Data acquisition and control system: the entire process as well as the recording of the data is done by a computer-based system. Among the controlled steps are the eluent composition, the temperature, and the injection of sample solution. The processed and stored data includes the spectra as well as information about the system performance such as mobile-phase composition, temperature, and backpressure.

3.4 Research topic

The area of research described herein is about the production of an amorphous drug loaded systems composed of a polymer matrix loaded with API amounts between 0,1 and 0,5 % mass fraction.

Such low concentrations in API may be of interest if formulations for high potency APIs are being created. In the context of this research, API amounts may reach as little as milli- or even micrograms. In the case of pharmaceuticals, the aspect of main concern is that of homogeneity and content uniformity, which both lead to challenges in the production process [48].

3.4.1 Current production technique and its limitations

Currently, such low concentrations are reached by creating a pre-blend of the desired composition of API- and matrix material [18, 52]. That approach has two fundamental drawbacks, which are caused by very different effects. The one is, that this production technique is a discontinuous process, the second-one being, that it is accompanied by risks of quality defects.

The quality-issue in the process is triggered by the formation of a pre-blend. Local concentration variations impair the final product and therefore have to be avoided. Such variations can be the result from insufficient mixing of the pre-mix. However, also phase segregation after the mixing is completed, may be an issue. An aspect that is especially critical for this matter is a possible difference in particle sizes (e.g. pellets with powder), but also other powder properties may have a disadvantageous effect [17].

In general, a discontinuous process calls for more monitoring, versus a continuous one. A discontinuous process can, for example, be a batch process, where one batch of material is being transferred one-by-one, through each processing step. As a consequence, the product quality has to be analyzed and tested for each batch, creating further, additional effort.

3.4.2 New micro-feeding solution and its challenges

The above-mentioned problems triggered by a batch-wise production technique can be avoided in a continuous production process.

In this thesis, a continuous hot-melt extrusion process for the production of polymer extrudates with a low API concentration of down to 0,1 $\omega/\omega\%$ is developed and investigated. With this type of continuous process, the issue around segregation does not arise, as the materials are being mixed and directly processed into their final, solid form. For polymers, a suitable technique for creating an amorphous system of API and matrix is hot melt extrusion [14, 36, 66].

Especially twin-screw extruders are a suitable technology to guarantee proper mixing of the components during the process [35]. Such extruders can be operated in a continuous fashion, only relying on the peripheral process-components preceding and following the extruder. Until now, a problem of a continuous extrusion process for low dose drug formulations has been the feeding of the API into the process. Insufficient feeder capabilities, caused by the feeding technology, prevented the direct feeding of low API amounts, directly into the HME-compounding process [25]. For the approach of this thesis, a novel microfeeder was applied, which supplies reliable feed rates of down to one gram per hour directly into the HME-compounding process [5].

To guarantee the product quality, an inline process analytical tool in the form of an UV/Vis spectrometer was integrated in the process. Through this approach, a constant monitoring of the processes stability and quality was supposed to be monitored with a chemometric model, with the aim of avoiding the need for constant off-line quality testing. The feasibility and stability of the process was then reviewed by checking the extrudates via HPLC analysis.

4 Materials and methods

4.1 Materials

4.1.1 API

The drug chosen for the experiments described in this thesis was Fenofibrate (Haihang Industry Co., CN). It is a crystalline white solid with low water solubility. Fenofibrate (FFB) can be extruded in an amorphous solution via hot melt extrusion but shows fast recrystallization due to its low glass transition temperature [16]. All relevant temperatures for processing are shown in Table 2.

Table 2: Characteristic temperatures of Fenofibrate

Temperature	(°C)	Literature
glass transition temperature (T_g)	-21,3	[68]
melting temperature (T_m)	78	[32]
	80-81	[42]
thermal degradation temperature ($T_{deg.}$)	180	[32, 42]

Fenofibrate was chosen due to several aspects, the most important one being that it is safe. For Fenofibrate, no immediate safety hazards have been found, which are relevant when carefully working with this substance. Also cost-drivers, such as the use of a high-potency-laboratory, could be avoided.

A third aspect was the compatibility of Fenofibrate with the chosen matrix polymer Kollidon VA64 (BASF, DE). Especially the solubility of Fenofibrate in the matrix at processing temperatures was of particular relevance. The coherence of relevant temperatures, as presented above, in relation to the same temperatures of the matrix-polymer are of vital importance. This allows to establish an HME process where both components are mixed, without degradation of material, leading to a desired process output.

For the in-line monitoring of the process via an UV/Vis spectroscopy-based PAT, the measurability of the FFB concentration in the polymer matrix was essential. The necessary absorption wavelength for the applied spectrometer had to be in the range of 280 nm, with an absorption of 0,5 to 1 AU (absorbance unit), due to the spectrometer's optimization for this area. With an absorption maximum at 305 nm and with an absorbance of approximately 0,75 AU, Fenofibrate has such properties, as was reported by El-Gindy et al. [19].

Additional aspects for the selection of Fenofibrate was the, even though only limited, prior experience with Fenofibrate in combination with the chosen polymer as well as the availability of the substance.

4.1.2 Matrix

The chosen matrix-polymer for this thesis was Kollidon[®] VA64 (BASF, DE). Kollidon VA64 (also known as "Copovidone", "Copolyvidone", "VP/VAc copolymer 60/40") is an amphiphilic copolymer of 1-vinyl-2-pyrrolidone and vinyl acetate in the mass ratio of 6 to 4 (therefor the name VA64). The amphiphilic character comes from the vinylpyrrolidones hydrophilic- and the vinyl acetates lipophilic character (chemical structure shown in Figure 11). Therefore, it dissolves in all hydrophilic solvents. The average molecular mass M_w (determined via measuring of the light scattered by a solution) is between 45.000 and 70.000 and the number-average of the molecular weight M_n (determined by membrane filtration) lies between 15.000 and 20.000. All relevant temperatures for processing are shown in Table 3 [2, 3, 13, 42].

Table 3: Characteristic temperatures of Kollidon VA64

Temperature	(°C)	Literature
glass transition temperature (T_g)	101	[42]
thermal degradation temperature ($T_{deg.}$)	230	[42]
recommended extrusion temperature range	155 - 200	[42]

Kollidon VA64 is a white to slightly yellowish, free flowing powder. Two grades are available, one being Kollidon VA64 with a volume average diameter between 50 – 65 μm , the other one being Kollidon VA64 Fine with a volume average diameter 10 - 20 μm as determined by laser diffraction [13]. For all experiments, the coarser grade was used. Stored as a pure product, the polymer is very stable at room temperature, for over three years [12]. The material moisture measured with a HC103 Moisture Analyzer (Mettler Toledo, USA) at a drying temperature of 105 °C was 2,68 %MC (moisture content) and could only be reduced to 1,68 %MC after drying in an oven at 70 °C for 4 days. Therefore, and since the processability appeared not to be influenced by this moisture difference, the polymer was not dried before extrusion.

Applications in the pharmaceutical industry include: as binder in tablets, as a retarding agent, as film former in coatings, and as a granulating agent. It is approved for application in drug formulations in USA, Europe, Japan, and holds the GRAS Status in USA [12, 42].

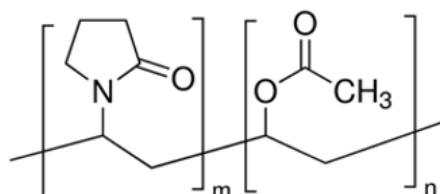


Figure 11: Chemical structure of Kollidon VA64 [61]

4.2 Equipment and methods

4.2.1 UV/Vis spectroscopy for API feasibility test

To ensure the applicability of Fenofibrate for the UV/Vis in-line detection in a Kollidon VA64 matrix, preceding experiments were conducted. The tests were done with a Shimadzu UV/Vis spectrophotometer UV 2700 (Shimadzu, JP) with double beam optics. The spectra were recorded in the range from 650 to 185 nm with the sample being measured by one beam and a standard consisting of water and acetonitrile (1 : 1) by the second beam simultaneously.

4.2.2 Microfeeder

The microfeeder used for the experiments in this thesis is a slightly adapted version of the one described in [5]. Its main components are a syringe pump, holding a cylindrical powder reservoir with a piston and a scraper composed out of razor blade mounted on a laboratory stirrer. Additional components are a plate, on which the material is transferred to a vertical pipe to guide the falling powder. The original microfeeder has been reconstructed to archive a reduction in size. This became necessary, to enable a proper mounting of the microfeeder on the extruder. The redesigned microfeeder is shown in Figure 12.

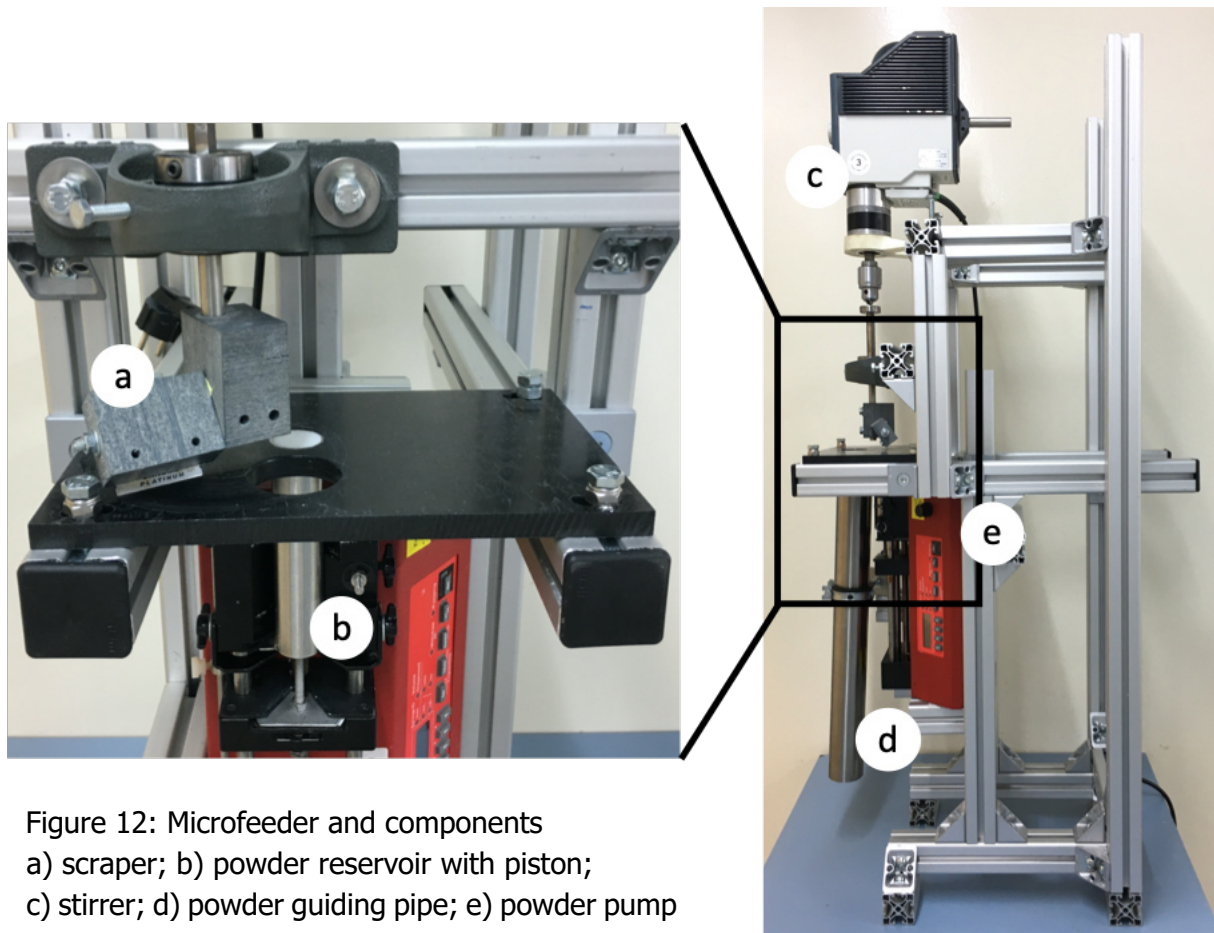


Figure 12: Microfeeder and components
a) scraper; b) powder reservoir with piston;
c) stirrer; d) powder guiding pipe; e) powder pump

The powder to be fed is introduced manually into the reservoir, from the top. During the feeding process, the piston is moved upwards with a defined speed by the powder-pump. The powder exiting the reservoir is periodically moved to the powder-guiding pipe by the scraper. Through the powder guiding pipe the material falls into any subsequent process or device [5].

The feed rate is defined by the reduction of powder filled volume in the powder reservoir. Therefore, it can be affected by two parameters. One is the diameter of the cylinder which can be reduced to reduce the powder-volume for each increment the piston is moved upwards. A change of reservoir parameter is, however, not easily facilitated and is impossible to perform during an ongoing process. The other parameter is the speed of the piston moving upwards. It is controlled by the syringe-pump and can easily be adapted during the process.

An important aspect of a constant powder feed rate is the density gradient in the powder reservoir. It develops through the piston pushing the powder from below as well as from the friction between powder and reservoir-wall. The formation of those powder-wall-interactions can be reduced by an increase in the reservoir's diameter. Material-related parameters influencing the powder density gradient are the initial bulk density as well as powder properties (such as particle size) and interparticle forces (such as cohesiveness). Those factors play an important role for the compaction of the material. Additionally, higher piston speeds negatively affect the compression of the powder in the reservoir [5].

To avoid an influence of the feed rate by a density gradient, a uniform powder density in the reservoir is paramount. To achieve this, a preconditioning of the powder in the cylinder can be performed by tapping and knocking on the cylinder and the surrounding components to compact the powder and reach a higher density (considered as the "tapped density" as opposed to the "bulk density" before the preconditioning). Powders with a very low bulk density can additionally be pre-compacted to promote a uniform powder density, further diminishing the effect of powder properties on the feeding process [5]. Nevertheless, a certain amount of "start-up time" for the feeding process is usually necessary until a constant feed rate is reached. Once the feed rate reaches a steady state, very constant feed rates can be achieved. Since the powder density after pre-conditioning and the feed rate slope during the start-up of the process are very reproducible and constant, they can be pre-determined and applied for all subsequent processes with the same material. Thus, an overall high reproducibility and robustness of the feeding process can be adjudged to the described feeding principle [5].

The continuity of the feeding process is adjusted by the rotational speed of the stirrer holding the scraper. For all experiments the stirrers rotational speed was set to 10 rpm, resulting in a material transfer to the pipe every 6 seconds. This interval is, by far, small enough to be obliterated by the extrusion process' residence time. The scraper-blade itself is mounted in the stirrer with a specific angle, for optimal powder transfer, without any material loss.

The powder guiding pipe had a slightly bigger diameter than the hole in the plate, through which the material is transferred. This is important to assure a free falling of the powder. Some powders may exhibit a strong tendency to adhere to any surface they are touching. This would strongly influence the feeding consistency.

The experimental procedure for the micro-feeding process was as following:

1. The piston is moved to the bottom position and powder is filled into the powder reservoir.
2. The powder is then preconditioned to reduce the density gradient via tapping and knocking on the reservoir and the plate.
3. The free volume in the reservoir created by sagging of the powder is filled up with powder and preconditioned by tapping again.
4. The piston speed calculated for the desired feed rate is entered into the syringe pump and the scraper is activated, initializing the start-up phase of the process. Until the feed rate is constant (timing known from prerecorded trials – see "5.2.1 Microfeeder"), the material is being collected and not transferred into any process.
5. Once the feed rate has reached a stable level, the material can be introduced into the desired process.
6. After the feeding process, the residual material is emptied by moving the piston to the upper position, and the entire unit is cleaned.

The implementation of the microfeeder in the extrusion process is discussed in section "5.3.3 Compounding experiments with microfeeder".

4.2.3 Pre-blend preparation

Five different pre-blends were made with FFB concentrations between 0,1 and 0,5 $\omega/\omega\%$ in 0,1 $\omega/\omega\%$ steps. For the fabrication, one-liter containers were used. They were filled with 500 g of Kollidon VA64 Fine in three layers. Fenofibrate was distributed between the layers, in order to promote proper distribution of the API in the polymer as well as to prevent wall-adhesion of the API to the container. Mixing was done in a turbula mixer Model TF2, (WAB, CH) for 10 min, at around 30 rpm. An additional blending experiment has been conducted with the same parameters, but with a color pigment instead of Fenofibrate to briefly verify the proper mixing of the two components, visually.

4.2.4 Twin-screw extruder

The extruder used for this thesis was the twin-screw extruder ZSK18 ML (Coperion, DE). It is specially developed for the application in pharmaceutical laboratories, for small scale extrusion processes. It has two 18 mm screws as well as integrated heating (electrical) and cooling (water) in all 10 zones, a vacuum pump, a control display, and a power unit. Zone 1 had an opening for the intake of material, while zones 4 and 8 had ventilation openings. The die-head was mounted on an adapter plate (not heated) and could be heated via two heating cartridges. For all experiments, the die had a diameter of 2,8 mm. The extruder with the used LIW-feeder on top is shown in Figure 13.

After each individual process, the cleaning of the extruder was performed by extruding pure Kollidon VA64 for around 10 minutes followed by the emptying of the barrel by keeping the

extruder running until no further material was being extruded. Before each new extrusion process, pure Kollidon VA64 was extruded for a minimum of 10 min, in order to remove the leftover polymer in the extruder from the last experiment. Unless stated differently, a ventilation unit was operating close to the intake zone (see Figure 13), during all experiments. This led to the subtraction (and therefor loss) of significant amounts of polymer from the process as will be discussed in "5.3.3 Compounding experiments with microfeeder". However, this could not have been avoided due to the sever formation of polymer dust during the feeding process.



Figure 13: Coperion ZSK 18 ML with LIW feeder

4.2.4.1 Screw profiles

Three different screw profiles have been used during the entire range of experiments. Screw-profile 1 (see Figure 14) was a screw configuration, with an overall length of 720 mm which was derived from an existing screw profile. The screw has several mixing blocks. Block one (in zone 3) is for melting the polymer while the other blocks are supposed to promote filler distribution. A backward pumping element in zone 7 causes a fully filled section acting as a seal before the atmospheric degassing unit. The barrel features an intake for the polymer supplied by the K-Tron feeder in zone 1, an opening for the introduction of API by the microfeeder is shown in zone 4, zone 8 had an opening for the atmospheric degassing, and zone 10 featured a pressure sensor. Zone 11 depicts the adapter plate for mounting the UV/Vis probes. Since the probe-tips enter the barrel, the screw ended in zone 10. The die is not shown.

4 Materials and methods

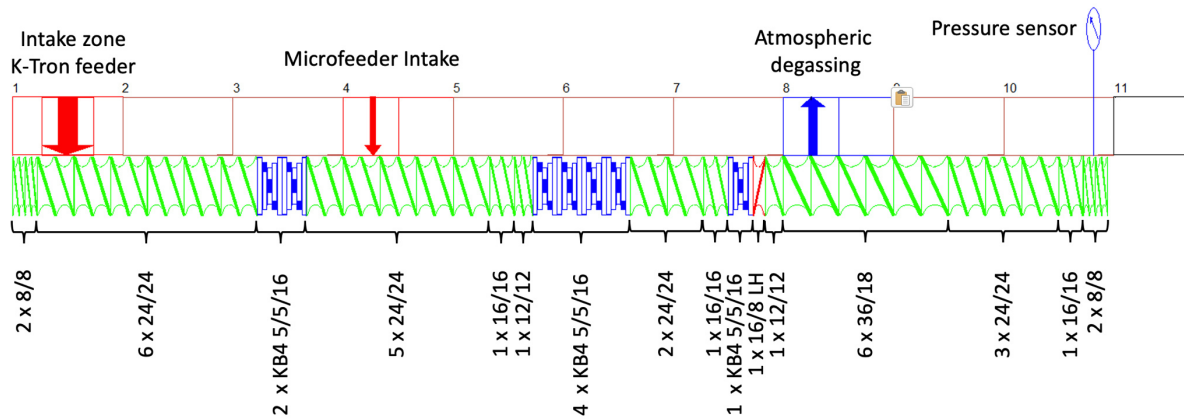


Figure 14: Screw-profile 1

Due to the large number of kneading elements and the “aggressiveness” of screw-profile 1 as a result, an alteration with fewer kneading elements was designed. Additional adaptations were the introduction of SK-elements in the intake zone to promote the powder intake and the exchange of the third kneading block with an SME-element to improve mixing. Screw-profile 2 is shown in Figure 15.

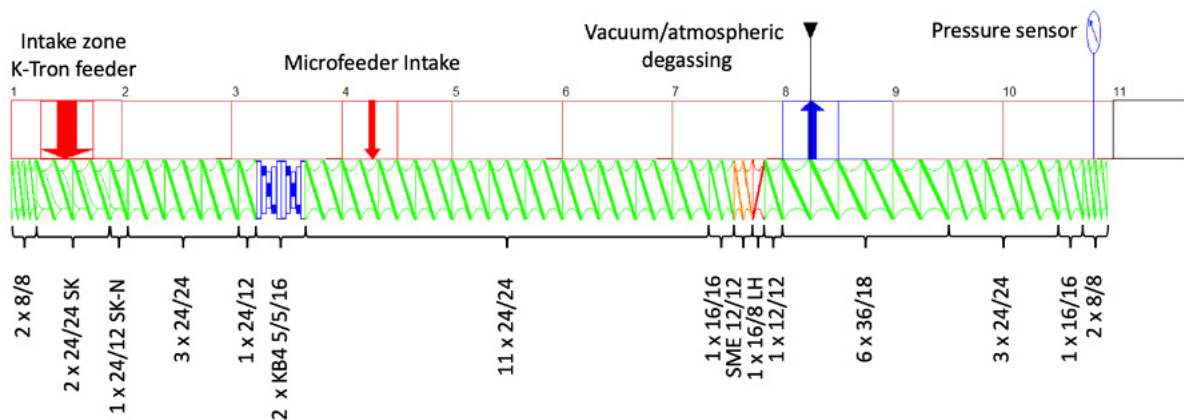


Figure 15: Screw-profile 2

Screw-profile 3 (Figure 16) is basically identical to Screw-profile 2, with the only difference being that the length of the screw is now 764 mm instead of 720 mm through the addition of two conveying elements in zone 10. Due to the screw now reaching until the end of the adapter plate (zone 11), the use of UV/Vis probes is not feasible anymore. Additionally, the microfeeder intake in zone 4 was shifted to zone 1, where both feeders are introducing the material into the extrusion process.

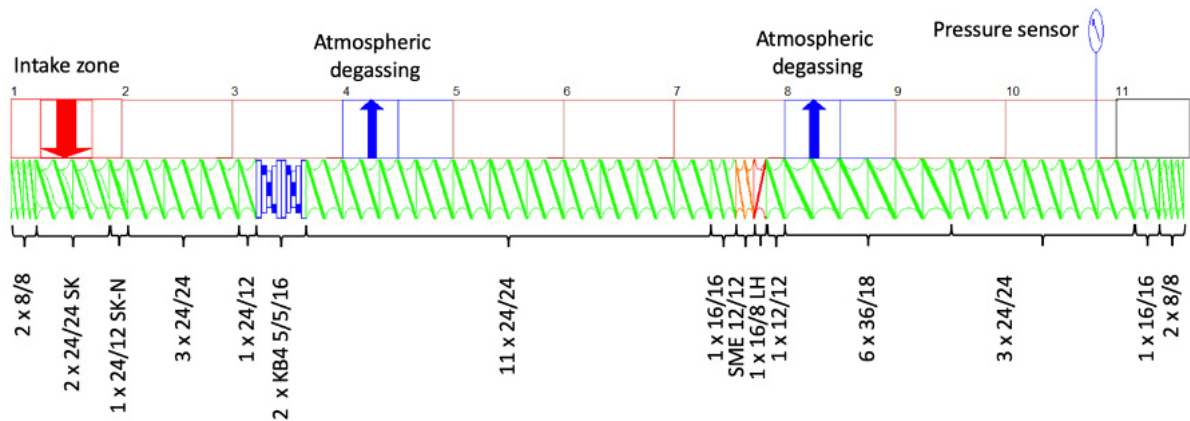


Figure 16: Screw profile 3

4.2.4.2 Temperature profile

The temperature profile for the extrusion processes is shown in Table 4. It shows a gradually rising temperature profile until barrel-zone 5, from where on the temperature is kept constant at 165 °C until the die is reached. Zone 11 did not provide a possibility for temperature control or measurement. With this temperature profile, the lower limit of the Kollidon VA64's suggested extrusion temperature range (between 155 °C and 200 °C; $T_{deg.} = 230$ °C) is chosen, however it is close to the thermal degradation temperature of Fenofibrate ($T_{deg.} = 180$ °C).

Table 4: Set temperature profile for extrusion processes

Barrel-zone	1	2	3	4	5	6	7	8	9	10	11	Die
Temperature (°C)	25	55	95	135	165	165	165	165	165	165	-	170

4.2.4.3 LIW-feeder

A Coperion K-TRON KT 20 (Coperion K-Tron, CH) LIW-feeder was used to feed the Kollidon VA64 polymer. It has a combined error of +/- 0,03 % and can feed up to 20 kg/h. It was equipped with long dual concave screws and an agitator in the hopper. The feeder was mounted on top of the extruder as can be seen in Figure 13, so that the feeder outlet was directly above the extruder intake opening. Before each operation, the feeder was calibrated, and the scale was tared. For all experiments the feed rate was set to 1,0000 kg/h. After each experiment the hopper was emptied, and residual polymer powder was removed with a vacuum cleaner.

4.2.5 UV/Vis spectroscopy as PAT

For the in-line monitoring of the FFB concentration in the extrusion process, an "InSpectro X Inline process UV/Vis spectro- and colourimeter" (ColVisTec, DE) in combination with a transmission polymer melt probe set "TPMP" (ColVisTec, DE) was used. The probes are connected with the spectrometer via glass-fibers. A Xenon flash lamp with up to 2 Hz is integrated together with a spectrometer that can measure in the range from 220 to 820 nm in 1 nm steps. The software applied was "EquiColour RTM4.0" (Equitech, USA) on a "Windows 7" operation system.

All experiments were conducted in transmission mode with the probes inserted into the melt channel as shown in Figure 17. In this setup, the gap between the probe-tips was 5 mm. A slight deviation from a perfect alignment was caused by the adapter-plates bores. A spectrum was recorded every 6 seconds (1/6 Hz).

Before each measurement, the probes were optimized to achieve a signal intensity between 50.000 and 60.000 counts for the highest peak. This is done by altering the amount of flashes for recording the spectra during the process. For all measurements, the amount of flashes was set to 7 with an exposure time of 14 ms. Additionally, the TPMP - calibration procedure was undertaken after each restart of the spectrometer. The 100 % transmission target was achieved by calibration against the polymer melt, the black standard by detaching the probe from the spectrometer. After each experiment, the probes were removed from the adapter plate and thoroughly cleaned while the polymer was still in a molten state.

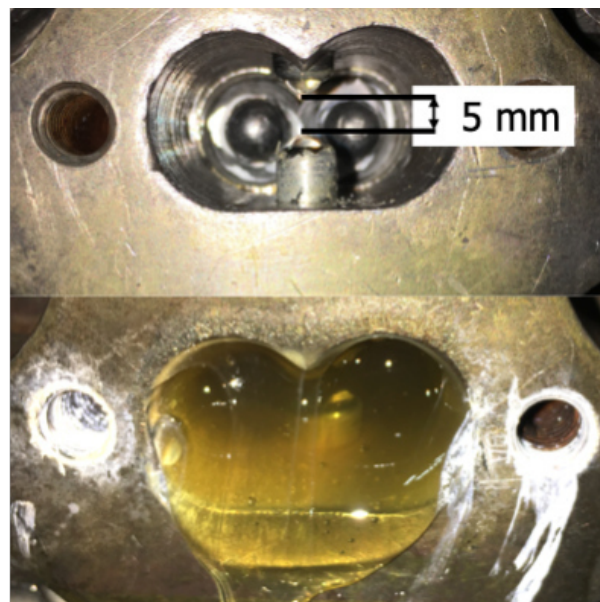


Figure 17: UV-Vis probes inserted into the extruder barrel (above: empty barrel before extrusion; below: filled barrel after extrusion)

4.2.6 Residence time distribution

The residence time distribution of the extrusion process was determined by image processing as described in [45]. A videoclip was recorded to monitor the color change in the extrudate directly after it left the die. The camera used was a Fujifilm FinePix HS25EXR (Fujifilm, Japan). The recording was started at the same moment as a spatula-tip of red food coloring "F 1088-B Rot" (Wurth Essenzenfabrik GmbH, Austria) as tracer was introduced into the extruder-barrel at the intake during the running process. From this video clip, an area of interest from the extrudate strand was chosen for analysis of the color change (example visualized as a black rectangle in Figure 18). The pixels from this region were then processed in MatLab (Mathworks, USA). Here they were transformed from RGB (red-green-blue color space) to "CIE L*a*b" space. This is done in order to eliminate the effect of changes in color brightness. In L*a*b space the "L" coordinate represents the lightness, "a" the color change from green to red, and "b" the color change from blue to yellow [71]. The "b"-values change from the pixels selected were analyzed over the duration of the video-clip to create a curve depicting the change of color-concentration over time. This curve is representative for the residence time distribution of the extrusion process. The entire procedure has been published by Kruisz et al. in [44] and [45].

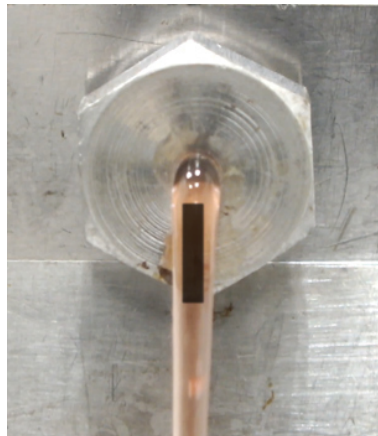


Figure 18: Marked area of interest from extrudate strand

4.2.7 HPLC analysis

A reverse phase high performance liquid chromatography (RP-HPLC) system "1260 Infinity II LC System" (Agilent Technologies, USA) together with the software Empower® (Waters Corporation, USA) was used to determine the amount of Fenofibrate in the extrudate-samples. The 150 mm long stationary phase consisted of Luna C18 (Phenomenex Inc., USA) with an internal diameter of 4.6 mm and a particle size of 3 μm . The column temperature was set to 40 °C. The total run time per injection was 10 min in which the flow was kept constant at 1 mL/min with an injection volume of 5 μL . The wavelength for detection was 286 nm.

The mobile phase consisted of 80 % HPLC-grade acetonitrile (Sigma-Aldrich, USA) and 20 % purified water with a pH set to 2,5 by orthophosphoric acid. The purge and washing solution consisted of 50 % purified water and acetonitrile filtered through a 0,22 μm Nylon membrane.

5 Experiments

5.1 Feasibility test of API

Two stock solutions were made for the experiment: 1) 5 mg of FFB were dissolved in 25 ml of a solvent consisting of water and acetonitrile (ACN) in the ratio of 1 : 1 to acquire a solution of 0,2 g/l FFB ; 2) 5 mg of Kollidon VA64 were dissolved in 25 ml of a solvent consisting of water and ACN in the ratio of 1 : 1 to acquire a solution of 0,2 g/l Kollidon VA64.

In both cases the component was first dissolved in the pure ACN, in which they exhibited good solubility characteristics, and then water was added to ensure complete dissolution. From these two solutions, three samples were made: a) 1,5 ml of solution 1 were mixed with 1,5 ml of water and ACN (1 : 1) creating a solution with 0,1 g/l FFB ; b) 1,5 ml of solution 2 were mixed with 1,5 ml of water and ACN (1 : 1) creating a solution with 0,1 g/l Kollidon VA64; c) equal amounts of solution 1 and 2 were mixed together to acquire a solution of 0,1 g/l FFB and Kollidon VA64 respectively.

5.2 Capability analysis of equipment

5.2.1 Microfeeder

To guarantee the proper feeding behavior of the microfeeder, a feed rate analysis has been conducted prior to the extrusion experiments. For this, a high precision scale "XPE 204" (Mettler Toledo, CH) connected to a data-logging software was placed under the outlet of the microfeeder. With this scale, the amount of fed material was recorded in 1 sec intervals. From the recorded data, the feed rate was determined by calculating the difference between two successive mass recordings of the scale. For the experiments the feeding process has been recorded from the very beginning (from the moment the piston started moving up) onwards to illustrate and analyze the start-up time of the process.

For the first experiments of each feed rate FR (g/h), the piston speed v_p (mm/min) for the desired feed rate has then been calculated. The calculation is shown in (6) with $V_{res.}$ (mm³) being the volume of the reservoir, $m_{res.}$ (g) the mass of the preconditioned powder in the reservoir, and A_{pist} (mm²) being the cross-section area of the reservoir.

$$v_{pist.} = \frac{FR * V_{res.}}{m_{res.} * A_{pist.} * 60} \quad (6)$$

The feed rates resulting from the calculated piston speeds were reviewed after the feeding experiments and proved to be very close to the actually desired feed rates.

Experiments were conducted for the highest (5 g/h) and lowest (1 g/h) nominal feed rate required over a time of 120 min each. Both experiments were performed in triplicate. Additionally, a "step-trial" has been conducted to prove the possibility of changing the feed rate during the process and additionally examine the feeder behavior at feed rates of 2, 3, and

4 g/h. Therefore, the feeding process was started with a *FR* of 1 g/h. After a stable process was reached (timing known from previous experiments with *FR* 1 g/h) the feed rate was consecutively increased after 30 min of feeding at a constant rate.

5.2.2 HPLC analysis

A system-suitability-analysis was performed to validate the analytical procedure. Sample stability and system suitability have been proven by repetitive measurement of the Fenofibrate content from a single solution containing 0,05 mg/ml FFB five times. Second standard recovery was tested by measuring a sample with the same concentration. Systems linearity was tested with five samples containing the FFB amount of 0,01; 0,02; 0,05; 0,10; and 0,20 mg/ml.

5.3 Compounding experiments

5.3.1 Preceding extrusion trials

First extrusion experiments were conducted with screw configuration one (see 4.2.4.1) and pure Kollidon VA64 polymer. During these processes the polymer was guided from the LIW-feeder into the extruder by a funnel placed directly onto the intake zone from the extruder barrel. The setup of the entire process is shown in Figure 19 with the LIW-feeder mounted on the extruder and the UV/Vis probes inserted into the adapter plate.

The main objective was to examine the process parameters and the processes stability as well as the extrudability of the polymer. Another important aspect was to assess the signals from the implemented UV/Vis spectrometer. Unfortunately, the melt did not let enough light pass through between the UV/Vis probes, so that barely a signal was obtained. From these signals, no applicable spectrum could be created. Figure 20 shows the difference between the maximum possible spectrum taken in an empty extruder barrel (green spectrum in left graph), and the one taken during the extrusion process (green spectrum in right graph). The red spectrum in both graphs represents the maximally possible signal intensity.

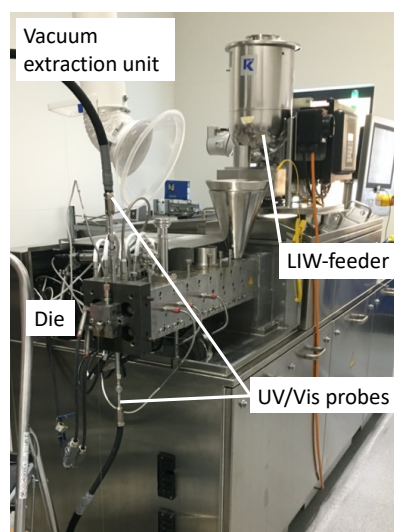


Figure 19: Primary process setup

5 Experiments

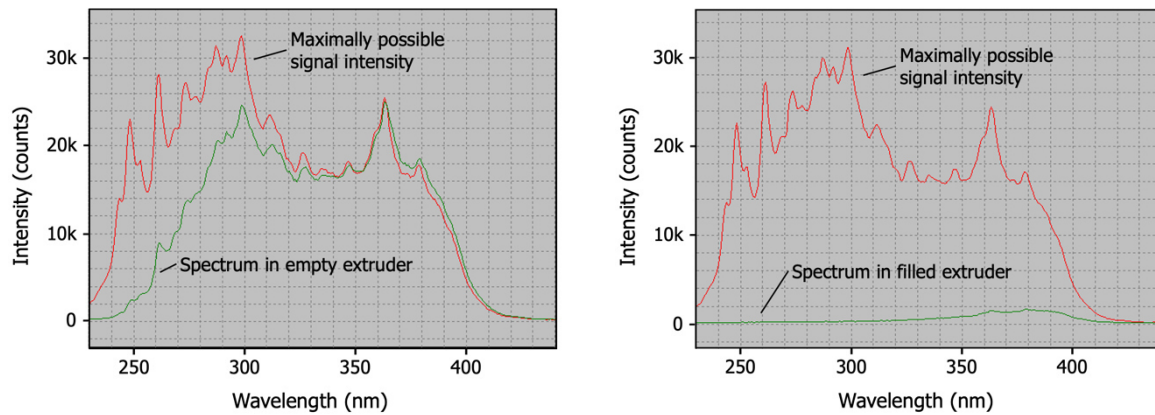


Figure 20: Spectra with UV-Vis spectrometer maximal possible signal (left) and signal through polymer melt (right)

Due to the bad results, the melt between the probes was inspected at the end of the extrusion process (see also 4.2.5 on page 38). It was concluded that the slightly opaque color, most probably, caused by material degradation in the countless kneading zones, and bubbles of gas trapped in the melt, were the main factors for the weak UV/Vis signal.

Therefore, a redesign of the screw to reduce material degradation from mechanical stress applied by the kneading zones was carried out (see "screw profile 2" in "4.2.4.1 Screw profiles"). Additionally, a vacuum degassing unit was implemented to reduce the amount of gas bubbles in the melt. With these alterations, the quality of the UV/Vis spectrum during an extrusion trial could be improved (see Figure 21). Even though the improvement was not as significant as it was hoped, it was assumed to be sufficient for further experiments.

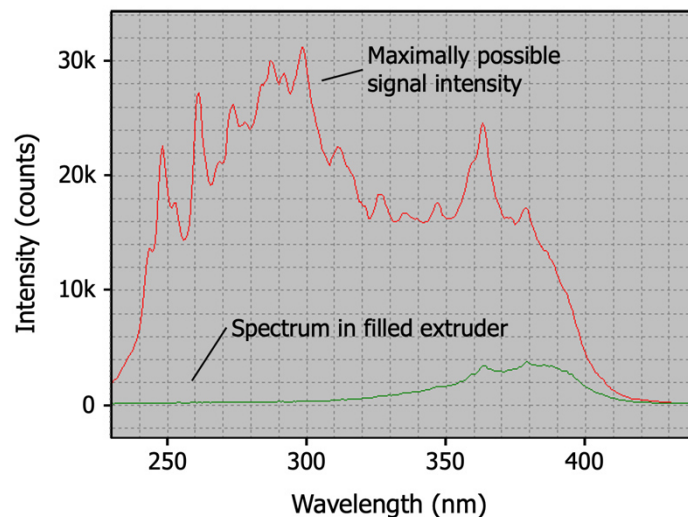


Figure 21: Improved UV/Vis spectrum

5.3.2 Pre-blend experiment with PAT

The extrusion experiments with the pre-blends were performed with the above-mentioned setup. For each of the six concentrations (0 to 0,5 $\omega/\omega\%$ in 0,1 $\omega/\omega\%$ steps) 500 g of material were put into the LIW-feeders hopper. A transition between the blends was performed after all of the current blend's material was emptied from the LIW-feeder. Then, the hopper was vacuumed to remove as much residual material as possible and refilled with the next batch. To avoid influences from cross contamination, the blends were extruded in ascending order according to the FFB concentration. During the material change, the extruder was operating with constant settings, to additionally empty the extruder barrel as much as possible from residual polymer. Since, even with those measures taken, a sharp batch-transition was still not possible, the sampling of the extrudates was adapted to compensate the batch transition time. During the 30 min of extrusion for each batch, a sample was taken at minute 15, 20, and 25 for further analyzation.

5.3.2.1 In-line UV/Vis spectroscopy

During the entire pre-blend extrusion process, the UV/Vis spectrometer recorded a spectrum every 6 seconds. The variations in the recorded spectra were to be used as basis for the creation of a chemometric model with "SIMCA" software. In this chemometric model, differences in the spectra over time would be used as indicators for a change of the melt's composition. All recorded spectra from this experiment are shown in Figure 22. The alterations considered as relevant are boxed in. Here, even though only slightly, several groups of curves with different gradient for the marked wavelength range can be seen. These groups indicate that spectra have stayed similar several times over a certain duration. This would suit the batchwise consecutive rise in FFB concentration during the extrusion experiment. Nevertheless, the signals were too weak, making in-line monitoring of API concentration impossible (see 6.3.1.1 "In-line UV/Vis spectroscopy").

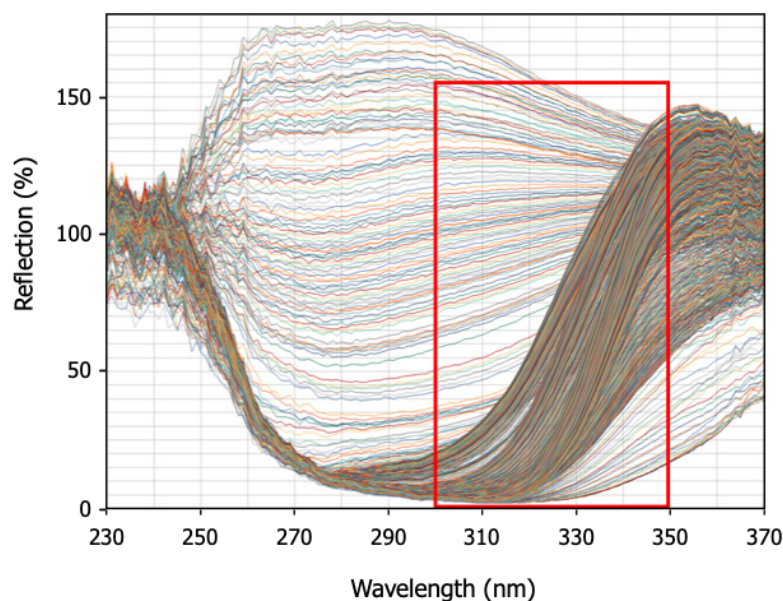


Figure 22: Spectra recorded during the extrusion process

5.3.2.2 Pre-blend sample analysis with HPLC

For the analysis, a standard stock solution with 1000 ppm was prepared by weighing 25 mg of FFB in a 25 ml flask and adding around 20 ml of mobile phase. The flask was then shaken carefully until the Fenofibrate was dissolved, before it was filled up with mobile phase. From this standard stock solution, a standard solution (100 ppm) was prepared by transferring 1 ml of standard stock solution into a 10 ml flask and filling it up with mobile phase. After shaking it manually, the standard solution was transferred into a HPLC-vial through a 0,22 µm Nylon filter. This procedure had to be done in duplicate.

For sample solutions, approximately 500 mg of extrudate were weighed in and the precise weight was noted (five significant digits). Then, around 20 ml of mobile phase were added and the extrudate was dissolved in an ultrasonic bath at room temperature for 30 min. The solutions were cooled to room temperature afterwards, if so necessary as a result of the bath warming up. Then the flask was filled up with mobile phase and homogenized by shaking manually. This sample solution was then filtered into a HPLC-vial through a 0,22 µm Nylon filter, flushing the first milliliters.

5.3.3 Compounding experiments with microfeeder

Since the implementation of the UV/Vis was not successful, the spectrometers probes were replaced with blind plugs. To avoid the formation of an unnecessary long melt-plug in front of the die, the screws length was increased leading to screw design three (see 4.2.4.1 "Screw profiles"). Furthermore, due to lack of space and no further need for it, the vacuum degassing unit was omitted.

5.3.3.1 Implementation of the microfeeder

In the first approach to implement the microfeeder into the extrusion process, the API was introduced into the extruder barrel in zone 4. Here the polymer has passed the kneading blocks and is therefore in a completely molten state. The loss of screw-length was not expected to reduce the mixing capacity of the extruder sufficiently to have a credible disadvantage, especially due to the mixing blocks effect.

The microfeeder was placed on a platform next to the extruder barrel. Due to the feeder's high construction, a guiding system for the falling powder had to be applied. From the feeder, the powder falls through a stainless-steel tube with an inner diameter of 4,5 cm. This diameter was necessary due to the microfeeder's scraper-construction (see also Figure 12 on page 32). To guide the API into the extruder barrel, a glass funnel was placed directly onto the barrel. The cardboard walls around the scraper were set up to protect the process from the ventilation unit. The setup is shown in Figure 23.

Experiments quickly showed that the humidity from the polymer exiting the barrel and that from the surrounding air, together with the barrels (and therefore also the funnels) temperature lead to an adhering of the API on the funnel's walls.

An attempt to solve this problem, was to separate any powder-guiding parts from the extruder barrel. Therefore, the glass funnel was moved directly under the hole in the microfeeder's

plate and a smaller pipe was used that slightly reached into the barrel to directly guide the API into the melt. This setup was supported by a tripod and all parts were grounded to reduce influence from static charges. The setup is shown in Figure 24.



Figure 23: First microfeeder setup

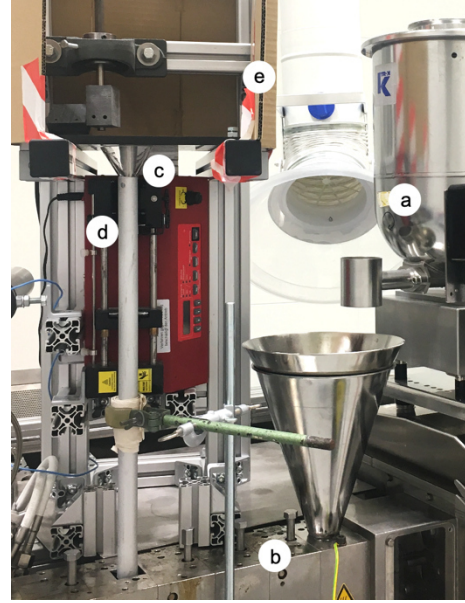


Figure 24: Second microfeeder setup

a) LIW-feeder; b) extruder barrel; c) glass funnel; d) pipe; e) cardboard wall

As before, the temperature and especially the humidity rising from the extruder barrel lead to powder adhering to the pipes and funnels surfaces. Drying of the polymer before the extrusion process did not bring any perceptible improvements.

Therefore, a completely different approach was chosen. Instead of introducing the API into the process separately from the polymer in zone 4, API was introduced in the extruder intake in zone 1. The main benefit expected from this change was the lower temperature in this zone 1 of 25 °C. The concept is demonstrated in Figure 25. A major challenge created by this rearrangement of the feeder was the lack of space and the proper guiding of powder into the extruder's intake.

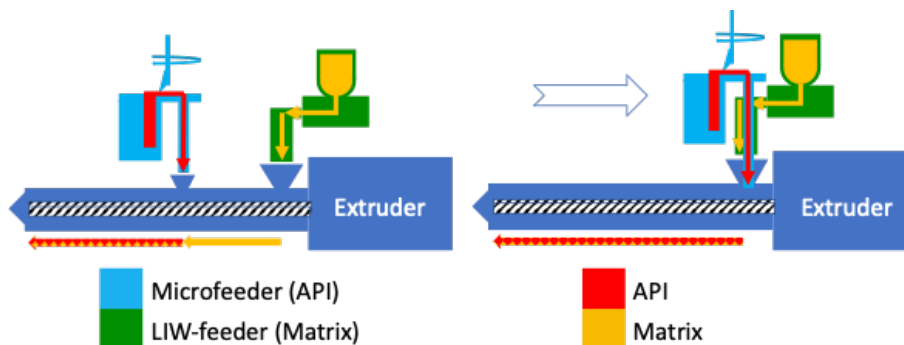


Figure 25: Microfeeder implementation concepts

After several attempts with different funnel-constructions, a funnel with an optimized geometry was designed for the polymer's guidance. An extension of the LIW-feeders outlet guided the polymer powder into this funnel. Both were made of a thin transparent Teflon® foil, having the advantage of reducing wall friction and additionally providing good visibility into the polymer feeding process. The API was collected by a funnel under the microfeeder's plate and passed through a thin polished stainless-steel tube with an inner diameter of 1 cm directly onto the extruder screws. The entire construction was supported by a stand. The challenge here was, that the API's tube had to pass through the LIW-feeders outlet without touching it. This would have biased the feeding performance of the LIW-feeder. The entire construction is shown in Figure 26. To ensure that the API guiding construction works properly, pilot tests have been conducted to monitor the behavior of the API in the new funnel and the relatively thin pipe. In those tests, without an operating extruder, barely any material adhered to the surfaces.

Additional pilot tests have been performed with a colored API being fed by the microfeeder into the extrusion process to investigate any displacement of API during the process. Once again, no undesired behavior could be observed.

Therefore, this setup was used for all of the following experiments. The only shortfall of this construction was, that the ventilation unit is situated close to the extruder's intake zone. It was necessary to reduce the dust pollution from the polymer powder falling into the funnel. However, this led to the extraction of significant amounts of polymer powder from the process. All in all, its effect on the extrusion throughput had to be taken into account and compensated in the evaluation of the process.

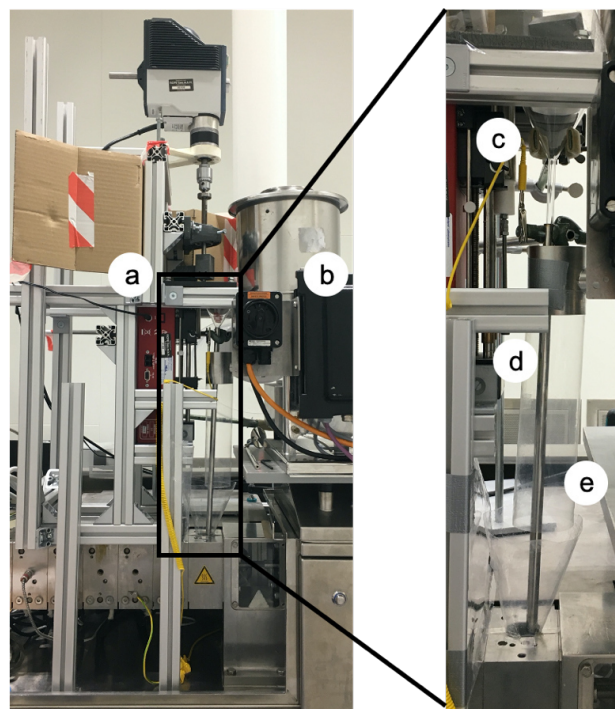


Figure 26: Final microfeeder setup
a) microfeeder; b) LIW-feeder; c) glass funnel;
d) API guiding pipe; e) powder guiding construction;

5.3.3.2 Description of procedure

Two different types of experiments have been conducted. One being a compounding process with a constant API concentration in the extrudate, the other one a compounding process with a stepwise increase in API concentration during the process.

5.3.3.2.1 Experiments with constant API concentration

The aim of this type of experiment was to produce an extrudate with a constant API loading for the duration of one hour. It was performed for concentrations of 0,5 $\omega/\omega\%$, 0,2 $\omega/\omega\%$, and 0,1 $\omega/\omega\%$. In the first experiment with 0,5 $\omega/\omega\%$ FFB, three separate runs were made to analyze the reproducibility of the process. For the other two concentrations three consecutive runs were made to analyze the repeatability of the process. A schematic depiction of the process is shown in Figure 27.

First the microfeeder was filled and started with the desired feed rate. The API was collected in a tray instead of being introduced into the extruder during the start-up interval (min. 40 min for all experiments) in order to guarantee a constant feed rate. During this time, the extrusion process was started, and the LIW-feeder was calibrated with a set feed rate of 1 kg/h. Then, pure Kollidon VA64 was extruded for 30 minutes to guarantee that all the material from the previous run was removed from the extruder and that no traces of API were present. After these 30 min, the tray for collecting the API during the microfeeders start-up phase was removed so that the API was introduced into the process. The duration of this compounding process then lasted 60 minutes, after which the API from the feeder was collected in a tray again for 30 min. This procedure was done three times, consecutively. For the first experiments with 0,5 $\omega/\omega\%$, the process was stopped following the 30 min of pure Kollidon extrusion after the 1 h compounding process, and the entire equipment was cleaned. Then the next run was performed.

For these experiments, samples were taken in 5-minute intervals after the first 15 minutes of extrusion process, until the end of the entire process. To do so, the extrudate was collected for 20 seconds and stored in separate bags to avoid cross-contamination. After the 20 second interval, the extrudate was collected for 4:40 minutes and the mass of this segment was weighed. This was done to deduce the actual mass throughput of the extruder affected by the ventilation unit's influence.

To avoid buildup of polymer powder and API on the funnels over time, they were tapped every time, after a sample was taken, to secure regular intervals and to avoid fluctuations in the results from this. Additionally, any beginning build-up of polymer in the intake zone was removed as soon as possible with a wooden stick to avoid bridging and therefore an interruption of the process. This, however, was only necessary during the experiments with 0,1 $\omega/\omega\%$ and 0,2 $\omega/\omega\%$, but not for the shorter experiments with 0,5 $\omega/\omega\%$.

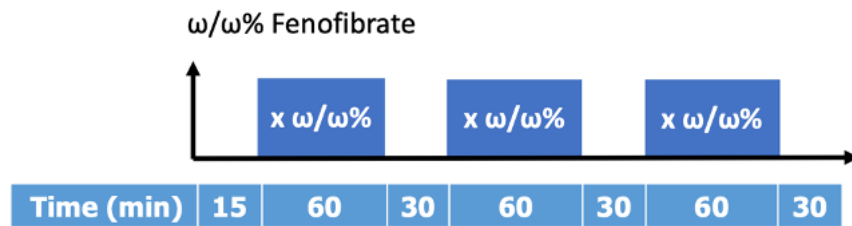


Figure 27: Visualization of experiments with constant API concentration

5.3.3.2.2 Step trial

The approach of this experiment was very similar to the ones with constant API concentration. However, here the concentration of API in the compounding process was increased from 0 to 0,5 $\omega/\omega\%$ of API by 0,1 $\omega/\omega\%$ steps as shown in Figure 28. This increase was done without interruption of the process after 40 minutes of processing with one concentration by simply increasing the microfeeders lead-screw speed. The start-up procedure was basically identical to the one described above with the microfeeder running for 40 minutes prior to being introduced into the process to achieve a constant feed rate.

To increase the resolution of the results and to improve the analysis' result of the concentration changes in the extrudate after change in API-feeding, the sampling interval was reduced to 2:30 min. The sample was taken for 30 seconds, followed by 2 minutes of collecting the extrudate for the mass throughput analysis. Samples were taken from 10 minutes before the switching the microfeeder into the process until 30 minutes after the microfeeder was removed from the process. Again, after each sample the funnels were tapped to avoid buildup of powder. Also bridging was avoided by regular removal of any polymer formations in the intake zone.

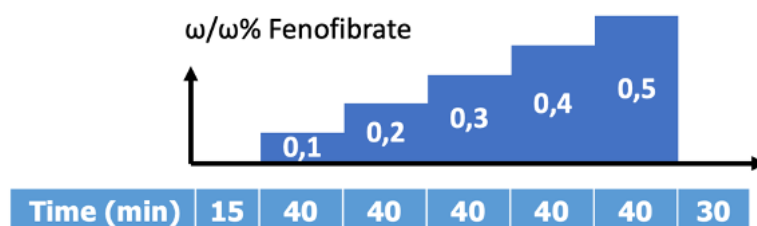


Figure 28: Visualization of step trial

5.3.3.3 Verification with HPLC

The samples collected during the compounding processes were analyzed identically to the ones from the pre-blend experiments.

6 Results and discussion

6.1 Feasibility test of API

The relevant wavelength-range from the resulting UV/Vis spectra of Fenofibrate and Kollidon VA64 are shown below in Figure 29, which illustrates the maximum absorption of Fenofibrate at about 0,55 AU and slightly below 290 nm. This also proves that Kollidon VA64 has no measurable effect on the UV/Vis absorbance spectrum of Fenofibrate in the relevant range between 250 and 350 nm.

Therefore, the results indicate, that an in-line monitoring of the FFB concentration with UV/Vis spectroscopy should be plausible. An aspect not taken into account yet is a possible biasing of the results by measuring both components in a melt instead of in solution.

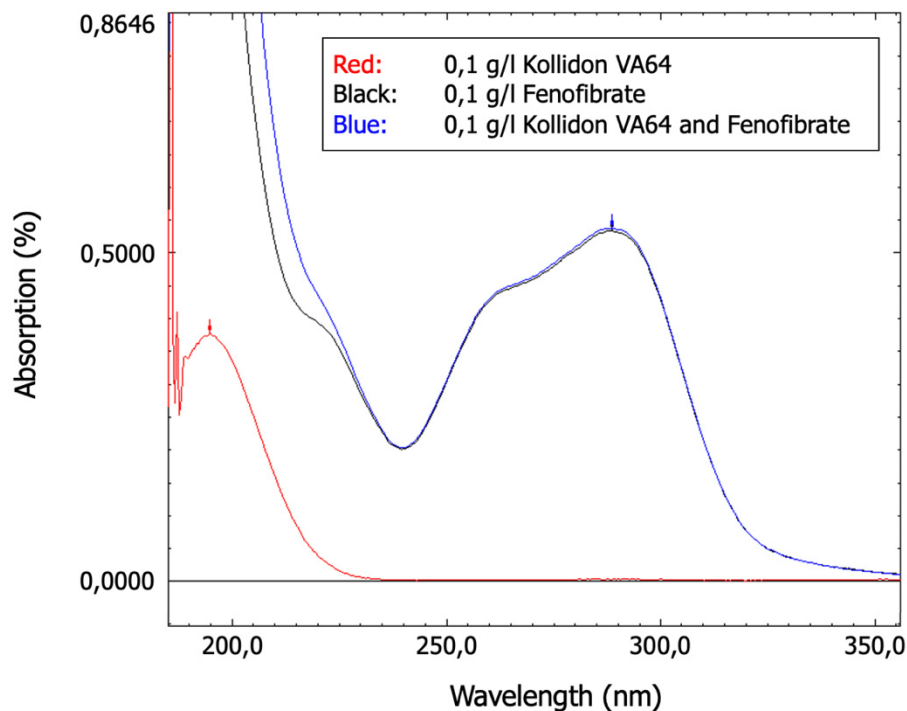


Figure 29: UV/Vis spectra of Kollidon VA64 and Fenofibrate

6.2 Capability analysis of equipment

6.2.1 Microfeeder

Figures 30, 31, and 32 show the results from the three feeding experiments with a feed rate of 1 g/h. The datapoints shown in the graphs represent the mean value for one minute of feeding time. The "start-up" time for the process with a certain "dead-time", followed by a slow rise in the feed rate, can be seen in the 40 minutes interval at the beginning of all three graphs. The repeatability of this "start-up" phase can be seen when comparing all three

experiments, especially in terms of the time until a stable process is reached. Individual, slightly bigger, peaks in the feeding process are caused by agglomerates of powder which have built-up on the inside of the powder guiding tube and which have loosened. The statistical analysis of the feed rates is shown in Table 5.

Feeding experiment nr. 1 with 1 g/h

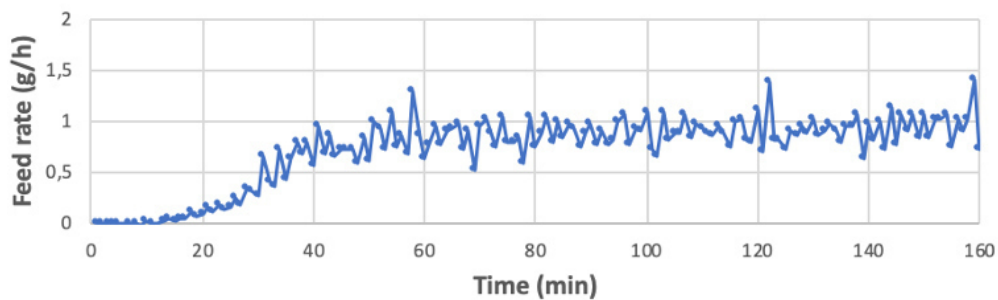


Figure 30: Capability analysis of microfeeder with feed rate 1 g/h (experiment nr. 1)

Feeding experiment nr. 2 with 1 g/h

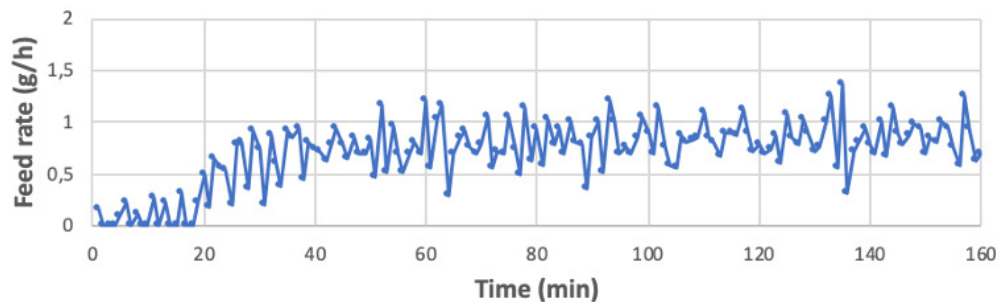


Figure 31: Capability analysis of microfeeder with feed rate 1 g/h (experiment nr. 2)

Feeding experiment nr. 3 with 1 g/h

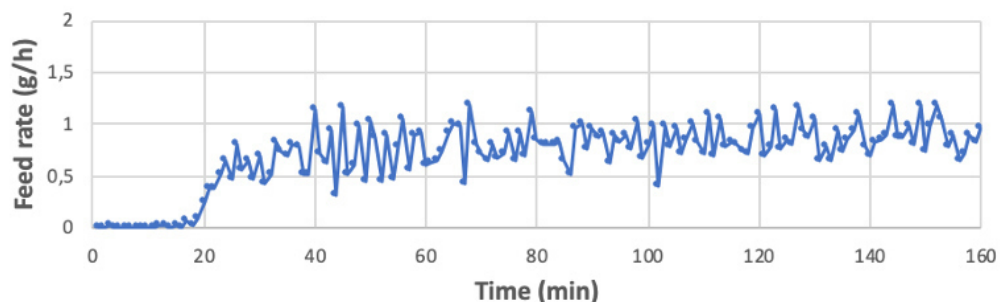


Figure 32: Capability analysis of microfeeder with feed rate 1 g/h (experiment nr. 3)

The results from the three feeding experiments, with a feed rate of 5 g/h, are shown in Figures 33, 34, and 35. Again, the "start-up" time for the process with a certain "dead-time", followed by a rise in the feed rate, is clearly demonstrated. The duration of the "start-up" phases can be determined with 20 minutes of all three graphs.

Feeding experiment nr. 4 with 5 g/h

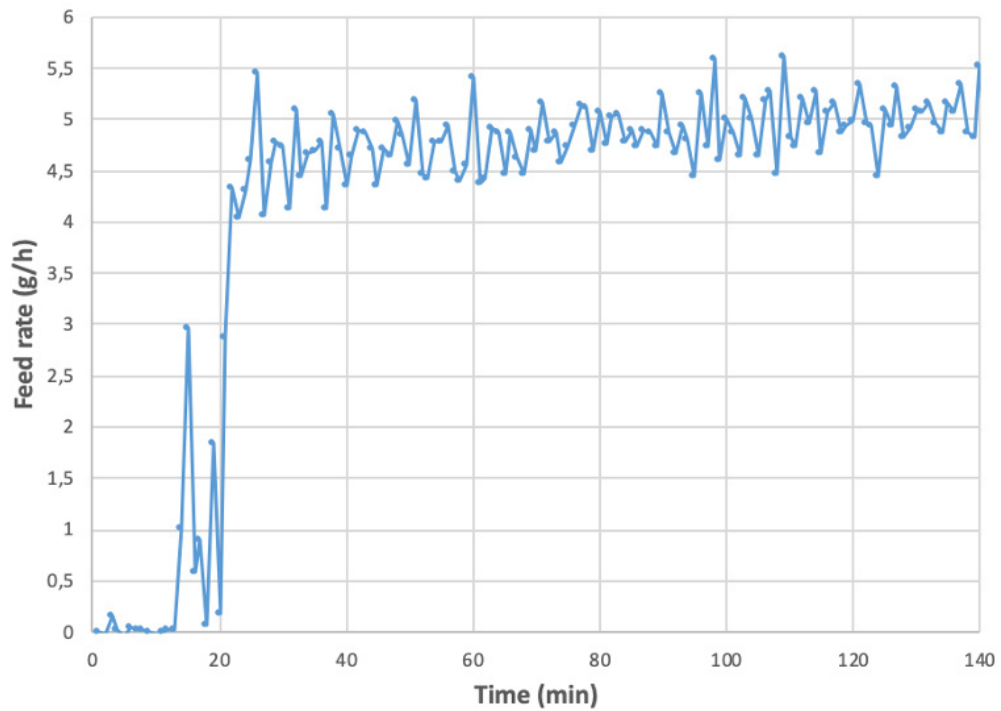


Figure 33: Capability analysis of microfeeder with feed rate 5 g/h (experiment nr. 4)

Feeding experiment nr. 5 with 5 g/h

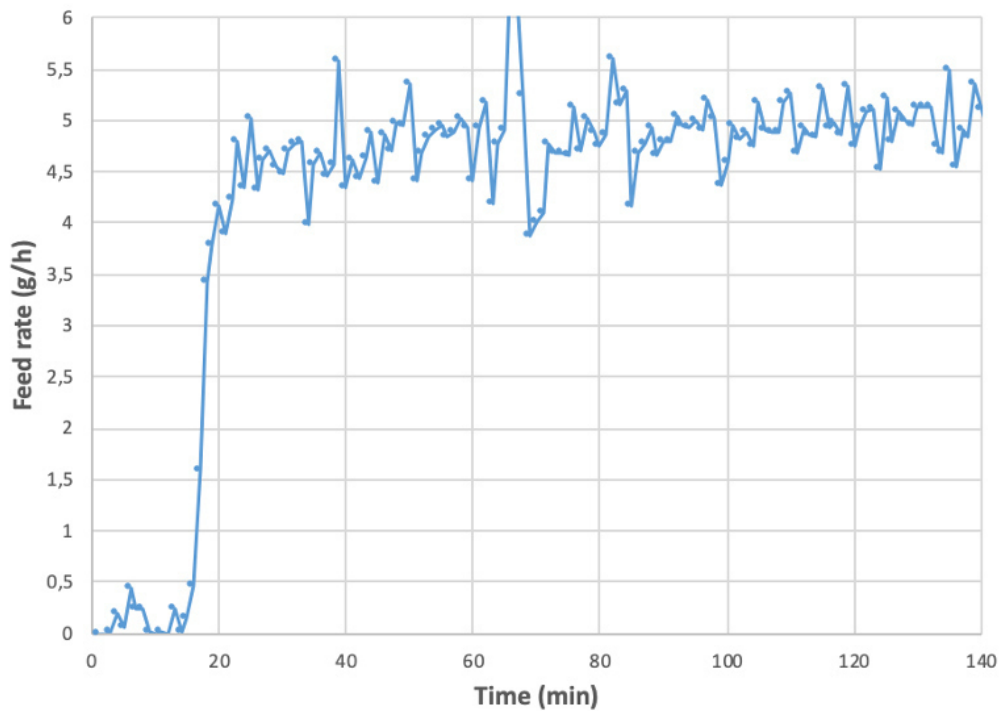


Figure 34: Capability analysis of microfeeder with feed rate 5 g/h (experiment nr. 5)

Feeding experiment nr. 6 with 5 g/h

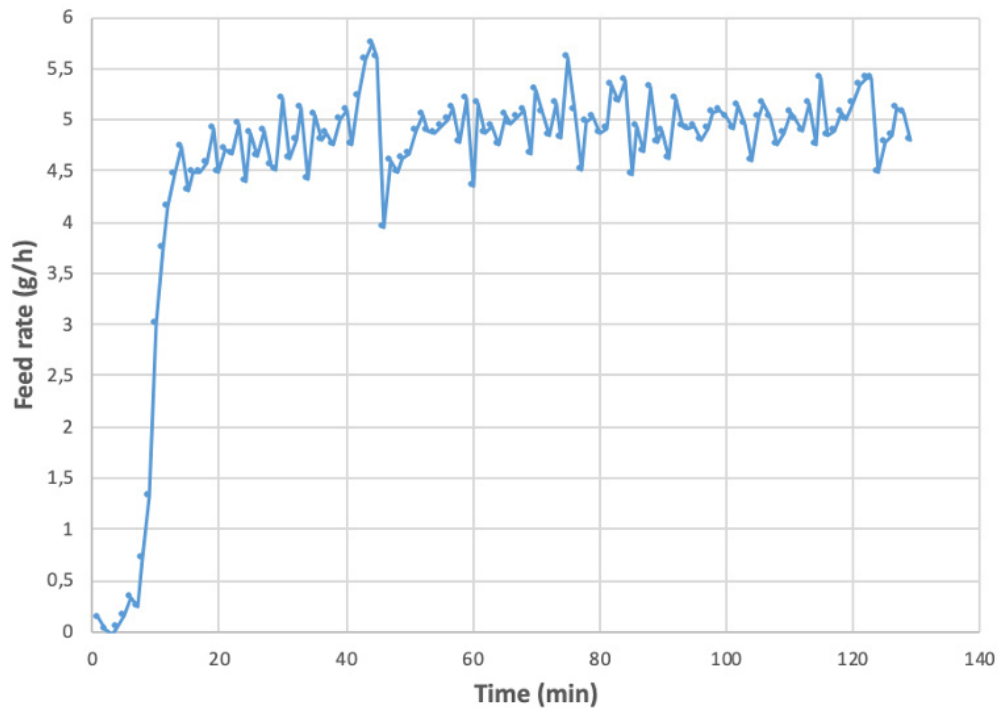


Figure 35: Capability analysis of microfeeder with feed rate 5 g/h (experiment nr. 6)

Table 5 compares the behavior of all six individual microfeeding experiments, after the start-up phase (40 min for 1 g/h and 20 min for 5 g/h). The table illustrates the nominal feed rate, the mean feed rate which was achieved, the accuracy of the process (defined as 100 % minus the relative deviation between nominal and mean feed rate), and the relative standard deviation (RSD) of the process.

Table 5: Statistical analysis of feed rates 1 g/h and 5 g/h

Experiment	Nominal feed rate (g/h)	Mean feed rate (g/h)	Accuracy (%)	RSD (%)
Nr. 1	1,00	0,89	88,59	17,12
Nr. 2		0,82	81,69	24,19
Nr. 3		0,83	83,09	21,57
Average		<i>0,84</i>	<i>84,46</i>	<i>20,96</i>
Nr. 4	5,00	4,82	96,43	7,46
Nr. 5		4,84	96,85	7,95
Nr. 6		4,94	98,74	5,78
Average		<i>4,87</i>	<i>97,34</i>	<i>7,06</i>

In Figure 36 the behavior of the “step-trial” experiment is displayed. The 50 min long start-up phase at the beginning of the experiment, until a stable feed rate of 1 g/h was achieved, can be interpreted as being similar to the one from the other 1 g/h feeding experiments.

The steps in the graph (indicated by the dotted lines) reflect the rise in the feed rate by nominally 1 g/h. The change of feed rate during the ongoing process is a very discrete step which occurs immediately after the change of the piston speed. This graph also shows the accuracy of the feeding process for all steps between 1 and 5 g/h.

Feeding experiment nr. 7 with stepwise feed rate increase

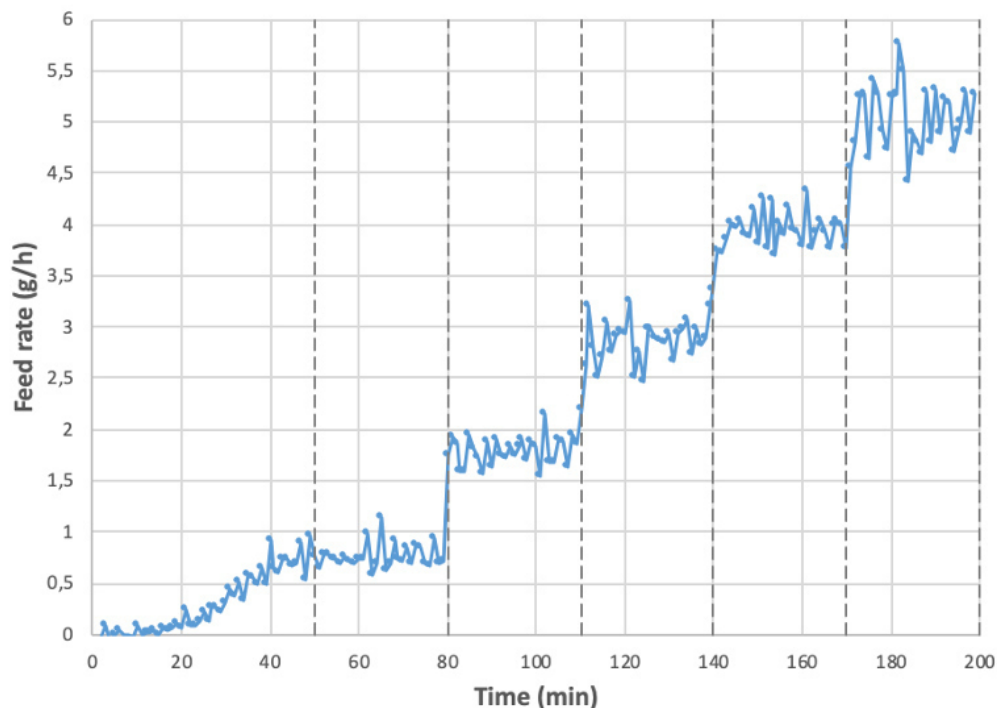


Figure 36: Capability analysis of microfeeder with stepwise feed rate increase

In Table 6 the behavior of the five phases with constant feed rate of experiment nr. 7 after a start-up phase of 50 min are analyzed.

In general, a good suitability of the microfeeder for the examined processes, with Fenofibrate as fed material, can be determined from all of the above experiments. The start-up phase is within a reliable interval for all runs and therefore does not represent a problem for the implementation of the microfeeder in a not-monitored process. The start-up time is mainly influenced by the powder properties and its preconditioning in the powder reservoir. By further improving the preconditioning, a reduction of start-up time is most certainly feasible and should lead to an additional reduction in the variations of the start-up-times.

Table 6: Statistical analysis of the experiments with stepwise feed rate increase

Experiment	Nominal feed rate (g/h)	Mean feed rate (g/h)	Accuracy (%)	RSD (%)
Nr. 7	1,00	0,76	75,96	15,27
	2,00	1,79	89,40	7,88
	3,00	2,85	94,87	8,15
	4,00	3,93	98,27	4,95
	5,00	5,00	99,92	7,76

The feed rate curves following the start-up time show constant fluctuations in the range of $\pm 0,5$ g in all experiments, with only a few outliers. Those fluctuations can be explained by several factors:

- Since the scale records the data in 1 sec intervals, but the microfeeder supplies the material in 6 sec intervals (due to the stirrer's rotational speed), interferences between the two tools can arise. If powder falls onto the scale within the scale's data-recording-interval, the impulse from the landing powder is biasing the logged result. This effect can also occur if the results are displayed in one-minute-intervals, because either ten or nine "powder-deliveries" on the scale can occur during this period of time. Additionally, slight deviations in the stirrer's rotational speed can also trigger such an effect.
- Due to the "prototype-character" of the microfeeder, some small tolerances in the range of micrometers between the powder-guiding components exist. These minor imperfections are sufficient to generate periodically repeating small variations in the feed rate. One example is the clearance between the scraper and the plate. If the plate is not perfectly aligned to the scraper blade, fine powder-particles can accumulate in the gap between scraper and plate and moved by the scraper, once this gap is filled.
- Bigger peaks in the graphs can be explained by chunks of powder which loosen from the powder guiding pipe and fall onto the scale. Those chunks are the result of small amounts of slightly electrostatic powder adhering to the inner pipe surface, when falling through. Once a certain agglomerate-size is reached, they can break loose and fall down, on the scale. In the experiments described, it was not possible to entirely avoid the buildup of those chunks. This is triggered by the material-characteristics of the powder and the powder-guiding pipes, such as the quality of the inner surface and the length of the pipes. In contrary to the chunks, which adhere to the pipe and remain there, the pieces which fall off primarily influence the RSD of the process, but barely have an impact on the mean feed rate.
- One further aspect that biases the results in the above curves are vibrations in the room where the measurement has been conducted. Even though all experiments have been performed in a mostly empty room, it was impossible to avoid the occasional opening of a door or vibrations of someone passing by, as factors influencing the measurements. Due to the high precision of the used scale and the small amount of powder used, such effects can lead to considerable consequences in the data.

Another aspect of the feeding process is the behavior of the feed rate after the start-up phase. Here, a gradual rise in the feed rate over time can occur. In all of the above experiments, barely any gradient can be identified. Only experiment nr. 4 with 5 g/h shows a very minor linear feed rate rise. Apart from the powder-properties, the biggest influential factor to cause a feed rate gradient is the preconditioning of the powder. If a further compaction of the powder, caused by the moving piston pushing the powder upwards, can be avoided through preconditioning of the powder, such effect can be avoided. Further options are the implementation of an external feed rate control or the correction of the feed rate during the process, based on experiences from previous tests.

Insights gained from further experiments following the same methodology as described above may help to optimize the feeding process even more. This may specially be true for incrementally adapting the mean feed rate to get even closer to the nominal feed rate. This way a mean feed rates accuracy of almost 100 % may be in reach, especially when looking at the higher feed rates, in experiment nr. 7, the RSD of the experiments is smaller. However, due to the extruders residence time distribution, the RSD should have no negative impact on the extrudates content uniformity for low feed rates.

6.2.2 HPLC analysis

The review of the analyzation method described in 5.2.2 proved to be linear, with a $R^2=0,9997$ over the concentration range of 0,3 - 200 ppm. The limit of detection (LOD) was 0,1 ppm and the limit of quantification (LOQ) was 0,3 ppm, determined by the signal-noise ratio.

6.2.3 Residence time distribution

The RTD data gained from video analysis was analytically fitted to gain the tracer concentration over time, which is a function of the Péclet number (Pe), the mean residence time (τ), an offset (d), and a scaling factor (s) as shown in (7) [69].

$$c_{tracer} = \tilde{f}(Pe, \tau, d, s) \quad (7)$$

Due to the dominance of the dispersion effect opposed to the diffusion effect in extrusion, here, the Péclet number is defined as the ratio between the convective transport and the axial dispersion coefficient (D) (opposed to the diffusion constant (E)) as shown in (8). The convective transport is the product of the average axial velocity (U) and the characteristic length (L) [69].

$$Pe = \frac{U * L}{D} = \frac{\text{convective transport}}{\text{dispersive transport}} \quad (8)$$

The Péclet number can allow a simple estimation of the RTD's characteristic. The higher Pe is, the higher is the convective transport and the lower is the contribution of dispersive processes such as back-mixing. Therefore: a higher Pe indicates a narrow RTD [69].

Two measurements of the RTD were performed with the final extrusion setup described in 5.3.3.1. The resulting curves for the color spaces "b" value are shown in Figure 37 (for measurement 1) and Figure 38 (for measurement 2).

The calculated Péclet number Pe , the mean residence time τ , and the estimated maximal residence time RT_{max} are shown in Table 7. The outcome of the two measurements is similar, with a mean residence time of about 3:30 min and a maximum residence time of approximately 10 min. As can be seen by comparing Figure 37 and Figure 38, the first RTD measurement was most likely stopped, before the tracer left the extruder barrel completely. This could happen because the end of the experiment was determined by visual estimation of the extrudates color. This however makes it slightly harder to estimate the true RT_{max} . The influence of the experiment's early terminations on τ , on the other hand, is comparably small.

Table 7: Results of RTD measurements

	Pe ()	τ (s)	RT_{max} (s)
Measurement 1	10,08	200	550
Measurement 2	7,62	214	660
Average	8,85	207	605

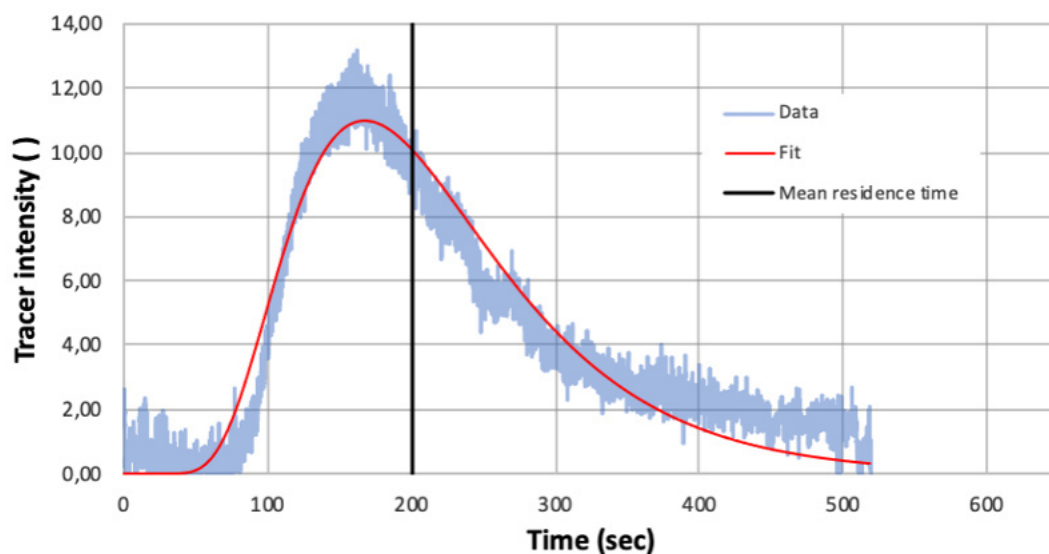


Figure 37: RTD curve of measurement 1

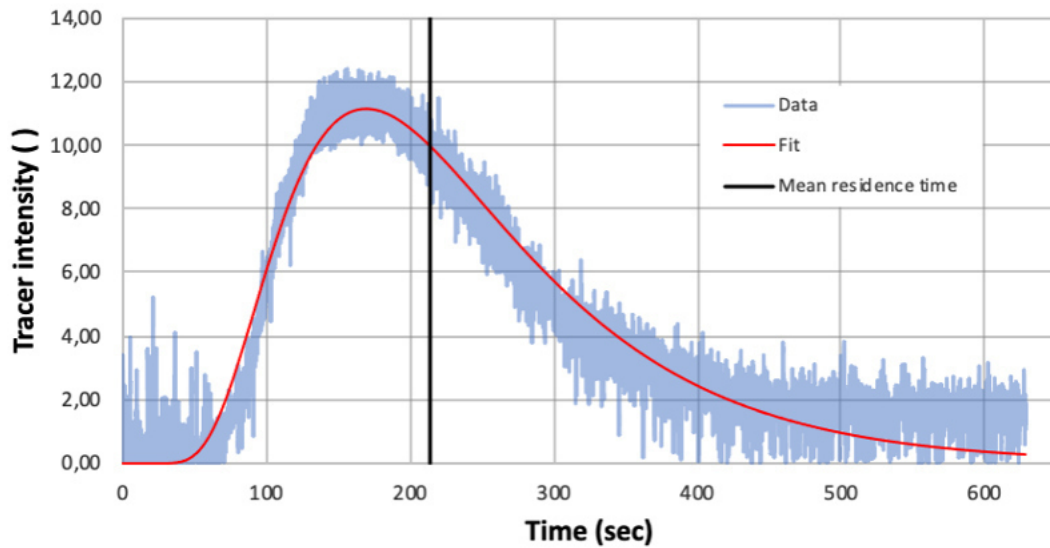


Figure 38: RTD curve of measurement 2

6.3 Compounding experiments

6.3.1 Pre-blend experiment with PAT

6.3.1.1 In-line UV/Vis spectroscopy

Based on the recorded spectra from the extrusion process (described in 5.3.1), a chemometric model for determining the API concentration in the melt should have been created. To analyze the informative value of the recorded data, the spectra were imported into the "SIMCA" software. With the help of multivariate data analysis, a correlation between the change in the spectra and the concentration of API at different process times was investigated.

One way to determine the existence of such correlations is to search for patterns in a score-scatter-plot. Scores are the new variables ($t[1]$ and $t[2]$) created by the software out of the original variables, from the collected data. Those scores are completely independent of each other (orthogonal). A third variable is introduced into the plot via the scores color representing the process-time. The ellipse shown in the plot represents the confidence region containing 95 % of the data.

Therefore, ideally, six independent clusters of scores with different colors can be seen in the plot, each representing a different concentration of API in the extrudate for a certain period of time. In Figure 39 a certain pattern indicating several time intervals can be seen. Several lines with various orientation and position may indicate the different concentration steps in the process. Due to their proximity or even overlapping characteristics, however, it was concluded that it was not possible to create a useful chemometric model, from the existing data and the available resources.

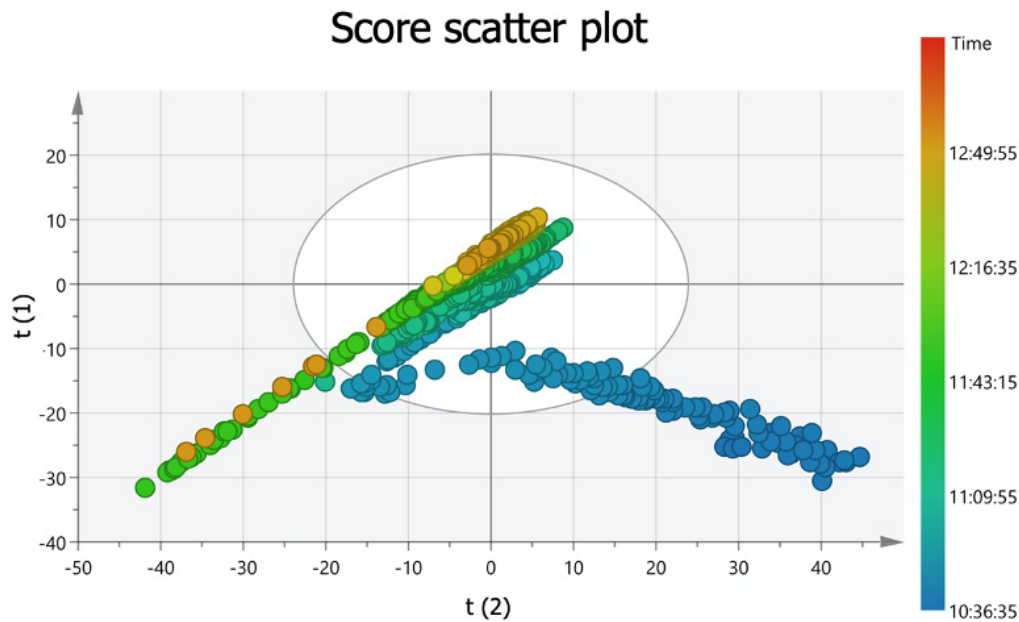


Figure 39: SIMCA analysis of recorded spectra

6.3.1.2 Pre-blend sample analysis with HPLC

The samples for analysis from the pre-blend experiment mentioned in "5.3.2 Pre-blend experiment with PAT" were taken and prepared as described (in 5.3.2.2). The samples from minutes 15, 20 and 25 of each concentration from 0 to 0,5 $\omega/\omega\%$ FFB in the extrudate are shown in Figure 40. The blue dashed line depicts the nominal concentration, whereas the red dots represent the individual samples. The absence of the sample at minute 15 of the batch with a concentration of 0,4 $\omega/\omega\%$ FFB and the bad accuracy of the subsequent sample are caused by problems during the extrusion process. Due to difficulties while refilling the LIW-feeder, the extruder had to be stopped and the restarting procedure resulted in a certain material loss.

The results were analyzed (even though only with limited significance due to the small sample size) and the outcomes are shown in Table 8.

Even when taking the samples with a concentration of 0,4 $\omega/\omega\%$ into consideration, it was possible to reach an accuracy of above 90 %. A positive surprise is, how good the results for lower concentrations have been reached. Nevertheless, due to the high exactness when weighing in the Fenofibrate during fabrication of the pre-blends, an even higher accuracy of the FFB concentration in the samples was expected for the higher concentrations. A possible reason for this is thermal degradation of Fenofibrate during the extrusion process, caused by the extruders high processing temperature in the die-zone of only 10 °C below the thermal degradation temperature of Fenofibrate. Additionally, various effects, such as adhesion of powder to equipment walls, could be responsible for some loss of API during the process. Nevertheless, for most concentrations the standard deviation is far below 10 %, indicating a uniform concentration in the extrudate and therefore indicating a generally stable process.

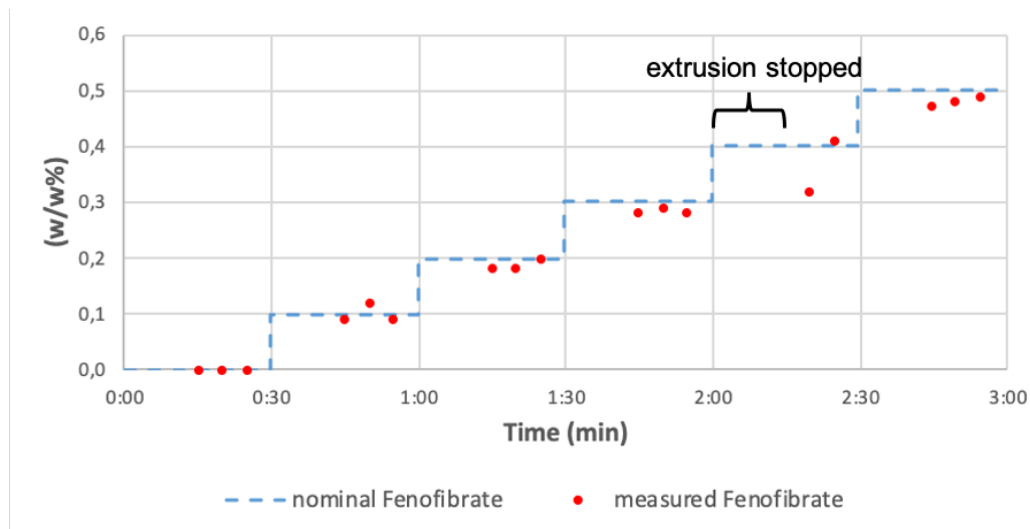


Figure 40: HPLC results from pre-blend experiments

Table 8: Results of pre-blend experiments

Process-time (min)	0:00	0:30	1:00	1:30	2:00	2:30
	–	–	–	–	–	–
	0:30	1:00	1:30	2:00	2:30	3:00
Nominal ($\omega/\omega\%$)	0,00	0,10	0,20	0,30	0,40	0,50
Measured average ($\omega/\omega\%$)	0,00	0,10	0,19	0,28	0,37	0,48
Accuracy (%)	100	100	93,33	94,44	91,25	96
RSD (%)	-	17,32	6,19	2,04	17,44	2,08

6.3.2 Compounding experiments with microfeeder

6.3.2.1 Constant API concentration

6.3.2.1.1 Experiments with 0,5 $\omega/\omega\%$ Fenofibrate in extrudate

As described in 5.3.3.2 "Description of procedure", the compounding experiments with a concentration of 0,5 $\omega/\omega\%$ FFB were performed in three separate runs. This was done to investigate the reproducibility of the process with identical starting conditions for the duration of one hour. Due to a minor error in the sampling method, experiment nr. 2 lasted 5 min longer than intended. This, however, should not have any significant influence on the results and will therefore be taken as it is. The graphic representation of the results can be seen in Figures 41, 42, and 43.

The blue, dashed line represents the nominal, and therefore expected, concentration of FFB in the extrudate. The grey dots represent the expected FFB concentration when the amount of polymer powder withdrawn from the process by the ventilation unit is taken into account. This "correction" was done by measuring the extruders mass throughput in between the samples by collecting the extrudates and weighing them. Then, the average of one samples adjacent measured mass-throughputs was taken as reference mass throughput, to calculate the "expected" FFB concentration. Therefore, these dots represent the concentration of FFB, which should be achieved if the full amount of Fenofibrate is introduced into the reduced (by the ventilation unit) polymer mass flow. Each red dot represents the actual concentration of Fenofibrate determined by HPLC analysis of an individual extrudate sample.

In all three experiments, the influence of the extruders RTD can be clearly seen. After activating the microfeeder (nominal FFB concentration rises to 0,5 $\omega/\omega\%$) it takes around 10 min until the desired concentration is actually reached. The same is true for the reverse process, if the microfeeder is stopped and the FFB concentration decreases. Of course, it has to be considered, that the low sampling resolution reduces the significance of this observation. The concentration-measurements after 1:30 h show that the removal of all Fenofibrate traces from the extruder is working, as anticipated.

Compounding experiment nr. 1 with 0,5 $\omega/\omega\%$ Fenofibrate

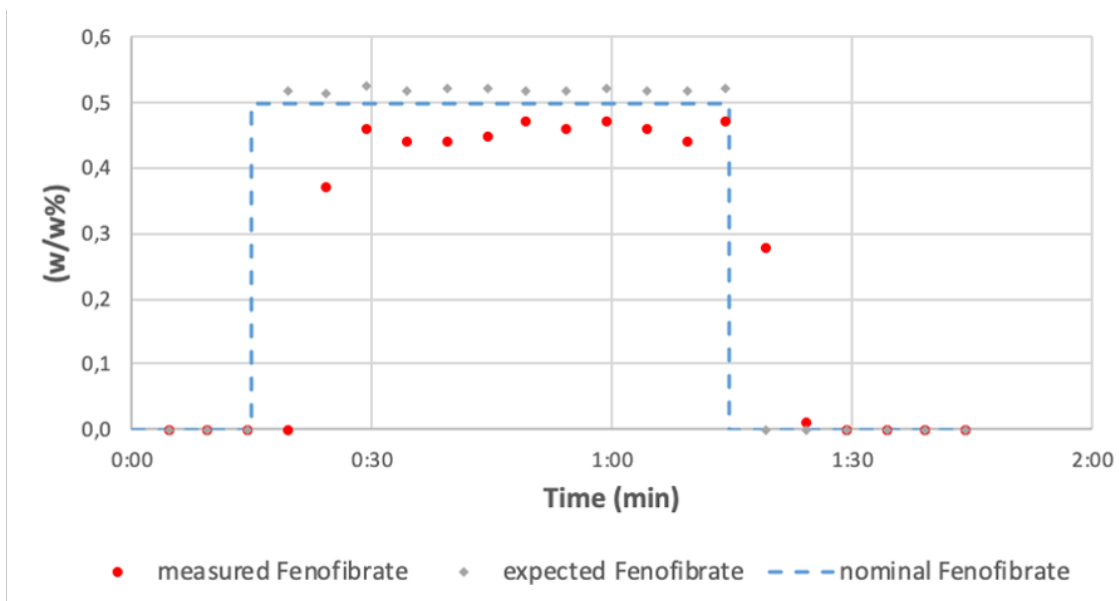


Figure 41: HPLC results from experiment nr. 1 with 0,5 $\omega/\omega\%$ Fenofibrate

Compounding experiment nr. 2 with 0,5 $\omega/\omega\%$ Fenofibrate

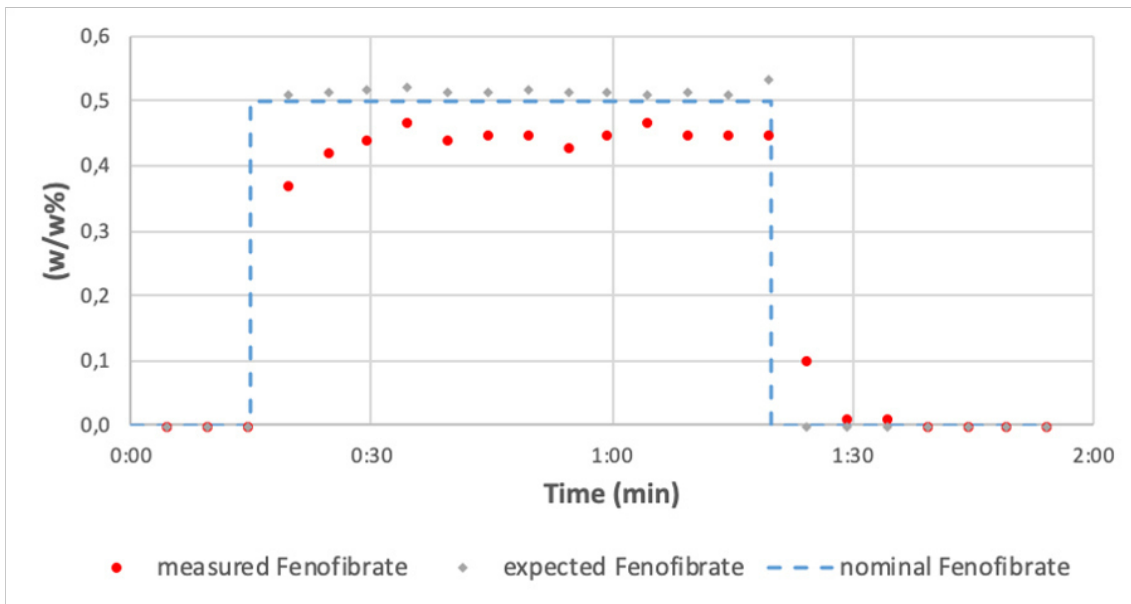


Figure 42: HPLC results from experiment nr. 2 with 0,5 $\omega/\omega\%$ Fenofibrate

Compounding experiment nr. 3 with 0,5 $\omega/\omega\%$ Fenofibrate

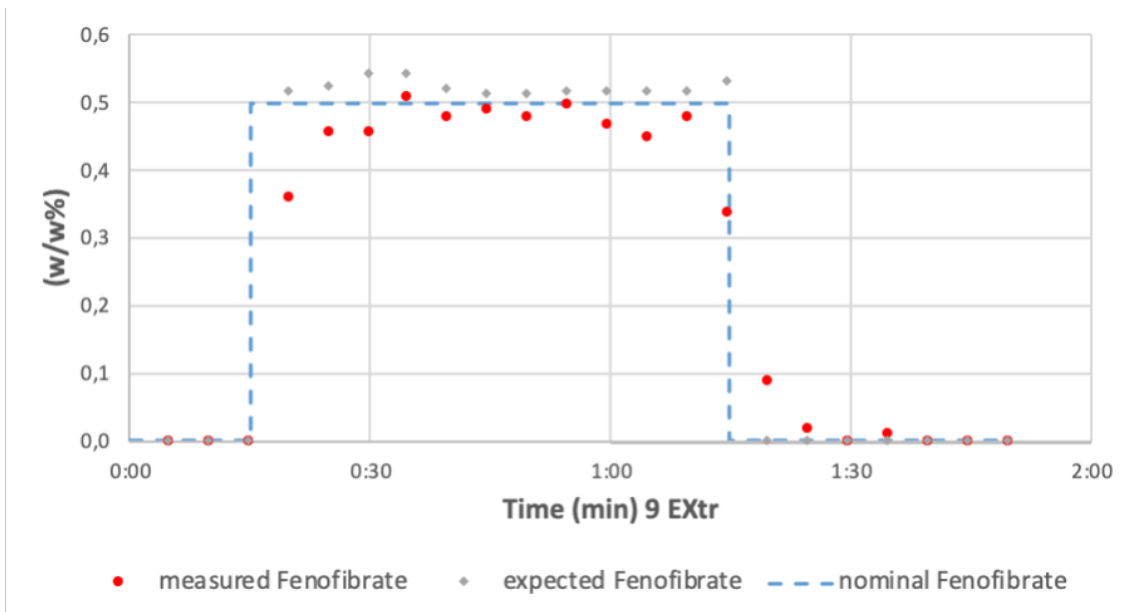


Figure 43: HPLC results from experiment nr. 3 with 0,5 $\omega/\omega\%$ Fenofibrate

The measurements for all three experiments were analyzed and the results are shown in Table 9. That table shows the nominal Fenofibrate concentration, the arithmetic average of the "expected Fenofibrate" and the "measured Fenofibrate" concentrations in the extrudates, the deviation of the measured from the expected Fenofibrate concentration, the accuracy of the "measured Fenofibrate" defined as 100 % minus the relative deviation between nominal

and measured concentration, and the relative standard deviation (RSD) of the expected and the measured results. All values are calculated for the timespan, where the nominal concentration is above zero. Therefore, also the influence from the extruders RTD, biasing the results at the beginning of each block (first time the nominal FFB concentration is 0.5 $\omega/\omega\%$), is comprised in the results.

The results for all three experiments are very good. The accuracy of all the experiments is particularly pleasing with 87,27 % of the intended concentration reached. When disregarding the first two samples of each block (in order to eliminate the effect of the extruders RTD) the accuracy rises even higher to over 90 %. This further pushes down the already low RSD of the measured samples to below 3 %, for experiment 2. The low RSD of the expected Fenofibrate concentration indicates that the influence of the ventilation unit is a constant and a barely fluctuating impact, therefore not seriously limiting the processes stability. A pleasant effect which can be observed in all experiments is, that the loss of polymer and Fenofibrate during the process compensate each other to a certain degree. Besides the loss of polymer and Fenofibrate due to ventilation unit and wall adhesion as main influential factors, other process-biasing aspects are the variations in feeder stability for both feeders. Additionally, small errors in the results may be caused by the precision of the scale, when preparing the samples for HPLC analysis.

Overall, this compounding process can be attested with a satisfactory stability and reproducibility for API concentrations of 0,5 $\omega/\omega\%$. Especially when taking in consideration that the entire process is still in its prototype phase.

Table 9: Results of experiments nr. 1-3 with 0,5 $\omega/\omega\%$ Fenofibrate

Experiment nr.	1	2	3	Average
Process-time (min)	0:15 – 1:15	0:15 – 1:20	0:15 – 1:15	
Nominal ($\omega/\omega\%$)	0,50			0,50
Expected average ($\omega/\omega\%$)	0,52			0,52
Measured average ($\omega/\omega\%$)	0,41	0,44	0,46	<i>0,44</i>
Deviation from expected (%)	-21,10	-14,67	-12,83	<i>-16,20</i>
Accuracy (%)	82,17	88,31	91,33	<i>87,27</i>
RSD from expected (%)	0,54	1,11	1,93	<i>1,19</i>
RSD from measured (%)	32,18	5,76	11,56	<i>16,50</i>

6.3.2.1.2 Experiments with 0,2 $\omega/\omega\%$ Fenofibrate in extrudate

Different to the compounding experiments with 0,5 $\omega/\omega\%$ FFB, the experiment for 0,2 $\omega/\omega\%$ FFB was performed in one single continuous run. This was done to examine the repeatability of the process and to analyze the process behavior for duration of more than two hours. The graphical display of the compounding experiment (Figure 44) and the analysis of results (Table 10) was performed identical to the methodology as described above.

In the first "API block" (first time the nominal FFB concentration is 0,2 $\omega/\omega\%$) the rise in the measured concentration is in agreement with the extruders RTD. The same is valid for the decline in FFB concentration at the end of this block. In this first block, an exceptional compliance between nominal and measured FFB concentration was achieved with an accuracy of 96,25 % and an RSD of only 12,94 % even when taking the first two samples into account.

The first issues in the process become visible at the beginning of the second block. The slow rise in FFB concentration is caused by a thin layer of fine Kollidon dust, which settled on the funnel below the microfeeder. This dust reduced the sliding capability of the small amounts of Fenofibrate falling through this funnel. Therefore, the Fenofibrate was delayed until a sufficient amount of powder was able to push through this obstacle. Apparently, the regular tapping and knocking on the funnel etc., was not enough to prevent this effect.

To avoid this effect in the third block, the Kollidon dust in the mentioned funnel was removed before the introduction of Fenofibrate started again. Therefore, no such retention in FFB concentration rise occurred in this block. However, after three hours of continuous process, first formations of bridging by molten polymer in the extruder intake evolved. They, of course, had a significant impact on the process stability. The FFB concentration was especially influenced by the increasing amount of polymer dust, settling on all surfaces and hindering the Fenofibrates feeding. The formation of a completely closed extruder intake from bridging was avoided by regularly removing the adhering polymer from the intakes wall.

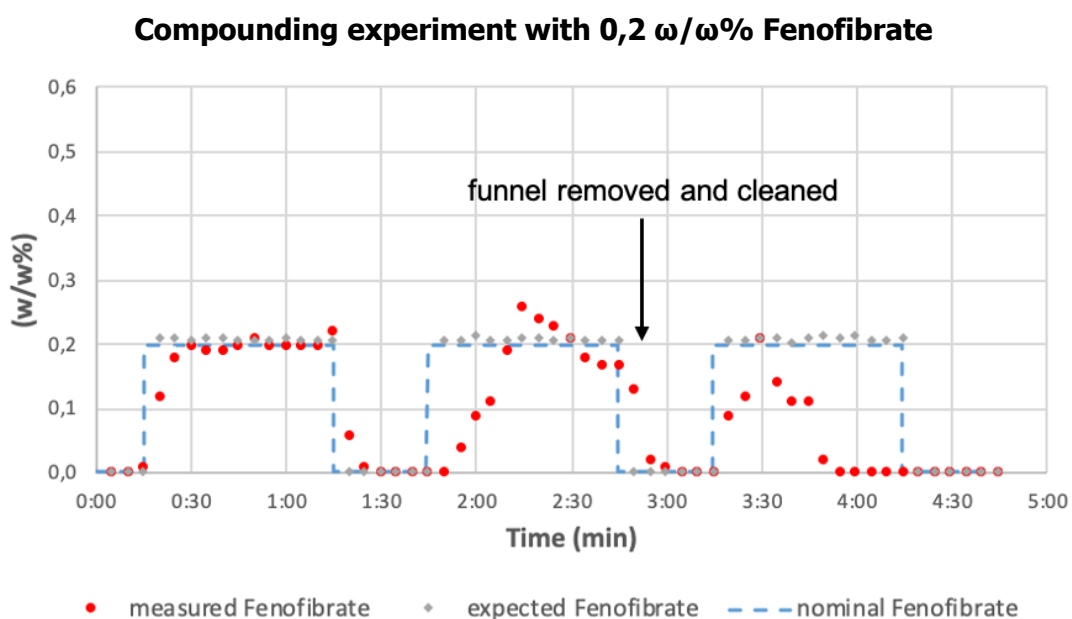


Figure 44: HPLC results from experiment with 0,2 $\omega/\omega\%$ Fenofibrate

The results in Table 10 reflect the above described findings. The first block shows good results and can be compared to the experiments with 0,5 $\omega/\omega\%$ FFB above. The accuracy is even better than before with 96,25 % of the intended concentration reached (again including the first two samples). The RSD of the first block even reaches below 4,50 %, when excluding the first two samples. The results from block two and three resemble the appearance of the graph (Figure 44). While the first results in the first block are shaped by feeder problems, the third block cannot be considered a successful repeat because of the bad results. Nevertheless, the RSD of the expected FFB concentration for all blocks indicates a stable polymer extrusion process, regardless of the experienced problems with polymer bridging.

In summary it can be concluded, that a stable compounding process, creating extrudates with an API concentration of 0,2 $\omega/\omega\%$, can be attained for at least one hour of processing. However, problems with the material intake in this process setup limit its maximal duration and repeatability.

Again, influential factors on the results besides the feeding problems may be caused by the precision of the scale when preparing the samples for HPLC analysis.

Table 10: Results of experiment with 0,2 $\omega/\omega\%$ Fenofibrate

Process-time (min)	0:15	1:45	3:15
	–	–	–
	1:15	2:45	4:15
Nominal ($\omega/\omega\%$)	0,20		
Expected average ($\omega/\omega\%$)	0,21		
Measured average ($\omega/\omega\%$)	0,19	0,16	0,07
Deviation from expected (%)	-7,20	-24,01	-68,01
Accuracy (%)	96,25	78,75	33,33
RSD from expected (%)	0,65	1,15	1,55
RSD from measured (%)	12,94	51,59	108,42

6.3.2.1.3 Experiments with 0,1 $\omega/\omega\%$ Fenofibrate in extrudate

The lowest concentration of API examined in a compounding experiment was 0,1 $\omega/\omega\%$ FFB. After the test with the concentration of 0,2 $\omega/\omega\%$, which have been partially successful, this was done to study the lower end of the possible concentrations. Again, the experiment for 0,1 $\omega/\omega\%$ FFB was performed in one single continuous run. The graphical display of the compounding experiment (Figure 45) and the following analysis of the results (Table 11) was done in the same way as previously described.

When working with such low concentration, the required feed rate becomes as little as 1 g/h. Therefore, each time the microfeeders scraper transports material into the process, only around 1,67 μg of material are moved. Hence, it is evident that the slightest influences such as material losses by wall-adhesion are a major influential factor. Additionally, feeding uniformity becomes a major impact factor and plays an important role.

Figure 45 shows, that besides all of the mentioned challenges, a microfeeder based compounding process could be accomplished. Even though the accuracy for the first block is at only 69,17 %, the fact that a stable result (RSD at 22,62 %) could be achieved, is a success in its own. With such low concentration, the rounding errors in the results become a noticeable influence due to the (in our case) HPLC-analysis' limitation to two decimal digits in the result.

For the second and third block it was not possible to detect any significant traces of Fenofibrate in the extrudates. Possible causes are the adherence of Fenofibrate to the inner walls of the powder guiding pipe, or of other components of the setup. The funnel (being a problem in previous experiments) was cleaned before each block, to guarantee proper slipping of the API. Another reason for the absence of Fenofibrate in the extrudate (especially for the third block) is, again, the formation of molten polymer in the extruder's intake zone. These depositions (especially when appearing close or underneath the powder guiding tube) can heavily influence the API concentration. Some samples of the second and third block were performed in duplicate to rule out errors in the extrudate analyzation.

Compounding experiment with 0,1 $\omega/\omega\%$ Fenofibrate

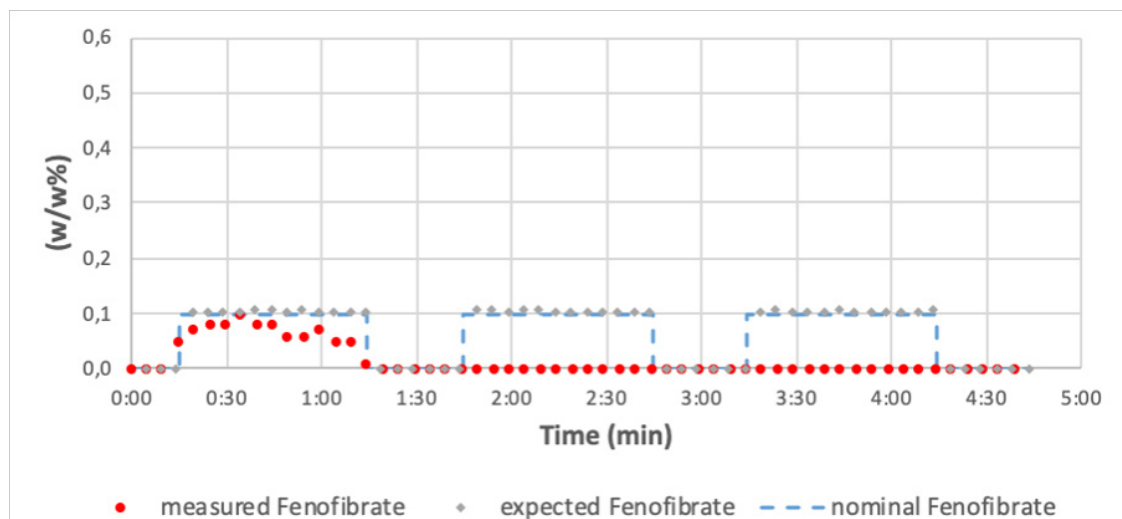


Figure 45: HPLC results from experiment with 0,1 $\omega/\omega\%$ Fenofibrate

Table 11: Results of experiment with 0,1 $\omega/\omega\%$ Fenofibrate

Process-time (min)	0:15	1:45	3:15
	-	-	-
	1:15	2:45	4:15
Nominal ($\omega/\omega\%$)	0,10		
Expected average ($\omega/\omega\%$)	0,10		
Measured average ($\omega/\omega\%$)	0,07	0,00	0,00
Deviation from expected (%)	-33,44	-100,00	-100,00
Accuracy (%)	69,17	0,00	0,00
RSD from expected (%)	1,06	1,40	0,78
RSD from measured (%)	22,62	-	-

6.3.2.2 Step trial

In the last compounding experiment, the microfeeder was operating continuously and the feed rate was adapted in the defined steps during the running process. The intended FFB concentrations in the extrudate were between 0,1 and 0,5 $\omega/\omega\%$ in 0,1 $\omega/\omega\%$ steps.

The aim of this experiment was to prove that the APIs concentration can be altered during the running process, through the change of the microfeeders feed rate, and to examine the process behavior for continuous operation, with active microfeeder for more than three hours.

The experimental procedure is described in 5.3.3.2.2 "Step trial" and consists of 40 min long blocks, for each concentration. To increase the resolution of the results, the sampling time was reduced to 2:30 min. This, however, made a proper determination of the extruders mass throughputs by individual measurements between the samples unfeasible due to a lack of time. Thus, the mass throughput for each "concentration-step" was averaged. The graphic representation of the results can be seen in Figure 46. Table 12 shows the results from the statistical analysis of the experiments samples.

The first three concentration steps show excellent results. At 81,88 %, the accuracy of the "0,1 $\omega/\omega\%$ step" exceeds the one from the previous experiment with the same FFB concentration. With accuracies of above 90 % and RSDs of the measured concentration being around 10 %, also the two following steps reach good results. Between the individual steps, the influence of the extruders RTD can once more be identified. Nevertheless, a uniform and defined change in concentration can be seen. The datapoint at 1:35 can be considered as an outlier, probably caused by an API agglomerate falling into the extruder.

After around two hours of continuous compounding process, the recurring problem of polymer bridging occurred. This is very much resembled in the last two "concentration steps". Still, the results from the last two steps are, considering the already accomplished process time, unexpectedly good with accuracies above 95 % and RSDs below 10%.

These results strongly support the assumption, that the main reason for the low API concentrations achieved in the second and third block of the experiments with 0,1 and 0,2 $\omega/\omega\%$, are caused by problems of Fenofibrate being hampered by polymer powder accumulating on powder guiding parts, while the microfeeder pauses.

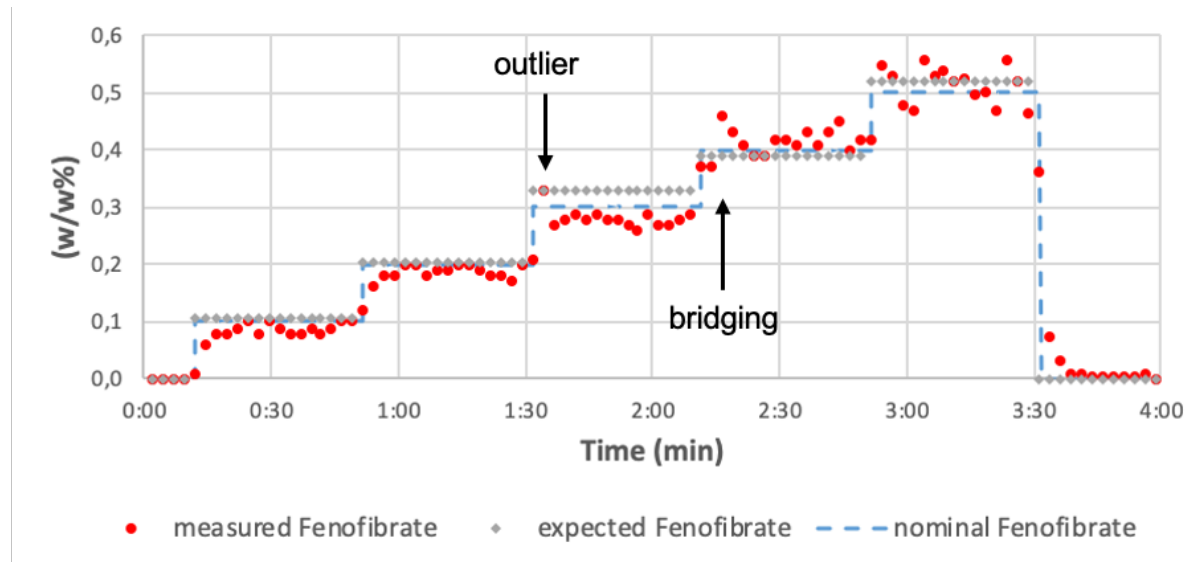


Figure 46: HPLC results from experiment with stepwise Fenofibrate concentration

Table 12: Results of experiment with stepwise Fenofibrate concentration

Process-time (min)	0:10	0:50	1:30	2:10	2:50
	0:50	1:30	2:10	2:50	3:30
Nominal ($\omega/\omega\%$)	0,10	0,20	0,30	0,40	0,50
Expected average ($\omega/\omega\%$)	0,10	0,21	0,33	0,39	0,52
Measured average ($\omega/\omega\%$)	0,08	0,18	0,28	0,41	0,51
Deviation from expected (%)	-21,75	-11,41	-15,32	5,60	-2,30
Accuracy (%)	81,88	91,25	92,50	96,72	98,40
RSD expected (%)	0,57	0,22	0,77	1,44	0,84
RSD measured (%)	26,84	11,23	8,58	6,11	7,71

6.4 Comparison between pre-blend feeding and microfeeding

In 3.4 "Research topic", the current pre-blend production technique and the new compounding technique with the implemented microfeeder for the production of low-API-concentration formulations are compared. The contemporary method has two major drawbacks.

Firstly, API-segregation and local concentration variations can occur in the pre-blend and thereby bias the uniformity of the API concentration in the extrudate. This was not particularly investigated in this thesis, but even with the limited amount of generated data, a careful interpretation can be made. Similar results were reached when comparing values (especially the achieved accuracy) from the pre-blend experiments with the ones from the compounding experiments, with a stepwise increase in API concentration. Without doubt, the pre-blend method supplied a more stable process during long extrusion experiments. This, however, is primarily due to the prototype characteristics and the therefrom occurring susceptibility of the newly developed microfeeder compounding process.

The benefit of a more streamlined process monitoring scheme by a continuously monitored production process cannot be assessed in the scope of this thesis, due to the not successful implementation of a PAT.

The second drawback of the batch-wise production technique is the increased workload from the separate creation of a pre-blend, with the desired API concentration. With the above described experiments, it is proven, that extrudates with concentrations between 0,1 and 0,5 $\omega/\omega\%$ can be produced in a single continuous process. The quality of the two production techniques is compared in Table 13.

When comparing the accuracy and the RSD of the different production techniques for a single API concentration, the following can be stated:

- The accuracy of the microfeeder compounding process does not yet reach the levels of a batch-production method, for the lower concentration of 0,1 and 0,2 $\omega/\omega\%$ API. For the higher concentrations, however, the results are similar or better to the ones of the batch production method. Even more so, when considering the impact of the extruders RTD on the results.
- In all cases, the RSD of the pre-blend method surpasses the one from the microfeeder compounding method. An exception here is the result from the step with 0,4 $\omega/\omega\%$ API, where an experimental error is responsible for the high RSD.

It is imperative to note that the sample size between pre-blend and microfeeder compounding trials greatly differs, which reduces the validity of the comparison.

Table 13: comparison between batch- and microfeeder compounding-technique

Nominal API concentration ($\omega/\omega\%$)	Method	Measured average ($\omega/\omega\%$)	Accuracy (%)	RSD measured (%)
0,1	pre-blend	0,10	100,00	17,32
	microfeeder	0,08	81,88	26,84
0,2	pre-blend	0,19	93,33	6,19
	microfeeder	0,18	91,25	11,23
0,3	pre-blend	0,28	94,44	2,04
	microfeeder	0,28	92,50	8,58
0,4	pre-blend	0,37	91,25	17,44
	microfeeder	0,41	96,72	6,11
0,5	pre-blend	0,48	96,00	2,08
	microfeeder	0,51	98,40	7,71

7 Conclusion and perspective

A compounding process was established through the combination of a twin-screw extruder and a novel volumetric microfeeder, with the intention to develop a new continuous production process for the fabrication of polymer extrudates with drug loadings down to 0,1 $\omega/\omega\%$ API. One envisioned example of application for this production technique is the continuous production of low dose drug eluting polymers. The main advantage of this new method compared to the batch-processing as is currently commonly used, is its continuous, uninterrupted character. Furthermore, the application of a process analytical technology to monitor the APIs concentration in the extrudate in-line, was explored.

In the course of this thesis, a formulation for the intended use was searched and investigated. Furthermore, all essential methods and devices were tested for their suitability. The ones of major interest were the applied microfeeder, the extruder, the UV/Vis based PAT method, and the HPLC for extrudate analysis. Several different approaches for the assembly of the compounding process, and especially the integration of the microfeeder, were made, and the most suitable was selected for conducting the compounding experiments.

Besides a review of the batch-processing technique, compounding experiments with the microfeeder have been conducted for concentrations of 0,5 $\omega/\omega\%$, 0,2 $\omega/\omega\%$, and 0,1 $\omega/\omega\%$ of API in the extrudate. The repeatability as well as the reproducibility of the processes were assessed and compared to the batch-process. Additionally, the possibility to change the API concentration in the polymer during the ongoing process has been evaluated in a separate experiment.

In reference to the objectives of this thesis, the following conclusions can be made:

- 1) It was possible to achieve reproducible feed rates with the applied microfeeder for the API used in this study. Average accuracies of 84,5 % were reached for feed rates of 0,1 g/h and an average of 97,3 % for feed rates of 5 g/h over a process duration of 2 hours.
- 2) The implementation of a UV/Vis based PAT method, to in-line monitor the API concentration in the extrudate was examined. While the concept as well as the implementation appears credible, difficulties with the signal intensity caused by the chosen formulation made it unfeasible to actively apply this technology under given circumstances. Additionally, an off-line analysis of the extrudates via HPLC was successfully conducted to study the API-content and its distribution in the extrudates.
- 3) Two types of experiments were performed to examine the processes suitability for the production of extrudates with an API concentration between 0,1 and 0,5 $\omega/\omega\%$. To prove reproducibility of the process, three separate compounding experiments were performed with an API concentration of 0,5 $\omega/\omega\%$. In those experiments, an average API content accuracy of 87,3 % was reached. For each of the lower concentration's experiments (0,1 and 0,2 $\omega/\omega\%$ API), one compounding experiment with a total duration of 4:45 h, containing three separate intervals of API being fed into the extruder, was performed. Within the first section of each experiment, feasibility of the process

was proven. Proof of repeatability was only limited, especially for the concentration of 0,1 $\omega/\omega\%$ API. In a further experiment, the variability of API concentration was investigated by changing the microfeeders feed rate during the ongoing process. To do so, a 4 h lasting trial, which included the stepwise increase of API concentration from 0 to 0,5 $\omega/\omega\%$ API during the process, was performed. The change in API concentration proved successful for each one of the five changes in feed rate. The average accuracy of the API content in the extrudates from all steps was above 90 %.

It can therefore be concluded, that the development of this new compounding technique was over all successful.

Several aspects of the work accomplished in this thesis entail approaches for further investigation. The most apparent subject for further studies is the implementation of a successful PAT. Possible approaches in this context are either to change the analytical method itself, or to adapt the formulation for the compounding experiments. With further insight into the arisen problems, it may even be possible to achieve a functioning process-monitoring by adaptation of the existing process.

For a successful upscaling of the presented method towards a capable production process, the powder guiding system between the feeders and the extruders intake requires adaptations and improvements. Identified as the leading cause for problems with content uniformity and process stability, the elimination of powder bridging problems after a certain processing duration would drastically improve the accuracy of API content in the extrudates. Optimization of the extruding process with regards to temperature profile and screw geometry could bring further improvements in this matter.

Finally, the processability of a wider range of material combinations with various powder properties should be investigated to demonstrate the universal applicability of the process. Similar is true for feed rates beyond the range studied in this thesis. Especially feed rates above the ones researched here should undoubtedly be achievable

In conclusion it can be said, that this thesis' major objective, the development of a continuous compounding process for extrudates with API concentrations down to 0,1 $\omega/\omega\%$, was successfully accomplished within the realms of possibility.

8 Literature

- [1] Alsulays B. B., Park J.-B., Alshehri S. M., Morott J. T., Alshshrani S. M.: "Influence of molecular weight of carriers and processing parameters on the extrudability, drug release, and stability of fenofibrate formulations processed by hot-melt extrusion," *Journal of Drug Delivery Science and Technology*, vol. 29, pp. 189-198, 17 July 2015.
- [2] BASF Aktiengesellschaft: *Kollidon VA 64*, Germany, 2000.
- [3] BASF SE: *Kollidon VA 64*, BASF.
- [4] Baumgartner R., Eitzlmayr A., Matsko N., Tetyczka C., Khinast J.: "Nano-extrusion: A promising tool for continuous manufacturing of solid nano-formulations," *International Journal of Pharmaceutics*, Vols. 1-2, no. 477, pp. 1-11, 30 December 2014.
- [5] Besenhard M., Fathollahi S., Siegmann E., Slama E.: "Micro-feeding and dosing of powders via a small-scale powder pump," *International Journal of Pharmaceutics*, no. 519, pp. 314-322, 2017.
- [6] Besenhard M., Faulhammer E., Fathollahi S., Reif G.: "Accuracy of micro powder dosing via a vibratory sieve-chute system," *European Journal of Pharmaceutics and Biopharmaceutics*, vol. 94, pp. 264-272, 1 June 2015.
- [7] Besenhard M., Karkala S., Faulhammer E., Fathollahi S.: "Continuous feeding of low-dose APIs via periodic micro dosing," *International Journal of Pharmaceutics*, vol. 509, pp. 123-134, 19 May 2016.
- [8] Bhandari B., Ho T. M., Truong T., Roos Y. H.: *Non-Equilibrium States and Glass Transitions in Foods*, United States: Woodhead Publishing, 2017, pp. 111-136.
- [9] Blackshields C. A., Crean A. M.: "Continuous Powder Feeding for Pharmaceutical Solid Dosage Form Manufacture: A Short Review," *Pharmaceutical Development and Technology*, vol. 23, no. 6, pp. 554-560, 21 June 2017.
- [10] Breitzkreutz J.: "Prediction of Intestinal Drug Absorption Properties by Three-Dimensional Solubility Parameters," *Pharmaceutical Research*, vol. 15, no. 9, pp. 1371-1375, 1998.
- [11] Bruschi M. L.: *Strategies to Modify the Drug Release from Pharmaceutical Systems*, vol. 85, UK: Woodhead Publishing, 2015, p. 38.
- [12] Bühler V.: *Kollidon - Polyvinylpyrrolidone excipients for the pharmaceutical industry*, 9 ed., Germany: BASF SE, 2008.
- [13] Bühler V.: *Polyvinylpyrrolidone Excipients for Pharmaceuticals*, Germany: Springer-Verlag, 2005.
- [14] Chiou W. L., Riegelman S.: "Pharmaceutical Applications of Solid Dispersion Systems," *Journal of Pharmaceutical Sciences*, vol. 9, no. 60, pp. 1281-1302, September 1971.

- [15] Crowley M. M., Zhang F., Repka M. A., Thumma S.: "Pharmaceutical Applications of Hot-Melt Extrusion: Part I," *Drug Development and Industrial Pharmacy*, no. 33, pp. 909-926, 2007.
- [16] Deng W., Majumdar S., Singh A., Shah S.: "Stabilization of fenofibrate in low molecular weight hydroxypropylcellulose matrices produced by hot-melt extrusion," *Drug Development and Industrial Pharmacy*, vol. 39, no. 2, pp. 290-298, 2013.
- [17] Douroumis D.: *Hot-melt Extrusion: Pharmaceutical Applications*, Greenwich: Wiley, 2012.
- [18] Eggenreich K., Schrank S., Koscher G., Nickisch K., Roblegg E., Khinast J.: "Influence of process route on the mechanical properties of polymer based intravaginal drug delivery systems," in *AIP Conference Proceedings 1914*, 2017.
- [19] El-Gindy A., Emara S., Mesbah M. K., Hadad G. M.: "Spectrophotometric and liquid chromatographic determination of fenofibrate and vinpocetine and their hydrolysis products," *Il Farmaco*, no. 60, pp. 425-438, 27 April 2005.
- [20] English W. E., Muzzio F. J.: "Loss-in-Weight Feeding Trials Case Study: Pharmaceutical Formulation," *Journal of Pharmaceutical Innovation*, no. 10, pp. 56-75, 06 December 2014.
- [21] English W. E., Muzzio F. J.: "Method for characterization of loss-in-weight feeder equipment," *Powder Technology*, no. 228, pp. 395-403, 7 June 2012.
- [22] English W., Muzzio F.: "Using Residence Time Distributions (RTDs) to Address the Traceability of Raw Materials in Continuous Pharmaceutical Manufacturing," *Journal of Pharmaceutical Innovation*, no. 11, pp. 64-81, 14 November 2015.
- [23] European Food Safety Authority (EFSA): "Scientific Opinion on the safety of polyvinylpyrrolidone-vinyl acetate copolymer for the proposed uses as a food additive," *EFSA Journal*, vol. 8, no. 12, pp. 1-28, 2010.
- [24] Gabrielsson J., Lindberg N.-O., Lundstedt T.: "Multivariate methods in pharmaceutical applications," *JOURNAL OF CHEMOMETRICS*, no. 16, pp. 141-160, 2002.
- [25] Ghebre-Sellassie I., Martin C.: *Pharmaceutical Extrusion Technology*, New York: Marcel Dekker Inc., 2003.
- [26] Gilmore C., Balke S. T., Calidonio F., Rom-Roginski A.: "In-Line Color Monitoring of Polymers During Extrusion Using a Charge Coupled Device Spectrometer: Color Changeovers and Residence Time Distributions," *Polymer Engineering and Science*, vol. 2, no. 43, pp. 356-366, February 2003.
- [27] Griffin J. P.: *The Textbook of Pharmaceutical Medicine*, London: Wiley-Blackwell, 2009, pp. 171-172.
- [28] Guay D. R.: "Micronized fenofibrate: A new fibric acid hypolipidemic agent," *Annals of Pharmacotherapy*, vol. 33, no. 10, pp. 1083-1103, 1 October 1999.

- [29] Guay D. R.: "Update on fenofibrate," *Cardiovascular Drug Reviews*, vol. 20, no. 4, pp. 281-302, 2002.
- [30] Hancock B. C., Zografi G.: "Characteristics and Significance of the Amorphous State in Pharmaceutical Systems," *Journal of Pharmaceutical Sciences*, vol. 86, no. 1, pp. 1-12, January 1997.
- [31] Hansen C. M.: "50 Years with solubility parameters—past and future," *Progress in Organic Coatings*, vol. 51, pp. 77-84, 24 May 2004.
- [32] He H., Yang R., Tang X.: "In vitro and in vivo evaluation of fenofibrate solid dispersion prepared by hot-melt extrusion," *Drug Development and Industrial Pharmacy*, vol. 6, no. 36, pp. 681-687, 2010.
- [33] Heilmann K.: "Therapeutische Systeme - Eine neue Klasse von Darreichungsformen," *Deutsches Arztblatt*, no. 7, pp. 420-426, 15 Februar 1979.
- [34] Hitzer P., Bäuerle T., Drieschner T., Ostertag E.: "Process analytical techniques for hot-melt extrusion and their application to amorphous solid dispersions," *Anal Bioanal Chem*, no. 409, pp. 4321-4333, 25 March 2017.
- [35] Hörmann T. R., Rehl J., Scheibelhofer O., Schaden L.-M.: "Sensitivity of a continuous hot-melt extrusion and strand pelletization line to T control actions and composition variation," *International Journal of Pharmaceutics*, no. 566, pp. 239-253, 16 May 2019.
- [36] Hsiao W.-K., Hörmann T. R., Toson P., Paudel A.: "Feeding of particle-based materials in continuous solid dosage manufacturing: a material science perspective," *Drug Discovery Today*, pp. 1-7, 23 January 2020.
- [37] Janssens S., da Armas H. N., Remon J. P., Van den Mooter G.: "The use of a new hydrophilic polymer, Kollicoat IR®, in the formulation of solid dispersions of Itraconazole," *European journal of pharmaceutical sciences*, no. 30, pp. 288-294, 26 November 2007.
- [38] Karttunen A.-P., Hörmann T. R., Leersnyder F. D., Ketolainen J.: "Measurement of residence time distributions and material tracking on three T continuous manufacturing lines," *International Journal of Pharmaceutics*, pp. 184-197, 28 March 2019.
- [39] Kazakevich Y., Lobrutto R.: *HPLC for pharmaceutical scientists, USA, New Jersey: Wiley-Interscience, 2007*, pp. 3-13.
- [40] Kleinbudde P.: "Pharmazeutisches Produktdesign: Gezielte Freisetzung von Wirkstoffen durch unterschiedliche Extrusionstechniken," *Chemie Ingenieur Technik*, vol. 5, no. 83, pp. 1-10, 2011.
- [41] Kohlgrüber K.: *Co-Rotating Twin-Screw Extruders, Germany, Munich: Carl Hanser Verlag, 2008*.
- [42] Kolter K., Karl M., Gryczke A.: *Hot-Melt Extrusion with BASF Pharma Polymers, 2 ed., B. SE, Ed., Germany, 2012*.

- [43] Kreimer M., Aigner I., Lepek D., Khinast J.: "Continuous Drying of Pharmaceutical Powders Using a Twin-screw Extruder," *Organic Process Research & Development*, 5 June 2018.
- [44] Kruisz J., Rehl J., Faulhammer E., Witschnigg A., Khinast J.: "Material tracking in a continuous direct capsule-filling process via residence T time distribution measurements," *International Journal of Pharmaceutics*, pp. 347-358, 28 August 2018.
- [45] Kruisz J., Rehl J., Sacher S., Aigner I.: "RTD Modeling of a Continuous Dry Granulation Process for Process Control and Materials Diversion," *International Journal of Pharmaceutics*, 01 June 2017.
- [46] Kukkar V., Anand V., Kataria M., Gera M.: "Mixing and formulation of low dose drugs: underlying problems and solutions," *Thai Journal of Pharmaceutical Sciences*, vol. 32, pp. 43-58, 2008.
- [47] Langer R.: "Polymeric Delivery Systems for Controlled Drug Release," *Chemical Engineering Communications*, no. 6, pp. 1-48, 11 April 1980.
- [48] Lllusa M., Mohr S., Baumgartner R., Paudel A.: "Continuous Low-dose Feeding of Highly Active Pharmaceutical Ingredients in Hot-Melt Extrusion," *Drug Development and Industrial Pharmacy*, vol. 42, no. 8, pp. 1360-1364, 11 January 2016.
- [49] Maier H. G.: *Lebensmittel- und Umweltanalytik: Methoden und Anwendungen*, Darmstadt: Steinkopff-Verlag Heidelberg, 1990.
- [50] Maniruzzaman M., Boateng J. S., Snowden M. J., Douroumis D.: "A Review of Hot-Melt Extrusion: Process Technology to Pharmaceutical Products," *ISRN Pharmaceutics*, pp. 1-9, 30 October 2012.
- [51] Marsac P. J., Shamblin S. L., Taylor L. S.: "Theoretical and Practical Approaches for Prediction of Drug-Polymer Miscibility and Solubility," *Pharmaceutical Research*, vol. 10, no. 23, pp. 2417-2426, 10 October 2006.
- [52] Park J.-B., Kang C.-Y., Kang W.-S., Choi H.-G.: "New investigation of distribution imaging and content uniformity of very low dose drugs using hot-melt extrusion method," *International Journal of Pharmaceutics*, vol. 458, pp. 245-253, 21 October 2013.
- [53] Patil H., Tiwari R. V., Repka M. A.: "Hot-Melt Extrusion: from Theory to Application in Pharmaceutical Formulation," *AAPS PharmSciTech*, vol. 1, no. 17, pp. 20-42, 10 July 2015.
- [54] Perkampus H.-H.: *UV-VIS Spectroscopy and Its Applications*, Germany, Berlin: Springer, 1992.
- [55] Perrie Y., Rades T.: *Pharmaceutics - Drug Delivery and Targeting*, UK: RPS Publishing, 2010.

- [56] Rajalathi T., Kvalheim O. M.: "Multivariate data analysis in pharmaceuticals: A tutorial review," *International Journal of Pharmaceutics*, no. 417, pp. 280-290, 16 February 2011.
- [57] Robinson B. V., Sullivan F. M., Borzelleca J. F., Schwartz S. L.: PVP - A Critical Review of the Kinetics and Toxicology of Polyvinylpyrrolidone (Povidone), USA, Michigan: Lewis Publishers, 1990.
- [58] Saerens L., Varvaet C., Remon J. P., De Beer T.: "Process monitoring and visualization solutions for hot-melt extrusion: a review," *Journal of Pharmacy and Pharmacology*, no. 66, pp. 180-230, 4 July 2013.
- [59] Schneider C., Langer R., Loveday D., Hair D.: "Applications of ethylene vinyl acetate copolymers (EVA) in drug delivery systems," *Journal of Controlled Release*, no. 262, pp. 284-295, 05 August 2017.
- [60] Sigma Aldrich: "Merck - Fenofibrate," [Online]. Available: <https://www.sigmaaldrich.com/catalog/product/sigma/f6020>. [Accessed 25 04 2020].
- [61] Sigma Aldrich: "Merck - Poly(1-vinylpyrrolidone-co-vinyl acetate)," [Online]. Available: <https://www.sigmaaldrich.com/catalog/product/aldrich/190845>. [Accessed 20 05 2020].
- [62] Stankovic M., Frijlink H. W., Hinrichs W. L.: "Polymeric formulations for drug release prepared by hot melt extrusion: application and characterization," *Drug Discovery Today*, no. 00, pp. 1-11, February 2015.
- [63] Thelin B., Lundstedt T., Lundgren R., Olsson A., Batra S.: "Classification of Estradurin batches: correlation between ³¹P NMR and a biological duration test for batch approval," *Chemometrics and Intelligent Laboratory System*, no. 27, pp. 135-145, 10 June 1995.
- [64] ThermoSpectronic: "Basic UV-Vis Theory, Concepts and Applications," [Online]. Available: <http://www.molecularinfo.com/MTM/UV.pdf>. [Accessed 23 03 2020].
- [65] Tian Y., Booth J., Meehan E., Jones D. S., Li S.: "Construction of Drug–Polymer Thermodynamic Phase Diagrams Using Flory–Huggins Interaction Theory: Identifying the Relevance of Temperature and Drug Weight Fraction to Phase Separation within Solid Dispersions," *molecular pharmaceutics*, no. 10, pp. 236-248, 30 October 2012.
- [66] U.S. Department of Health and Human Services Food and Drug Administration: "Guidance for Industry, PAT — A Framework for Innovative Pharmaceutical Development, Manufacturing, and Quality Assurance," Maryland, USA, 2004.
- [67] U.S. Food & Drug Administration.: "Drugs@FDA Glossary of Terms," 14 November 2017. [Online]. Available: <https://www.fda.gov/drugs/drug-approvals-and-databases/drugsfda-glossary-terms#M>. [Accessed 25 March 2020].
- [68] Waard H. d., Hinrichs W., Visser M., Bologna C., Frijlink H.: "Unexpected differences in dissolution behavior of tablets prepared from solid dispersions with a surfactant

- physically mixed or incorporated," *International Journal of Pharmaceutics*, vol. 349, pp. 66-73, 24 July 2008.
- [69] Wahl P., Hörl G., Kaiser D., Sacher S., Khinast J.: "In-Line Measurement of Residence Time Distribution in Melt Extrusion via Video Analysis," *POLYMER ENGINEERING AND SCIENCE*, vol. 2, no. 58, pp. 170-179, 09 February 2018.
- [70] Wahl P. R., Treffer D., Roblegg E., Koscher G.: "Inline monitoring and a PAT strategy for pharmaceutical hot melt extrusion," *International Journal of Pharmaceutics*, pp. 159-168, 31 July 2013.
- [71] Wang X., Hänsch R., Ma L., Hellwich O.: "Comparison of Different Color Spaces for Image Segmentation using Graph-cut," in *VISAPP 2014*, Portugal, 2014.
- [72] Wang Y., Steinhoff B., Brinkmann C., Alig I.: "In-line monitoring of the thermal degradation of poly(L-lactic acid) during melt extrusion by UVevis spectroscopy," *Polymer*, no. 49, pp. 1257-1265, 11 January 2008.
- [73] Wesholowski J., Prill S., Berghaus A., Thommes M.: "Inline UV/Vis spectroscopy as PAT tool for hot-melt extrusion," *Drug Delivery and Translational Research*, no. 8, pp. 1595-1603, 11 January 2018.
- [74] William R. C.: "Safety of Fenofibrate - US and Worldwide Experience," *Cardiology*, no. 76, pp. 169-179, 1989.
- [75] Wintermantel E., Ha S.-W.: *Medizintechnik*, Berlin Heidelberg: Springer, 2009.
- [76] Yang R.: *Analytical Methods for Polymer Characterization*, USA, Florida: Taylor & Francis Group, 2018.
- [77] Yang Y., Li X.: "Experimental and analytical study of ultrasonic micro powder feeding," *Journal of Physics D: Applied Physics*, vol. 36, no. 11, pp. 1349-1354, 14 May 2003.

9 Appendix

9.1 Abbreviations and symbols

Symbol	Meaning	Unit
A	Absorbance	AU (or %)
$A_{pist.}$	Cross-section area of microfeeder reservoir	mm ²
c	Concentration	mol/dm ³
d	Offset	
D	Dispersion coefficient	m ² /s
E	Diffusion constant	m ² /s
FR	Feed rate	g/h
I	Transmitted radiation	
I_0	Initial radiation	
k	Molar attenuation coefficient	dm ³ /(mol cm)
l	Length of the optical path	cm
L	Characteristic length	m
m	Mass	kg
\dot{m}	Mass flow	kg/s
$m_{res.}$	Mass of powder in microfeeder reservoir	g
Pe	Péclet number	
RT_{max}	Maximal residence time	s
s	Scaling factor	
T	Transmission	%
$T_{deg.}$	Thermal degradation temperature	°C
T_g	Glass transition temperature	°C

T_m	Melting temperature	°C
t_x	Time x in RTD curve	s
U	Average axial velocity	m/s
V	Volume	m ³
\dot{V}	Volume flow	m ³ /s
v_p	Microfeeder piston speed	mm/min
$V_{res.}$	Microfeeder reservoir volume	mm ³
δ_d	Hansen solubility parameter for dispersion	MPa ^{1/2}
δ_g	Hansen solubility parameter for polarity	MPa ^{1/2}
δ_h	Hansen solubility parameter for hydrogen bonding	MPa ^{1/2}
$\delta_{tot.}$	Total Hansen solubility parameter	MPa ^{1/2}
τ	mean residence time	s
$\omega/\omega\%$	Mass fraction	%

Abbreviation Meaning

ACN	Acetonitrile
API	Active pharmaceutical ingredient
BCS	Biopharmaceutical classification system
FDA	Federal Drug Administration
FFB	Fenofibrate
HME	Hot melt extrusion
HPLC	High pressure liquid chromatography
LIW	Loss in weight
LOD	Limit of detection
LOQ	Limit of quantification

9 Appendix

MIR	Mid-infrared
NIR	Near-infrared
PAT	Process analytical tool
PCA	Principal component analysis
PVP	Polyvinylpyrrolidone
PVP-VA	Polyvinylpyrrolidone – vinyl acetate
QbD	Quality by Design
RT	Residence time
RTD	Residence time distribution
RSD	Relative Standard Deviation
SIMCA	Soft independent modelling of class analogy
SK	“Schub Kante”
TI	Therapeutic index
TSE	Twin-screw extruder
UV/Vis	Ultraviolet / visible light

9.2 List of figures

Figure 1: Concentration of API in plasma for different delivery forms [59]	4
Figure 2: Synthesis of N-Vinyl-2-pyrrolidone [13]	7
Figure 3: Polymerization of soluble PVP in water [13].....	8
Figure 4: Synthesis of PVP-VA via free radical polymerization [13].....	9
Figure 5: Chemical structure of Fenofibrate [60]	10
Figure 6: Processing zones of a twin-screw extruder (Figure adapted from [41]).....	13
Figure 7: Different screw elements.....	16
Figure 8: Residence time distribution (Figure adapted from [41])	18
Figure 9: Operating principle of LIW-feeder (Figure adapted from [17])	21
Figure 10: Operating principle of the microfeeders volumetric feeding system [5]	23
Figure 11: Chemical structure of Kollidon VA64 [61]	31
Figure 12: Microfeeder and components	32
Figure 13: Coperion ZSK 18 ML with LIW feeder	35
Figure 14: Screw-profile 1	36
Figure 15: Screw-profile 2.....	36
Figure 16: Screw profile 3	37
Figure 17: UV-Vis probes inserted into the extruder barrel	38
Figure 18: Marked area of interest from extrudate strand.....	39
Figure 19: Primary process setup	41
Figure 20: Spectra with UV-Vis spectrometer	42
Figure 21: Improved UV/Vis spectrum	42
Figure 22: Spectra recorded during the extrusion process	43
Figure 23: First microfeeder setup.....	45
Figure 24: Second microfeeder setup	45
Figure 25: Microfeeder implementation concepts.....	45
Figure 26: Final microfeeder setup	46
Figure 27: Visualization of experiments with constant API concentration	48
Figure 28: Visualization of step trial	48
Figure 29: UV/Vis spectra of Kollidon VA64 and Fenofibrate.....	49
Figure 30: Capability analysis of microfeeder with feed rate 1 g/h (experiment nr. 1).....	50
Figure 31: Capability analysis of microfeeder with feed rate 1 g/h (experiment nr. 2).....	50
Figure 32: Capability analysis of microfeeder with feed rate 1 g/h (experiment nr. 3).....	50
Figure 33: Capability analysis of microfeeder with feed rate 5 g/h (experiment nr. 4).....	51
Figure 34: Capability analysis of microfeeder with feed rate 5 g/h (experiment nr. 5).....	51
Figure 35: Capability analysis of microfeeder with feed rate 5 g/h (experiment nr. 6).....	52
Figure 36: Capability analysis of microfeeder with stepwise feed rate increase.....	53
Figure 37: RTD curve of measurement 1.....	56
Figure 38: RTD curve of measurement 2.....	57
Figure 39: SIMCA analysis of recorded spectra	58
Figure 40: HPLC results from pre-blend experiments.....	59
Figure 41: HPLC results from experiment nr. 1 with 0,5 $\omega/\omega\%$ Fenofibrate.....	60
Figure 42: HPLC results from experiment nr. 2 with 0,5 $\omega/\omega\%$ Fenofibrate.....	61
Figure 43: HPLC results from experiment nr. 3 with 0,5 $\omega/\omega\%$ Fenofibrate.....	61
Figure 44: HPLC results from experiment with 0,2 $\omega/\omega\%$ Fenofibrate.....	63
Figure 45: HPLC results from experiment with 0,1 $\omega/\omega\%$ Fenofibrate.....	65
Figure 46: HPLC results from experiment with stepwise Fenofibrate concentration.....	67

9.3 List of tables

Table 1: Hansen solubility parameters for used substances.....	12
Table 2: Characteristic temperatures of Fenofibrate.....	30
Table 3: Characteristic temperatures of Kollidon VA64	31
Table 4: Set temperature profile for extrusion processes	37
Table 5: Statistical analysis of feed rates 1 g/h and 5 g/h.....	52
Table 6: Statistical analysis of the experiments with stepwise feed rate increase	54
Table 7: Results of RTD measurements.....	56
Table 8: Results of pre-blend experiments.....	59
Table 9: Results of experiments nr. 1-3 with 0,5 $\omega/\omega\%$ Fenofibrate.....	62
Table 10: Results of experiment with 0,2 $\omega/\omega\%$ Fenofibrate.....	64
Table 11: Results of experiment with 0,1 $\omega/\omega\%$ Fenofibrate.....	66
Table 12: Results of experiment with stepwise Fenofibrate concentration	67
Table 13: comparison between batch- and microfeeder compounding-technique.....	69